1993

Studies in excitation-contraction coupling in isoproterenol-induced hypertrophied rat heart.

Lihui. Tang
University of Windsor

NOTICE

AVIS

The quality of this microform is heavily dependent upon the quality of the original thesis submitted for microfilming. Every effort has been made to ensure the highest quality of reproduction possible.

La qualité de cette microforme dépend grandement de la qualité de la thèse soumise au microfilmage. Nous avons tout fait pour assurer une qualité supérieure de reproduction.

If pages are missing, contact the university which granted the degree.

S'il manque des pages, veuillez communiquer avec l'université qui a conféré le grade.

Some pages may have indistinct print especially if the original pages were typed with a poor typewriter ribbon or if the university sent us an inferior photocopy.

La qualité d'impression de certaines pages peut laisser à désirer, surtout si les pages originales ont été dactylographiées à l'aide d'un ruban usé ou si l'université nous a fait parvenir une photocopie de qualité inférieure.

Reproduction in full or in part of this microform is governed by the Canadian Copyright Act, R.S.C. 1970, c. C-30, and subsequent amendments.

La reproduction, même partielle, de cette microforme est soumise à la Loi canadienne sur le droit d'auteur, SRC 1970, c. C-30, et ses amendements subséquents.

Canada

STUDIES IN EXCITATION-CONTRACTION COUPLING IN ISOPROTERENOL INDUCED HYPERTROPHIED RAT HEART

by

Lihui Tang

A Dissertation
Submitted to the Faculty of Graduate Studies and Research
through the Department of Biological Sciences
in Partial Fulfilment of the Requirements
for the Degree of Doctor of Philosophy
at the University of Windsor

Windsor, Ontario, Canada

1993

Name ___ *Li Hui Tang* ___

ohysics?

SUBJECT TERM

`0 4 3 3` U·M·I

SUBJECT CODE

Subject Categories

THE HUMANITIES AND SOCIAL SCIENCES

COMMUNICATIONS AND THE ARTS
Architecture	0729
Art History	0377
Cinema	0900
Dance	0378
Fine Arts	0357
Information Science	0723
Journalism	0391
Library Science	0399
Mass Communications	0708
Music	0413
Speech Communication	0459
Theater	0465

EDUCATION
General	0515
Administration	0514
Adult and Continuing	0516
Agricultural	0517
Art	0273
Bilingual and Multicultural	0282
Business	0688
Community College	0275
Curriculum and Instruction	0727
Early Childhood	0518
Elementary	0524
Finance	0277
Guidance and Counseling	0519
Health	0680
Higher	0745
History of	0520
Home Economics	0278
Industrial	0521
Language and Literature	0279
Mathematics	0280
Music	0522
Philosophy of	0998
Physical	0523

Psychology	0525
Reading	0535
Religious	0527
Sciences	0714
Secondary	0533
Social Sciences	0534
Sociology of	0340
Special	0529
Teacher Training	0530
Technology	0710
Tests and Measurements	0288
Vocational	0747

LANGUAGE, LITERATURE AND LINGUISTICS
Language	
General	0679
Ancient	0289
Linguistics	0290
Modern	0291
Literature	
General	0401
Classical	0294
Comparative	0295
Medieval	0297
Modern	0298
African	0316
American	0591
Asian	0305
Canadian (English)	0352
Canadian (French)	0355
English	0593
Germanic	0311
Latin American	0312
Middle Eastern	0315
Romance	0313
Slavic and East European	0314

PHILOSOPHY, RELIGION AND THEOLOGY
Philosophy	0422
Religion	
General	0318
Biblical Studies	0321
Clergy	0319
History of	0320
Philosophy of	0322
Theology	0469

SOCIAL SCIENCES
American Studies	0323
Anthropology	
Archaeology	0324
Cultural	0326
Physical	0327
Business Administration	
General	0310
Accounting	0272
Banking	0770
Management	0454
Marketing	0338
Canadian Studies	0385
Economics	
General	0501
Agricultural	0503
Commerce-Business	0505
Finance	0508
History	0509
Labor	0510
Theory	0511
Folklore	0358
Geography	0366
Gerontology	0351
History	
General	0578

Ancient	0579
Medieval	0581
Modern	0582
Black	0328
African	0331
Asia, Australia and Oceania	0332
Canadian	0334
European	0335
Latin American	0336
Middle Eastern	0333
United States	0337
History of Science	0585
Law	0398
Political Science	
General	0615
International Law and Relations	0616
Public Administration	0617
Recreation	0814
Social Work	0452
Sociology	
General	0626
Criminology and Penology	0627
Demography	0938
Ethnic and Racial Studies	0631
Individual and Family Studies	0628
Industrial and Labor Relations	0629
Public and Social Welfare	0630
Social Structure and Development	0700
Theory and Methods	0344
Transportation	0709
Urban and Regional Planning	0999
Women's Studies	0453

THE SCIENCES AND ENGINEERING

BIOLOGICAL SCIENCES
Agriculture	
General	0473
Agronomy	0285
Animal Culture and Nutrition	0475
Animal Pathology	0476
Food Science and Technology	0359
Forestry and Wildlife	0478
Plant Culture	0479
Plant Pathology	0480
Plant Physiology	0817
Range Management	0777
Wood Technology	0746
Biology	
General	0306
Anatomy	0287
Biostatistics	0308
Botany	0309
Cell	0379
Ecology	0329
Entomology	0353
Genetics	0369
Limnology	0793
Microbiology	0410
Molecular	0307
Neuroscience	0317
Oceanography	0416
Physiology	0433
Radiation	0821
Veterinary Science	0778
Zoology	0472
Biophysics	
General	0786
Medical	0760

EARTH SCIENCES
Biogeochemistry	0425
Geochemistry	0996

Geodesy	0370
Geology	0372
Geophysics	0373
Hydrology	0388
Mineralogy	0411
Paleobotany	0345
Paleoecology	0426
Paleontology	0418
Paleozoology	0985
Palynology	0427
Physical Geography	0368
Physical Oceanography	0415

HEALTH AND ENVIRONMENTAL SCIENCES
Environmental Sciences	0768
Health Sciences	
General	0566
Audiology	0300
Chemotherapy	0992
Dentistry	0567
Education	0350
Hospital Management	0769
Human Development	0758
Immunology	0982
Medicine and Surgery	0564
Mental Health	0347
Nursing	0569
Nutrition	0570
Obstetrics and Gynecology	0380
Occupational Health and Therapy	0354
Ophthalmology	0381
Pathology	0571
Pharmacology	0419
Pharmacy	0572
Physical Therapy	0382
Public Health	0573
Radiology	0574
Recreation	0575

Speech Pathology	0460
Toxicology	0383
Home Economics	0386

PHYSICAL SCIENCES

Pure Sciences
Chemistry	
General	0485
Agricultural	0749
Analytical	0486
Biochemistry	0487
Inorganic	0488
Nuclear	0738
Organic	0490
Pharmaceutical	0491
Physical	0494
Polymer	0495
Radiation	0754
Mathematics	0405
Physics	
General	0605
Acoustics	0986
Astronomy and Astrophysics	0606
Atmospheric Science	0608
Atomic	0748
Electronics and Electricity	0607
Elementary Particles and High Energy	0798
Fluid and Plasma	0759
Molecular	0609
Nuclear	0610
Optics	0752
Radiation	0756
Solid State	0611
Statistics	0463

Applied Sciences
Applied Mechanics	0346
Computer Science	0984

Engineering	
General	0537
Aerospace	0538
Agricultural	0539
Automotive	0540
Biomedical	0541
Chemical	0542
Civil	0543
Electronics and Electrical	0544
Heat and Thermodynamics	0348
Hydraulic	0545
Industrial	0546
Marine	0547
Materials Science	0794
Mechanical	0548
Metallurgy	0743
Mining	0551
Nuclear	0552
Packaging	0549
Petroleum	0765
Sanitary and Municipal	0554
System Science	0790
Geotechnology	0428
Operations Research	0796
Plastics Technology	0795
Textile Technology	0994

PSYCHOLOGY
|	
General	0621
Behavioral	0384
Clinical	0622
Developmental	0620
Experimental	0623
Industrial	0624
Personality	0625
Physiological	0989
Psychobiology	0349
Psychometrics	0632
Social	0451

ABSTRACT

Cardiac hypertrophy was induced by daily subcutaneous injections of isoproterenol (0.3 mg/kg. body weight) for 12 consecutive days. A significant increase in whole ventricular weight (35.7%) was achieved. Regionally, the right ventricle produced a greater hypertrophy response than the left ventricle. Contractile force, $+Dt/dt$, and $-DT/dt$ in right ventricular trabecular muscle were significantly increased, suggesting that either Ca^{2+} responsiveness of the myofilaments or the availability of $[Ca^{2+}]_i$ was increased.

The Ca^{2+} sensitivity of the myofilaments was investigated using a Triton-100 skinned trabecular preparation. The force-pCa relationship showed no difference in the myofilament Ca^{2+} sensitivity.

The force-interval relationship was studied to reflect the early recovery of SR Ca^{2+} release channels and the late diastolic Ca^{2+} influx via sarcolemmal Na-Ca exchange. The SR Ca^{2+} release characteristics were not altered, however, Ca^{2+} influx via sarcolemmal Na-Ca exchange was enhanced in hypertrophied muscle.

A biphasic rate staircase was found in trabecular muscle: negative from 0.1 to 0.5 Hz and positive from 0.5 to 2.5 Hz. Studies using rapid cooling contractures (RCCs) suggest that SR Ca^{2+} content determines the amounts of SR Ca^{2+} release. Ryanodine, which unloads SR Ca^{2+}, abolished the negative rate staircase. Nifedipine, I_{Ca} blocker, eliminated the positive response. These results suggest that diastolic SR Ca^{2+} loading, probably via Na-Ca exchange, contributes to the negative phase, whereas Ca^{2+} influx via L-type channel dominates the positive phase. In hypertrophied muscle ($[Ca^{2+}]_o$ = 0.5 mM), the positive rate staircase was significantly enhanced, indicating an
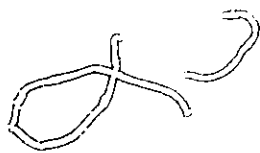
increased functioning of L-type Ca^{2+} channel and a greater SR Ca content.

There was a frequency-dependent prolongation of APD_{50} and the APD_{50} was significantly increased in hypertrophied muscle, suggesting that Ca^{2+} influx, probably via I_{Ca}, was increased with frequency and this pathway was significantly amplified in hypertrophied muscle.

The capacity to remove cytoplasmic Ca^{2+} was increased by either SR Ca-ATPase pump or sarcolemmal Na-Ca exchange in hypertrophied muscle.

In summary, the increased $[Ca^{2+}]_i$ handling pathways, such as I_{Ca}, SR Ca^{2+} content, Na-Ca exchange activity, and SR Ca-ATPase pump, contribute to the enhanced contractile function in hypertrophied muscle.

DEDICATION

To my wife and our parents

ACKNOWLEDGEMENTS

TABLE OF CONTENTS

LIST OF TABLES

LIST OF FIGURES

LIST OF ABBREVIATIONS

APD_{50}	Action potential duration at 50% amplitude
$[Ca^{2+}]_i$	Intracellular calcium
$[Ca^{2+}]_o$	Extracellular calcium
cAMP	Cyclic adenosine monophosphate
CaMK	Calcium/calmodulin kinase
CICR	Calcium induced calcium release
DG	Diacylglycerol
DT	Developed tension
+DT/dt	Maximum rate of contraction
-DT/dt	Maximum rate of relaxation
E-C coupling	Excitation-contraction coupling
H^+	Proton
Mg^{2+}	Magnesium
mN/mm^2	Millinewton per square millimetre of muscle cross-sectional area
Na^+	Sodium
I_{Ca}	Calcium influx via L-type channel
ISO	Isoproterenol
pH_i	Intracellular pH
PKC	Protein kinase C
PLC	Phospholipase C
RCC	Rapid cooling contracture
SL	Sarcolemma
SR	Sarcoplasmic reticulum

INTRODUCTION

I. CARDIAC HYPERTROPHY.

Cardiac muscle growth can be envisioned to be regulated by two sets of factors: those that maintain the proper allometric ratio of heart to body size during normal growth, and those that are responsible for matching heart size to altered hemodynamic requirements (Bugaisky et al. 1986). Hypertrophy, an increase in cell size without cell division, is a fundamental adaptive process employed by post-mitotic muscle cells. Because the adult myocardial cell is terminally differentiated and has lost the ability to proliferate, cardiac growth during the hypertrophic process results primarily from an increase in protein content per individual myocardial cell, with little or no change in muscle cell number (Morgan et al. 1987).

The central cellular features of myocardial hypertrophy are: (1) an increase in cell volume or size without a concomitant increase in cellular proliferation; (2) an increase in contractile protein content due to up-regulation of contractile protein genes, such as cardiac myosin light chain-2 gene (MLC-2) and cardiac α-actin gene (Lee et al. 1988); (3) an induction of contractile protein isoforms, such as an altered proportion of α- and β-myosin heavy chain (MHC) (Lee et al. 1988, Schwartz et al. 1986); (4) an activation of the immediate early (IE) genes (c-fos, c-jan, Egr-1, etc). The activation of

1

IE genes are one of the first detectable changes in cardiac hypertrophy (McDonough et al. 1992, Sadoshima et al. 1992); (5) a re-expression of embryonic genes for contractile proteins (skeletal α-actin and β-MHC genes) and non-contractile proteins [atrial nutriuretic factor (ANF)], which are normally expressed in embryonic tissue. Because the ANF gene is expressed in both atrial and ventricular tissues during embryonic development and the atria are the primary site of ANF synthesis shortly after birth, a reexpression of ANF in ventricular cells represents the activation of an embryonic program of gene expression, which occurs in various models of ventricular hypertrophy (Franch et al. 1988, Sadoshima et al. 1992), and finally (6) the differential activation in single gene expression coding for channel-, or pump-proteins such as the SR Ca-ATPase (Lakatta 1993).

In addition to alterations in cellular elements, morphological studies of hypertrophic myocytes reveal a relatively well preserved intracellular organization and cellular symmetry (Bouron et al. 1992); an apparent decrease in the number of mitochondria (Bishop 1990); a widening of the myofibrillar bundles (Bishop 1990), which could indicate an increase in the cross sectional area of individual cells; an enlargement of the transverse tubular system (Bishop 1990), which still maintains an unchanged ratio of sarcotubular membrane to myofibrillar volume; an increase in the number of glycogen granules; and an unchanged ratio of plasma membrane volume to cell volume.

Changes in cardiac excitation, myofilament activation, and contraction mechanisms also occur with cardiac hypertrophy. The altered contractile function has been extensively studied in pressure-overload hypertrophy, which is the most common form in the human. The abnormalities in cardiac excitation-contraction (E-C) coupling

include: prolonged action potential duration (Aronson 1980); prolonged contraction and relaxation times (Capasso et al. 1986); a shift in MHC isoform profile from a predominant V_1 to the V_3 with a reduction in myosin ATPase activity (Capasso et al. 1986); decreased velocity of force development; decreased SR Ca^{2+} pump activity (Dela Bastie et al. 1990); prolonged intracellular Ca^{2+} transient duration (Gwathmey et al. 1985). Over the range of $[Ca^{2+}]_i$ encountered in the intact cell during contraction, the myofilament Ca^{2+} sensitivity is not altered in experimental pressure overload in rodents, guinea pigs, rabbits and ferrets (Gwathmey et al. 1992). Accumulating evidence has indicated that altered Ca^{2+} handling may play a dominant role in the abnormalities of contractile function in cardiac hypertrophy (Henry et al. 1972, Gwathmey et al. 1985, Ventura-Clapier et al. 1988).

In the process of adapting to stress, fundamental changes occur in the cellular elements and their functional characteristics. Studies on the contractile changes in hypertrophied heart yield valuable clues in understanding the fundamental aspects of myocardial mechanics and suggest possible regulatory pathways. The present dissertation focused on the cellular mechanisms contributing to changes in cardiac E-C coupling in the hypertrophied myocardium. Evaluation of these pathways will require some background understanding of both cardiac hypertrophy and cardiac E-C coupling.

(I). MODELS OF CARDIAC HYPERTROPHY

A. Mechanical Stimuli In Cardiac Hypertrophy

In vivo studies. Cardiac hypertrophy usually results from an increased workload

3

that is imposed upon the heart. There are two typical models of experimental cardiac hypertrophy, which result from mechanical stimuli. One is pressure-overload due to an increased afterload on the heart; while the other is volume-overload hypertrophy due to a higher preload within the ventricles. Pressure-overload hypertrophy can be induced by (1) ascending (Cutilletta et al. 1975) or abdominal (Beznak et al. 1969) aortic stenosis; (2) hypertension; and (3) pulmonary artery stenosis (Cooper et al. 1981). Both aortic stenosis and hypertension result in left ventricular tissue growth, while pulmonary artery stenosis is mainly used to induce right ventricular hypertrophy. Various factors that increase preload of the heart can be used to create an animal model of volume-overload hypertrophy, such as arteriovenous fistula, aortic insufficiency, bradycardia and anaemia, etc. (Bishop 1982). The characteristics of tissue growth in response to mechanical stimuli vary widely, depending on experimental conditions. Commonly recognized variables are severity, duration, and type of overload (i.e., pressure versus volume), the rate of overload application (i.e., acute versus chronic), and the age and species of the animal. Pressure-overload hypertrophy is often associated with areas of focal necrosis (Cooper 1987). This raises the question as to whether the fast tissue growth in response to pressure-overload results directly from work overload or a compensation for loss of myocardial cells. Volume-overload usually results in slower rates of hypertrophy which may not be appropriate for studies on the mechanism of either accelerated rates of protein synthesis or decreased protein degradation (Morgan et al. 1987). In some instances, increased pressure or volume overload is associated with increased release of neurotransmitters and/or plasma concentrations of hormones that may also have direct effects on cardiac myocyte growth. In this situation, a rigorous assessment of the

4

direct effects of mechanical parameters such as increased active (pressure overload) or passive (volume overload) wall tension on growth is impossible.

In vitro studies. The effects of mechanical factors, such as deformation of tissue or cell by stretching or swelling, on the generation of cell growth could overcome some of the complexities associated with *in vivo* experiments. *In vitro* studies in isolated whole heart, Chua et al. (1987) reported that increased aortic pressure decreased the rate of protein degradation and accelerated the rates of ribosome formation. Peterson and Lesch (1972) first observed that stretch of quiescent papillary muscle could accelerate protein synthesis. Stimulation of the muscle to contract did not increase the rate of protein synthesis in stretched muscle; rather, myocardial protein synthesis increased in proportion to total muscle tension. In a single cell preparation, Sadoshima et al. (1992) recently provided information as to how mechanical load is converted into intracellular signals for gene regulation by using cultured neonatal cardiocytes grown on a stretchable substrate in a serum free medium. Static stretch of the myocytes (increasing resting length 20%) induced myocyte hypertrophy without cell injury. Stretch initiated the induction of immediate early (IE) genes such as c-fos, c-jun, c-myc, JE and Egr-1. The induction of IE genes was followed by the expression of "fetal" genes for skeletal α-actin, ANF, and β-MHC. These data indicate that an increase in hemodynamic loading itself is a sufficient stimulus for induction of tissue growth in the whole organ, small intact tissue preparations and in isolated single cells.

B. Neural Control In Cardiac Hypertrophy

In vivo studies. During the past several decades, many neural and hormonal stimuli have been implicated in cardiac muscle growth, including but not limited to α-

and β-adrenergic agonists, thyroxine, and angiotensin-II, etc. Accumulating evidence has indicated that adrenoceptor activation could be a primary effector initiating and maintaining cardiac hypertrophy as a result of increased cardiac sympathetic nerve activity and elevated levels of circulating catecholamines. As reported by Zierhut et al. (1989a) in the rat, norepinephrine or norfenephrine (α-adrenergic agonist) increased left ventricular weight-to-body weight ratio and was accompanied by an increase in total RNA. Prazosin (α_1-adrenoceptor blocker) and metoprolol (β-adrenoceptor blocker) each partially antagonized the increase in left ventricular weight. However, when administered simultaneously, they prevented the norepinephrine-induced increase in left ventricular mass. Changes in functional parameters caused by norepinephrine were reversed with verapamil (Ca^{2+} channel blocker); however, this treatment did not prevent the development of cardiac hypertrophy. These results suggest that cardiac hypertrophy in the rat in response to norepinephrine was directly mediated by stimulation of myocardial α- and β-adrenoceptors and was not secondary to hemodynamic changes.

Chronic, repeated injections of isoproterenol, a β-adrenergic agonist, have been used to induce cardiac hypertrophy (Baldwin et al. 1982, Taylor et al. 1988, Haddad et al. 1991, Allard 1990). Isoproterenol-induced cardiac hypertrophy, in the rat, is a dose- and time-dependent event. Generally, it is believed that evaluating the mechanism of isoproterenol-induced cardiac hypertrophy is complicated by altered contractility, heart rate, and necrosis of cardiac myocytes. However, an early study by Fried and Reid (1985) showed that the hemodynamic changes produced by isoproterenol were transient, being undetectable after one day. Further evidence indicating that hemodynamic alterations do not play a major role in isoproterenol-induced cardiac

6

hypertrophy comes from studies with transplanted, denervated rat hearts in which heart weight increased in the absence of a hemodynamic workload (Larson et al. 1985). Recent work using *in vivo* monoclonal antimyosin antibodies to identify myocyte necrosis has shown that the timing and the degree of hypertrophy do not follow the course of myocyte loss (Benjamin et al. 1989). Allard et al. (1990) also demonstrated a dissociation of myocardial hypertrophy and myocardial injury. These findings indicate that isoproterenol-induced cardiac hypertrophy is not merely a compensatory response to myocyte loss.

In vitro studies. A direct test of α_1-adrenergic agonists on tissue growth potential was provided by Fuller et al. (1990). They observed that accelerated protein synthesis appeared to be mediated by the α_1-adrenoceptor in myocytes and perfused hearts from adult rats and identified that the increased rates of α_1-adrenergic dependent protein synthesis was due to a faster rate in translation of preexisting mRNA. In the neonatal cardiac myocytes, which are capable of cell division, α_1-adrenergic agonists have been clearly demonstrated to result in myocyte hypertrophy as characterized by increased rate of protein synthesis, myocyte surface area, protein content, selective upregulation of the MLC gene, the early developmental contractile protein isogene, skeletal α-actin and β-MHC genes (Meidell et al. 1986, Simpson 1985, Lee et al. 1988, Simpson et al. 1989). These data suggest that α_1-adrenergic stimuli can mediate *in vitro* cardiomyocyte hypertrophy in both neonatal and adult myocardium.

The effects of β-adrenergic agonists on cardiac growth can be studied using isolated perfused whole hearts and cell culture techniques. The perfused heart is a complex preparation to study direct effects of β-receptor occupancy because of the accompanying changes in contractility, heart rate and ATP depletion. ATP depletion

can obscure the effects of catecholamines on protein synthesis and degradation. In cultured neonatal cardiac myocytes, chronic exposure to isoproterenol resulted in cell hypertrophy, but the effect was not as large as α_1-adrenergic stimulation (Simpson et al. 1982).

C. Endocrine Control In Cardiac Hypertrophy

Thyroid Hormone:

In vivo studies. Thyroid hormone has been shown to affect the developmental expression of ventricular isomyosin V_1, V_2, and V_3 (Chizzonite et al. 1984). During development, endogenous thyroid hormone induces the synthesis of ventricular α-MHC, which dimerizes to form the V_1 isomyosin. Chizzonite et al. (1984) reported that, in the rat, increased serum levels of endogenous thyroxine (T_4) and triiodiothyronine (T_3) correlated with the maximal expression of V_1 during development. High circulatory thyroid hormone levels, in cardiac hypertrophy, has been widely shown in either human or animal models (Cohen et al. 1966). The *in vivo* effects of thyroid hormone on cardiac hypertrophy include: 1) direct effects of the hormone on the heart and 2) indirect effects related to stimulation of the adrenergic nervous system and altered left ventricular loading conditions. Zierhut et al. (1989b) reported that after T_3 administration, there was an enhanced cardiac output and RNA concentration, and a significant ventricular hypertrophy. β-receptor blockade reduced left ventricular functional alterations but had no effect on the T_3-induced increase in RNA or on the development of cardiac hypertrophy. In addition, α-receptor blockade also had no effect on T_3-induced cardiac hypertrophy. These data suggest that exogenous thyroid hormone may directly mediate increased protein synthesis and the development of

8

cardiac hypertrophy.

In vitro studies. The *in vitro* studies have clearly shown that thyroid hormone directly controls gene expression and cellular growth. Mouse heart organ culture studies have shown that T_3 increased the rate of protein synthesis, with no observed change in contractility (Crie et al. 1983). In addition, cultured fetal cat myocyte studies showed that thyroid hormone caused a shift in the content of myosin isozyme from V_3 to V_1 (Nag et al. 1984), an accumulation of a-MHC mRNA, and an inhibition of the expression of β-MHC mRNA.

Angiotensin-II:

In vivo studies. The direct cardiac actions of angiotensin-II are mediated by membrane receptors and are coupled to effector responses by G-proteins and include stimulation of cardiac contractility; acceleration of protein synthesis that results in cardiac hypertrophy; and activation of a membrane phospholipase with resultant increases in inositol-triphosphate (IP_3), diacylglycerol (DG), and protein kinase C activity (PKC) (Baker et al. 1988). The classic example in the involvement of the renin-angiotensin system in cardiac hypertrophy is experimentally produced by renovascular hypertension. However, in this model, the possible direct hypertrophic effects of angiotensin-II were not separated from indirect effects that are mediated through increases in blood pressure and vascular resistance.

In vitro studies. It has been clearly demonstrated, *in vitro*, that angiotensin-II has a direct effect on cardiac hypertrophy. In cultured embryonic chick myocytes, angiotensin-II induced cellular hypertrophy that was associated with an increased rate of protein synthesis (Aceto et al. 1990). Angiotensin-II stimulated rates of protein

9

synthesis and cardiomyocyte growth were not secondary to an angiotensin II-induced

increase in chronotropic activity, because the hypertrophic response was the same in

non-beating potassium chloride-depolarized cells (Baker and Aceto 1990a).

D. Paracrine And Autocrine Control In Cardiac Hypertrophy

Because of the difficulty of isolating and quantitatively delivering a specific stimulus

in vivo, most of studies of the paracrine and autocrine mechanisms have been carried

out in cultured myocyte models. Growing evidence has suggested that peptide-derived

growth factors, including fibroblast (FGF) (Parker et al. 1990), transforming growth

factor (TGF-β) and other factors (Sen et al. 1990), can activate features of myocardial

cell hypertrophy in the *in vitro* model. This indicates that the autocrine mechanism may

exist for the initiation of the hypertrophic response. Recent studies have shown that

a powerful vasoconstrictor, endothelin-1 (ET-1), is a potent stimulus for myocardial cell

hypertrophy in a cultured myocardial cell model (Shubeita et al. 1990). As ET-1 is

released from endothelial cells that lie immediately adjacent to the myocytes within the

intact myocardium, the activation of myocardial cell hypertrophy by ET-1 represents

a potentially important paracrine mechanism for the regulation of myocardial growth

and hypertrophy. The role of ET-1 in the regulation of ventricular function has been a

subject of speculation. The results of a recent study provide compelling evidence that

ET-1 can activate a hypertrophic response in cultured neonatal rat ventricular

myocardial cells, including the acquisition of several features of cardiac hypertrophy,

such as an increase in cell size, activation of IE gene expression, activation of

contractile protein gene expression, and the reactivation of a program of embryonic

gene expression (Shubeita et al. 1990).

(II). POSSIBLE MECHANISMS OF CARDIAC HYPERTROPHY

A. Mechanical Stimuli

Although the exact mechanisms coupling the extracellular stimuli to the intracellular hypertrophic response are unclear, accumulating data have indicated that mechanical stimuli can mediate intracellular signal transduction pathways, including Na^+, Ca^{2+}, cAMP, inositol phosphates (IPs) and H^+ (Fig 1). Muscle cell membranes as well as many other tissues contain mechanotransducer (stretch) ion channels that are either activated or inactivated by cell deformation (Morris 1990). Kent et al. (1989) reported that Na^+ uptake was increased in quiescent or contracting ferret papillary muscle as the load on the muscle was increased. The elevation of intracellular Na^+ levels can augment the rate of RNA and protein synthesis in this preparation. The addition of streptomycin, a cationic blocker of mechanotransducer ion channels, had no effect on protein synthesis in slack muscles, but inhibited the faster rate of protein synthesis observed in stretched muscles. These data indicated that increased intracellular Na^+ levels due to muscle stretch are involved in the hypertrophic responses.

Because changes in intracellular Ca^{2+} levels accompany alterations in the contractile state of the myocardium, it has long been considered that alterations in intracellular Ca^{2+} might represent a logical stimulus for coupling changes in contractility with alterations in cardiac metabolism and gene expression during the imposition of a mechanical stimulus such as pressure or volume overload (Mochly-Rosen et al. 1990). A recent study using cultures of electrically stimulated neonatal rat ventricular myocytes showed that gene expression (ANF, MLC-2), cellular size and myofibrillar

organization dramatically depend on cytoplasmic free Ca^{2+} levels and calmodulin activity (McDonough et al. 1992). One of the possible mechanisms of elevated intracellular Ca^{2+} initiating cardiac hypertrophy may be the activation of Ca^{2+}-dependent calmodulin kinase (CaMK) complex. Activated CaMK can phosphorylate the trans-acting transcriptional activator, cAMP-response element-binding protein (CREB). Although CREB was originally shown to be regulated through cAMP-dependent protein kinase-mediated phosphorylation, it has recently been shown that CREB could be phosphorylated by CaMK (Sheng et al. 1991). Such phosphorylation appears to enhance the ability of CREB to activate transcription.

There is also evidence that an increase in pH_i is a necessary signal for the initiation of growth and development in many cell types. Regulation of pH_i is in large part controlled by Na-H exchanger (Moolenaar 1986). Recently published studies showed that a strong correlation exists between shape-dependent alkalination of capillary endothelial cells and increases in DNA synthesis as the result of cell-deformation (Ingber et al. 1990). Treatment of cells with a 5-amino derivative of amiloride, which has a selectivity for inhibiting the Na-H exchanger, prevented or reversed the increase in DNA synthesis associated with cell-deformation. These data indicate that cell deformation or stretch, results in cytoplasmic alkalinization (Schwartz et al. 1989, 1990) via activating Na-H exchanger, and modifies the rates of macromolecular synthesis.

Cellular deformation can directly stimulate cAMP accumulation (Watson 1989a). Singh (1982) reported that mechanical stretch of the isolated frog ventricle elicited a rapid rise in cAMP content. Increased cAMP content has been associated with an accelerated protein synthesis, ribosome formation and increased cAMP-dependent
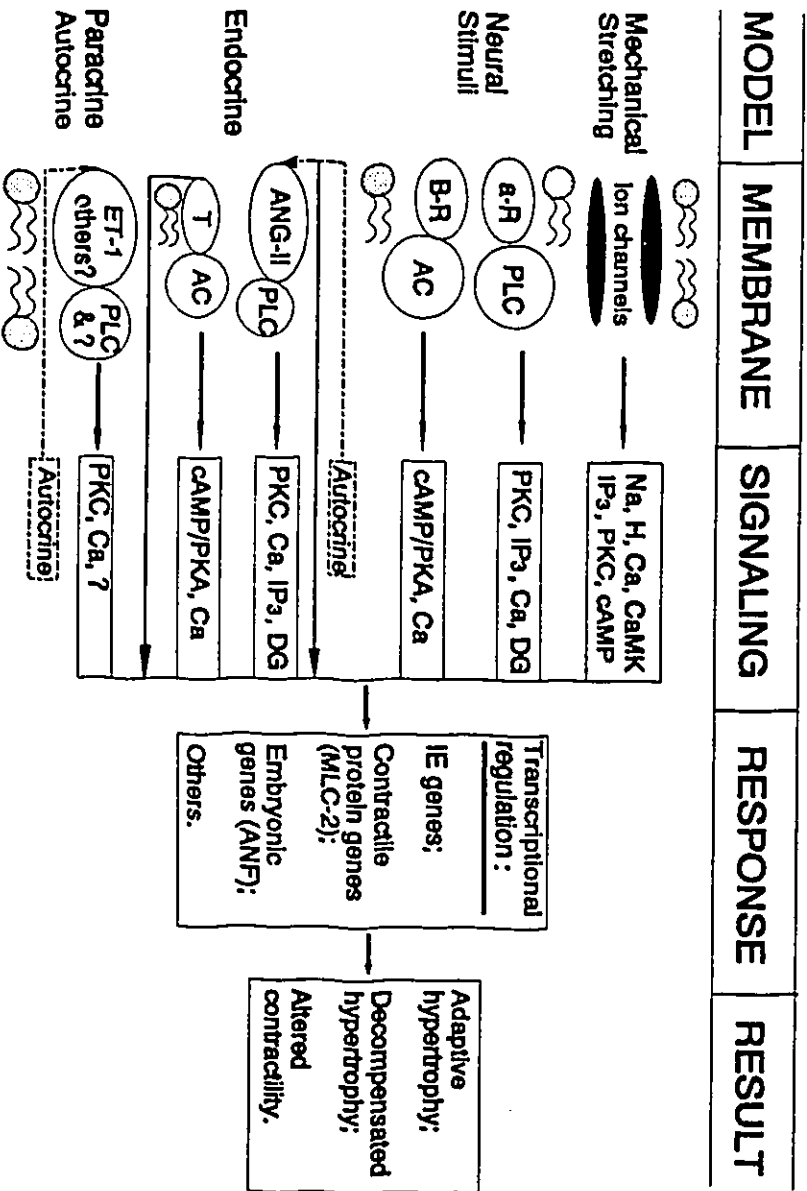
Figure 1. Possible pathways coupling stimuli to cardiac hypertrophy.

protein kinase activity in response to an elevation in aortic pressure in either beating or tetrodotoxin-arrested hearts (Watson et al. 1989b).

As currently understood, the phosphotidylinositol turnover pathway involves receptor stimulation of a phospholipase C (PLC), which selectively cleaves a plasma membrane lipid (PIP_2) and generates two biologically active intracellular messengers, DG and IP_3. DG stimulates PKC, and IP_3 can induce Ca^{2+} release from the SR. It has been reported that myocardial stretch can activate the phosphatidylinositol (PI) turnover pathway and result in the accumulation of inositol phosphate (IP), inositol biphosphate (IP_2) and IP_3 in isolated, perfused rat heart (Harsdorf et al. 1989). The activation of the PIP_2-IP_3-Ca^{2+} pathway or the DG-PKC pathway may have an important role in the development of cardiac hypertrophy (Shoki et al. 1992, Kawaguchi et al. 1993).

B. Neural Stimuli

Potential intracellular transducers involved in a_1-adrenergic-mediated hypertrophy in the heart include IP_3 and DG. DG activates PKC, which is an important mediator for the activation of cardiac hypertrophic response. Some experiments have shown that phorbol esters, which directly activate PKC, can lead to the development of several features of myocardial cell hypertrophy (Yang et al. 1989). These features include the activation of embryonic gene transcription (ANF), the accumulation and assembly of an individual contractile protein (MLC-2) into an organized sarcomeric unit, as well as the induction of a program of IE genes (c-fos, Egr-1) that have been implicated in the control of gene expression during growth factor stimulation (Buxton et al. 1986, Yang et al. 1989).

14

Overall, a_1-agonists stimulate cellular hypertrophic responses, and the signalling pathways appear to involve PLC, DG, and PKC. An increase in pH, due to activation of H-Na exchange via PKC may also be an important component in the growth response to a_1-adrenergic stimulation (Watson 1990).

The mechanisms of β-adrenoceptor-mediated tissue growth and hypertrophy are through the production of cytoplasmic cAMP via adenylate cyclase (AC) pathway (Fig 3). As discussed in the section on models, there are data to support a role for stretch-induced activation of AC and cAMP-dependent protein kinase in the regulation of protein synthesis and ribosome formation in isolated heart. The phosphorylation of some transcription factors (AP-2, CREB, etc) by cAMP-dependent protein kinase A (PKA), which is at the receiving end of a complex pathway responsible for transmitting the stimuli from the cell membrane to the transcriptional machinery, is involved in the regulation of gene transcription (Karin 1992).

C. Hormonal Stimuli

Thyroid hormone could act through changes in the tissue content of intracellular signalling compounds, such as cAMP, Ca^{2+}, or directly on gene transcription via nuclear thyroid hormone receptors (Fig 1)(Zimmer et al. 1986). The possible mechanisms by which increased cAMP and Ca^{2+} could contribute to cardiac hypertrophy were discussed above. The thyroid hormone receptor, which is located in the nucleus, is part of a family of ligand-dependent transcriptional factors. Members of this family activate transcription by binding of the hormone-receptor complex to specific DNA sequences on target genes (Gustafson et al. 1987). In cardiac tissue, thyroid hormone can act as either a positive (a-MHC) or negative (β-MHC) regulator of

transcription.

Angiotensin-II can directly induce structural changes in chromatin. Nuclear localization of angiotensin-II may be similar to that of thyroid hormone where angiotensin-II receptor internalization interacts with the regulatory site on DNA. Angiotensin-II receptor-mediated increase in DG and resultant translocation of PKC could also contribute to the effects of this peptide on cardiomyocyte growth (Tsuda et al. 1990). The autocrine and paracrine factors may also be involved in the regulation of angiotension-II on cardiac hypertrophy, since the intra-cardiac expression of renin, angiotensin I and angiotensin-II have all been detected (Re et al. 1983). Upregulation of left ventricular angiotensin mRNA has been described in association with pressure-overload cardiac hypertrophy, suggesting that an intra-localized renin-angiotensin system may be activated in this experimental model of hypertension (Baker et al. 1990b).

II. CARDIAC EXCITATION-CONTRACTION COUPLING

Figure 2 is an illustration of the current view of excitation-contraction (E-C) coupling in cardiac muscle and the ionic current movements associated with a typical action potential. The release and reuptake of sarcoplasmic reticulum Ca^{2+} is central to the normal systolic and diastolic function of the mammalian heart. There are two major Ca^{2+} dependent mechanisms that alter the contractile state of the heart: changing the availability of Ca^{2+} to the myofilaments, and changing the responsiveness of the myofilaments to activation by $[Ca^{2+}]_i$. The availability of $[Ca^{2+}]_i$ is mainly regulated by

the sarcolemma (SL) and the sarcoplasmic reticulum (SR) , while Ca^{2+} responsiveness is controlled by the myofilaments and the regulatory troponin complex.

The regulation of $[Ca^{2+}]_i$ concentration is critical in maintaining normal systolic and diastolic function. Because the background or resting concentration of $[Ca^{2+}]_i$ is normally quite low in cardiac muscle cells and is about $75 \sim 200$ nM, even a small change in absolute $[Ca^{2+}]_i$ can be associated with large Ca^{2+} dependent responses. Calcium homeostasis is maintained by the following mechanisms: (1) voltage-dependent Ca^{2+} channels that mediate Ca^{2+} entry from the extracellular space; (2) the SR, which can release Ca^{2+} into cytosol by the SR Ca^{2+} release channels during cell activation and resequesters Ca^{2+} by a ATP-driven Ca-pump during relaxation; (3) sarcolemmal ATP-driven Ca-pump that extrudes cytosolic Ca^{2+} across the sarcolemma; (4) Na-Ca exchange that can move Ca^{2+} either into or out of the cytosol across the sarcolemma, depending on the prevailing Na^+ electro-chemical gradient; (5) cytoplasmic Ca^{2+} buffering systems, such as troponin-C, calmodulin, ATP, phosphocreatine, outer mitochondrial membrane, outer SR and inner sarcolemma; and (6) mitochondria, which can also sequester Ca^{2+} by a ATP-driven transport mechanism and can release Ca^{2+} by a Na^+-dependent (Na-Ca exchange) mechanism.

Cardiac E-C coupling is initiated when the action potential permits Ca^{2+} to enter the myoplasm through voltage-dependent Ca^{2+} channels (I_{ca}) in the sarcolemma (Fig 2). The influx of Ca^{2+} triggers Ca^{2+} release from the SR. Both the released Ca^{2+} from the SR and a fraction of influx Ca^{2+} (depending on animal species) interact with troponin C, which is part of the regulatory complex on the myofilaments, to produce a conformational change that allows actin and myosin to interact and form cross-bridges. Relaxation occurs when Ca^{2+} dissociates from the contractile apparatus and is

17
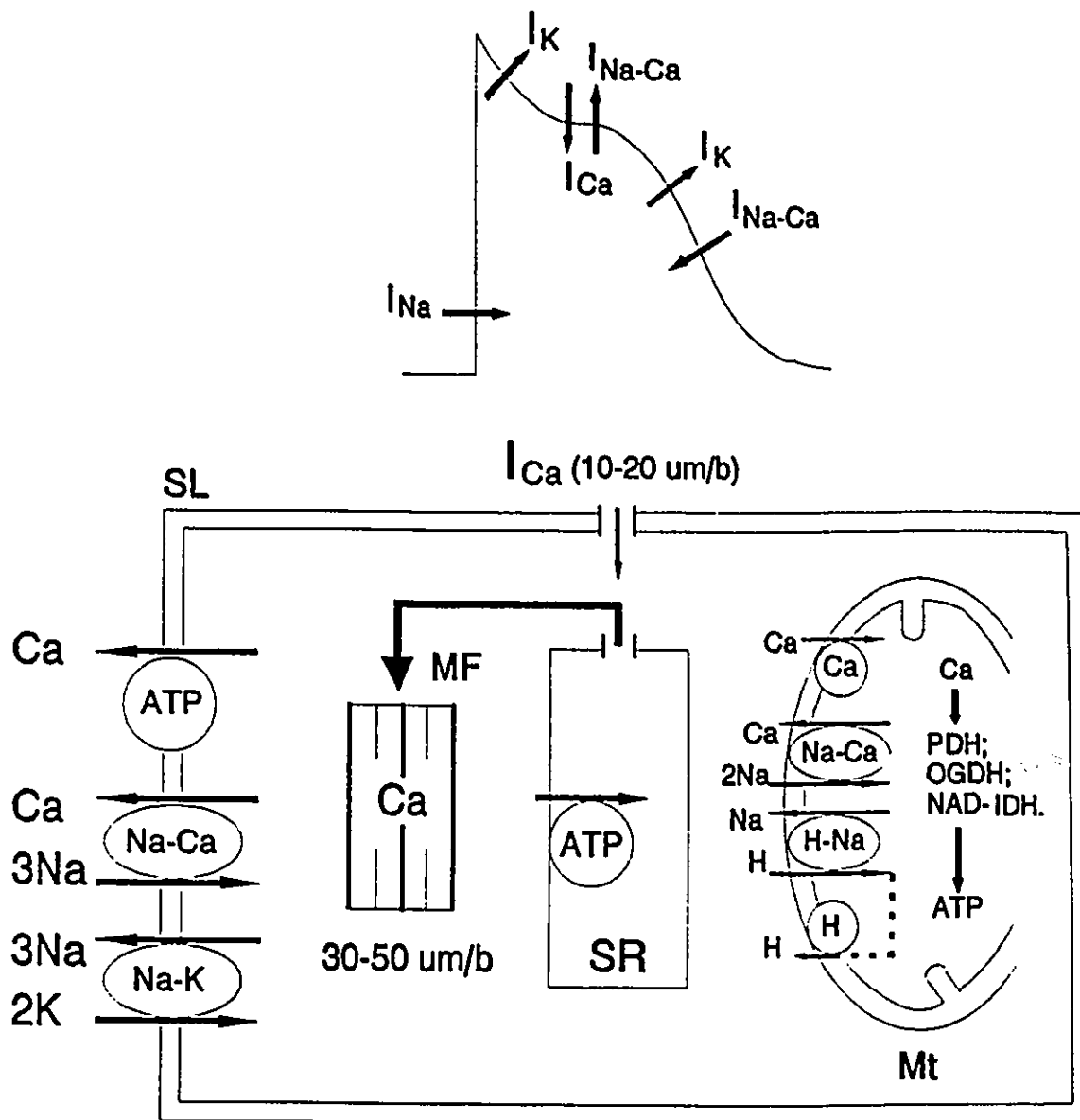
Figure 2. Model of cardiac E-C coupling (lower panel) . SL, sarcolemma. SR, sarcoplasmic reticulum. MF, myofilament. Mt, mitochondria. PDH, pyruvate dehydrogenase. OGDH, oxoglutarate dehydrogenase. NAD-IDH, NAD-linked isocritrate dehydrogenase. um/b, micromolar calcium per beat. Upper panel represents ionic currents consisting of a typical action potential. I_{Na}, fast inward sodium current. I_{K}, potassium current. I_{Ca}, L-type calcium current. The direction of the arrows for I_{Na-Ca} (Na-Ca exchange current) indicates the Na^{+} flow.

removed from the cytosol. A variable fraction of cytosolic Ca^{2+} is resequestered by the ATP-driven Ca^{2+} pump of the SR and the rest is extruded via Na-Ca exchange in the sarcolemma. The initial excitatory event of membrane depolarization is also associated with the entry of Na^+ into cells; the Na^+ is ultimately extruded by the energy-dependent Na-K pump or by the reversed Na-Ca exchange, which operates on the basis of concentration gradients.

(I). SARCOLEMMAL CALCIUM CHANNELS

A. Classification And Distribution Of Ca^{2+} Channels

Two classes of Ca^{2+} channels in the sarcolemma of cardiac cells , the T (Transient) and L (Long-lasting), were demonstrated first by Hagiwara et al. (1975). The relatively new technique of patch clamping of small cell membrane areas has been used to study the Ca^{2+} channels and their response to drugs. Based on differences in single channel conductance, inactivation kinetics, pharmacology and voltage dependence, Nowychy et al. (1985) characterized these Ca^{2+} channels and gave the nomenclature which has been generally adopted at the present time. T-type channels are characterized by a tiny conductance, transient openings, insensitivity to the family of 1,4-dihydropyridine (DHP) and activation at more negative membrane potentials. Normally, these T channels are depolarized at potentials more negative than -50 to -60 mv, peak at approximately -30 mv, and inactivation with time constants of 5 ~ 30 ms. L-type Ca^{2+} channels are characterized by a large conductance, long lasting openings, sensitivity to DHP. L channels activate at -40 to -30 mv, inactivate more slowly than

T channels, and carry three- to four-fold the Ca^{2+} current (Sperelakis 1988). The values for the conductance of L-type Ca^{2+} channel usually range between 5 and 25 pS (pico-Siemens). The T channels appear to be quite prominent in certain atrial cells and Purkinje cells (Bean 1985, Hirano et al. 1989), but are less prominent in most ventricular cells. The functional significance of the T channels is not known, though they might be involved in pacemaker activity (Hagiwara et al. 1988). The L-type Ca^{2+} channel appears to be the major pathway for Ca^{2+} entrying the ventricular myocyte during excitation for initiation and regulation of contractile force (Sperelakis 1988).

B. Regulatory Pathways Of L-type Ca^{2+} Channels

Accumulating results have implied that the cAMP plays a key role in the regulation of Ca^{2+} channel current in response to β-adrenergic agonists (Sperelakis 1984, Sperelakis et al. 1976). At present, the biochemical pathway for the regulation of the L-type Ca^{2+} channel has been clarified. The occupation of β-adrenergic receptor by sympathetic neurotransmitters leads to the activation of Gs proteins (stimulatory GTP-binding proteins) which, in turn, activate adenylate cyclase (AC) with a resultant elevation of cAMP levels (Fig 3). The cAMP activates cAMP-dependent protein kinase A (PKA) and PKA results in phosphorylation of the L-type Ca^{2+} channel by the catalytic subunit of cAMP-dependent PKA (Sperelakis 1988). In this model, the Gs protein can exert a direct effect on L-type Ca^{2+} channel current. This regulation is at the very least membrane delimited and independent of any changes in cytoplasmic levels of second messages such as the well established cAMP-dependent pathway and is very likely due to some type of direct interaction of the Gs protein (α-subunit) with the channel proteins. It has been suggested that a direct Gs effect may regulate basal channel

20

availability and that the cAMP-dependent phosphorylation effects modulate activity above the basal level (Homcy et al. 1991). The effects of β-adrenergic agonist on the characteristics of Ca^{2+} current have been demonstrated by Reuter et al. (1982, 1983). In patch clamp experiments on a single L-type Ca^{2+} channel in cultured neonatal rat heart cells, isoproterenol lengthened the mean open time of the channel and decreased the intervals between bursts. The conductance of the single channel was not increased by isoproterenol. Therefore, the increase in the total maximal slow conductance produced by isoproterenol could be produced by the observed increase in mean open time of each channel, as well as by an increase in the number of channels participating in the conductance.

The parasympathetic neurotransmitter, acetylcholine (ACH), binds to the muscarinic receptors which inhibit the catalytic subunits of AC via the G_i (inhibitory GTP-binding protein) coupling protein and thus cAMP level. ACH depresses Ca^{2+} current and contraction not only by reversing cAMP elevation produced by β-adrenergic agonists, but also by elevating cGMP pathway (Reuter 1983).

The L-type Ca^{2+} channel currents can be blocked by the organic Ca^{2+}-antagonistic drugs, such as nifedipine, and inorganic ions such as Mn^{2+}, Co^{2+}, La^{3+}. The general order of potency of the Ca^{2+}-antagonistic drugs in blocking the L-type Ca^{2+} channels of various heart tissues is nifedipine $>$ diltiazem $>$ verapamil $>$ bepridil (Li et al. 1983). The effect of most of the Ca^{2+}-antagonistic drugs on depression of the Ca^{2+} current is frequency dependent: the higher the frequency of the stimulation, the greater the blocking effect on the Ca^{2+} current. However, nifedipine and other dihydropyridines have less of a frequency dependence than other drugs of this class (Sperelakis 1988). Inorganic Ca^{2+} entry blockers, such as Mn^{2+}, Co^{2+} and La^{3+}, do not exhibit a
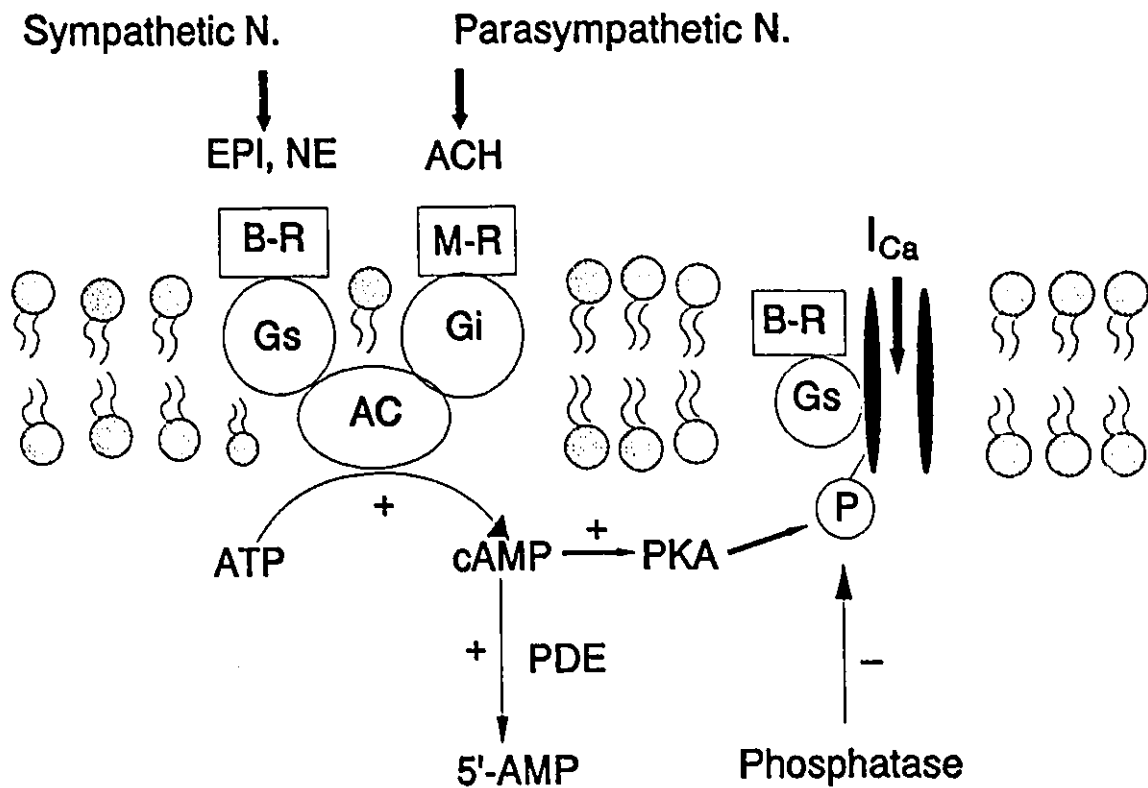
Figure 3. The regulatory pathways of the L-type Ca^{2+} channel via sympathetic and parasympathetic nervous system. EPI, epinephrine. NE, norepinephrine. ACH, acetylcholine. β-R, beta receptor. M-R, muscarinic receptor. I_{Ca}, Ca^{2+} current. G_i and G_s, respectively, indicates inhibitory and stimulatory G protein. AC, adenylate cyclase. PDE, phosphodiesterase. PKA, protein kinase A.

frequency dependence (Sperelakis 1988). It has been suggested that such compounds act to stabilize a specific channel conformation state (Hess et al. 1984).

The L-type Ca^{2+} channels also have some special properties, including functional dependence on metabolic energy, selective blockade by acidosis, and regulation by the

intracellular cyclic nucleotide levels (Irisawa et al. 1983, Vogel et al. 1977, Sperelakis 1988). Blockage of the Ca^{2+} channels may occur with acidification of the outer or inner surfaces of the cell membrane. Because of these special properties of the L-type Ca^{2+} channels, Ca^{2+} influx into the myocardial cell can be controlled by extrinsic factors such as autonomic nerve stimulation or circulating hormones and by intrinsic factors such as cellular pH or ATP levels.

In the pressure-overload hypertrophied heart, a down-regulation to the β-adrenergic stimuli has been found. In myocytes isolated from aortic constricted rats, β-adrenergic receptor stimulated Ca^{2+} current was reduced compared to cells from control hearts, and this difference was abolished by inclusion of cAMP within the patch electrode (Scamps et al. 1990). Radioligand binding assays also indicate a decreased β-receptor density and a reduction in high-affinity sites in pressure overload hypertrophied heart (Mansier et al. 1989). The contractile response to forskolin was also depressed in this model, suggesting that at least in part, changes in mechanisms distal to the β-receptor also occur (Mansier et al. 1989). The down-regulation to the β-adrenergic stimuli also occurs in severely hypertrophied hearts induced by isoproterenol (Tse et al. 1979). The total number of Ca^{2+} channels per left ventricle estimated from radioactive DHP labelling increase proportionally to the degree of hypertrophy (Mayou et al. 1988). However, the density of the Ca^{2+} channels remained constant during the hypertrophic process. The activity of these channels in pressure-overload hypertrophy, measured by patch clamp studies (Scamps et al. 1990), clearly indicated that the intensity (peak current) of the Ca^{2+} current per cell was increased, but the density normalized per unit membrane surface area remained unchanged, suggesting that the quantity of functional Ca^{2+} channels also increased with the degree of hypertrophy.

23

C. The Amount Of Ca^{2+} Influx Via L-Type Ca^{2+} Channels

In most animal species the $[Ca^{2+}]_o$ ranges from $2-5$ mM, while the resting free $[Ca^{2+}]_i$ is about $75-200$ nM (Blinks 1986). The sarcolemma maintains a Ca^{2+} gradient of about 15,000 between $[Ca^{2+}]_i$ and $[Ca^{2+}]_o$. A transient increase in cytosolic free Ca^{2+} from a level of $75-200$ nM to about $0.5-3$ uM will result in cardiac contraction (Blinks 1986). Based on the values assumed by Fabiato (1983), these cytosolic free Ca^{2+} concentrations of $0.5-3$ uM correspond to total Ca^{2+} (including the bound Ca^{2+}) of $15-50$ umol/kg wet wt, which can activate $5-70\%$ of maximum force development. Langer (1992) estimated that transsarcolemmal Ca^{2+} entry measured using isotopes, Ca^{2+}-sensitive electrodes or flourescent dyes, contributes about $15-20$ umol/kg wet wt/beat. These values are similar to those reported by Bers (1983) in which Ca^{2+} entry, based on extracellular Ca^{2+} depletions and voltage clamp analysis, was in the range of $10-18$ umol/kg wet wt/beat. According to Fabiato's estimates of intracellular Ca^{2+} buffering (1983), this would only be sufficient to raise $[Ca^{2+}]_i$ from ~ 125 nM to ~ 500 nM and activate only about $4-5\%$ of maximal force. Thus, it would seem that Ca^{2+} entry via sarcolemmal Ca^{2+} channels would not normally be sufficient to fully activate cardiac muscle contraction.

(II). SARCOLEMMAL Na-Ca EXCHANGE

The notion that external Na^+ apparently antagonized the delivery of Ca^{2+} to the contractile apparatus was verified by tracer flux studies of Niedergerke (1956). He showed that frog ventricular tissue gained Ca^{2+} when external Na^+ was reduced;

indeed, the gain in Ca^{2+} could be correlated with the increase in contractile force as external Na^+ was progressively reduced. However, the first direct evidence for a counterflow exchange of Na^+ for Ca^{2+} was obtained with tracer flux measurements in mammalian heart by Reuter and Seitz (1968). It is now accepted that this sarcolemmal Na-Ca exchange system can apparently operate in any one of the several (models): (a) "forward-mode", in which the $[Na^+]_o$ influx is in exchange with $[Ca^{2+}]_i$ efflux; (b) "reverse-mode", meaning that Na^+ efflux from cytosol exchanges the Ca^{2+} influx from extracellular space; (c) "$[Ca^{2+}]_i$-$[Ca^{2+}]_o$ exchange mode", in which the Na-Ca transport system could also operate in self-exchange mode as confirmed by tracer studies, but it is not important in physiological condition (Sheu et al. 1986). These models show that the Na-Ca exchange can move Ca^{2+} in either direction across the sarcolemma in exchange for Na^+. The direction of net Ca^{2+} movement appears to depend on the prevailing Na^+ electrochemical gradient. Bridge et al. (1990), using voltage-clamp procedures and rapid solution changes in isolated ventricular cells, have demonstrated that all Ca^{2+} entering the cell via Ca^{2+} channels could be removed via Na-Ca exchange during the course of a contraction cycle. The exchange operated predominantly in the Ca^{2+} efflux mode, however, relatively small increases in $[Na^+]_i$ can cause a reversal of the next Ca^{2+} flux. Extracellular Na^+-dependent Ca^{2+} efflux using inside-out vesicles shows a steep dependence on Na^+ concentration between 8 and 12 mM (Philipson et al. 1982). This range is reasonable for $[Na^+]_i$ during physiological and pharmacological interventions in the intact cell. Because it is widely reported that the inhibition of sarcolemmal Na-K-ATPase by digitalis glycosides results in elevation of $[Na^+]_i$ and produces a significant increase in contractile force (Cohn et al. 1982, Lee et al. 1980, Bers 1987), the energy required to move Ca^{2+} out of the cell

against a large electrochemical gradient via Na-Ca exchange could be provided by the downhill movement of Na$^+$ into the cells. The Na$^+$ electrochemical gradient, in turn, would be maintained by the ATP-dependent Na-K-pump (Kaplan 1985).

The stoichiometry of Na-Ca exchange is very close to 3Na$^+$ to 1Ca^{2+} in cardiac muscle (Fig 2). This Na-Ca exchange with a stoichiometry of 3 Na$^+$ to 1 Ca^{2+} has important implications for cardiac muscle. Under these circumstances, each exchange cycle will result in net transfer of charge across the membrane; that is, the exchange will be electrogenic and may thus make a contribution to the membrane potential (Langer 1992). The exchange may also be influenced by the electric field across the membrane and thus may be voltage-dependent. Mullins (1979) suggested that Na-Ca exchange may contribute significantly to the current carried during the cardiac action potential. When the cells depolarize and the transmembrane Na$^+$ electrochemical gradient is reduced, Ca^{2+} will be driven into the cells via the exchange; conversely, when the cells repolarize, and the transmembrane Na$^+$ electrochemical gradient increases greatly, the exchange should move Ca^{2+} out, therefore helping to restore the resting Ca^{2+} gradient.

Leblanc and Hume (1990) have recently proposed that a transient rise in [Na$^+$]$_i$ occurs in the diffusion-restricted region near the intracellular opening of the Na$^+$ channel during depolarization. This increase would cause a transient net influx of Ca^{2+} in the region of the SR "feet" through reversal of the Na-Ca exchange, producing Ca^{2+}-induced Ca^{2+} release and contractile activation. However, Sham et al. (1992) demonstrated that the Na-Ca exchange does not initiate Ca^{2+} release and only the Ca^{2+} channel gates the fast release of Ca^{2+} from the SR in the range of the action potential. In intact rabbit ventricular muscle, Bers et al. (1988) showed that Ca^{2+} entry

via Na-Ca exchange does not normally contribute significantly to the activation of contraction, but can if $[Na^+]_i$ is elevated (e.g. to $15 \sim 20$ mM).

Rich and Langer (1991) have reported that the flux rates of Na-Ca exchange are about 100 umol/kg wet wt/sec and the exchange can easily maintain $[Ca^{2+}]_i$ at a steady state at heart rates greater than 200 beats/min. By using patch-clamp, I_{Na-Ca} of 300 pA have been recorded in mammalian ventricular myocytes and this also corresponds to about 100 umol/kg wet wt/sec (Bers 1991a). The 300 pA I_{Na-Ca} is $10 \sim 30\%$ of the peak $[Ca^{2+}]_i$ transient in ventricular myocytes under normal circumstances and the Na-Ca exchange does not inactivate rapidly as does the Ca^{2+} channel current. Thus, it is becoming clear that Na-Ca exchange can contribute importantly to Ca^{2+} flux during the cardiac cycle. It is consistent with the notion that the Na-Ca exchange is the main means by which about $20 \sim 30\%$ of the Ca^{2+} is extruded from the cell, during relaxation and the remaining portion ($70 \sim 80\%$) is removed by the SR Ca-ATPase pump.

(III). SARCOLEMMAL Ca-ATPase PUMP

In addition to the importance of Na-Ca exchange, another mechanism responsible for $[Ca^{2+}]_i$ extrusion from myocytes is the sarcolemmal Ca-ATPase pump. This ATP dependent pump was first identified in heart sarcolemma by Caroni and Carofoli (1980). The purified SL Ca-ATPase pump can transport Ca^{2+} with a 1:1 stoichiometry to ATP (Niggli et al. 1981). This is 50% less efficient than the SR Ca-ATPase pump which operates at $2Ca^{2+}$ per ATP hydrolysed. Ca^{2+} extrusion by this pump appears

coupled to H^+ influx with a ratio of $1Ca^{2+}:1H^+$ (Kuyayama 1988), however, it is not yet clear whether the exchange is electroneutral or partially electrogenic. The maximal rate at which Ca^{2+} might be extruded from cardiac myocytes by this pump has been estimated to be 2.4 umol/kg wt wet/sec (Bers 1991a). If relaxation of cardiac muscle were solely dependent on the sarcolemmal Ca-pump, it would take 20~40 seconds for complete relaxation at maximal ATPase activity (Bers 1991a). Thus, this transport rate may be too slow to be important to Ca^{2+} efflux during the cardiac cycle. By comparison, it is probable that the rapid, high-capacity Na-Ca exchange is the system responsible for maintenance of beat-to-beat steady-state cellular Ca^{2+} levels.

(IV). MITOCHONDRIA

It has long been recognized that mitochondria can transport Ca^{2+} and account for approximately 20% of total cellular Ca^{2+} content (Walsh et al. 1988). Ca^{2+} enters the mitochondria via a uniport system down a large electrochemical gradient (Fig 2). The inner membrane potential of mitochondria is about -180 mV and promotes the charge influx, which is compensated for by the extrusion of two protons by the H^+-pump of the electron transport chain (Crompton 1985). Ca^{2+} entry via the uniporter exhibits a sigmoid dependence on $[Ca^{2+}]_i$ and has a $K_m > 30$ uM for $[Ca^{2+}]_i$ (Crompton 1985). Thus, if the $[Ca^{2+}]_i$ associated with the cardiac cycle is approximately 0.5~3 uM, the influx pathway will be at a relatively low level.

Ca^{2+} extrusion from the mitochondria is via a mitochondrial Na-Ca exchange system with a stoichiometry of $2Na^+$ influx to $1Ca^{2+}$ efflux (Fig 2) that seems to operate as

28

an electroneutral system (Crompton et al. 1976), in contrast to the sarcolemmal system, which is clearly electrogenic. The $[Na^+]_i$ dependence of this Na-Ca exchange (antiporter) is quite sensitive to a change of $[Na^+]_i$ in the physiological range with half-maximal Ca^{2+} extrusion at $5 \sim 8$ mM $[Na^+]_i$ (Fry et al. 1984). The inner mitochondrial membrane also has an active Na-H exchange system which can extrude the Na^+ from the matrix and associate with the H^+ influx. The intramitochondrial protons can be pumped out of the mitochondria during respiration and thus maintain the negative intramitochondrial potential.

Although there is a potentially enormous capacity for mitochondrial Ca^{2+} storage and transport, it is now accepted that mitochondrial Ca^{2+} transport is not a primary pathway in E-C coupling. It seems that Ca^{2+} transport is directed toward regulation of the various intramitochondrial enzymes responsible for control of oxidative metabolism (Denton et al. 1980).

To demonstrate the regulatory role of mitochondria in cytoplasmic Ca^{2+}, Crompton (1990) modeled quasi-steady-state behaviour of the rat heart mitochondrial Ca^{2+} transport cycle. He found that intramitochondrial Ca^{2+} does not fluctuate as much as cytosolic Ca^{2+} which oscillates between 0.2 and 2 uM with each beat. In intact cardiac muscle, Bers and Bridge (1989) showed that when the SR Ca^{2+} uptake and sarcolemmal Na-Ca exchange were inhibited, relaxation was slowed by more than an order of magnitude and was often incomplete. Thus, it is likely that mitochondria play a very minor role in Ca^{2+} movements during contraction and relaxation.

(V). SARCOPLASMIC RETICULUM

A. Ultrastructural Consideration Of The SR

The SR is an entirely intracellular, membrane bounded compartment which is not continuous with the sarcolemma. The main function of this organelle in muscle appears to be sequestration and release of Ca^{2+} to the myoplasm. Electron microscopic studies have shown that the continuous sealed network structure of the SR consists of two distinct components: (1) longitudinal SR that surrounds the myofilaments, and (2) junctional SR, the portion that comes into close apposition to the sarcolemma either at the level of the transverse (T) tubules to form diads or triads, which are called terminal cisternae.

The longitudinal SR membrane is fairly homogeneous and mainly contains the SR Ca-ATPase pump protein (Kaze et al. 1986) which is revealed as intramembrane particles ~8 nm in diameter with a density of 3000~5000 particles/um² of SR membrane. The longitudinal SR is generally regarded as being involved in Ca^{2+} uptake from the cytosol during relaxation. The maximum turnover rate for cardiac SR Ca-ATPase estimated from data of Levitsky et al. (1981) in guinea pig is about 10~15 Ca^{2+} ions/pump site/second. Shigekawa et al. (1976) estimated that the active, ATP-dependent rate of Ca^{2+} pumping by canine cardiac SR is about 16~20 Ca^{2+}/pump site/second. The major part of the terminal cisternae also appears to have a Ca-ATPase pump. Thus, the vast majority of the SR surface is likely to function primarily in removing Ca^{2+} from the cytoplasm.

The junction of the SR with the sarcolemma is highly specialized and contains spanning proteins which have been called "feet" by Franzini-Armstrong (1970). These

feet, which are located in the terminal cisternae of the SR, have been identified as the high affinity binding sites for ryanodine (a neutral plant alkaloid) and called the SR Ca^{2+} release channel in cardiac muscle (Caldwell et al. 1982, Lai et al. 1988). In mammalian ventricular muscle, the majority of L-type channels are located in the T-tubules that form the junctional complexes with these feet (no physical contact, but in a distance less than 100 nm) (Stern et al. 1992). A stoichiometry of one L-type Ca^{2+} channel (DHP receptor) to nine SR Ca^{2+}-release channels has been reported (Wibo et al. 1991). On the basis of this ultrastructural evidence, Stern and Lakatta (1992) proposed that Ca^{2+} from a single sarcolemmal Ca^{2+} channel triggers release from a cluster of SR Ca^{2+} release channels, producing a locally regenerative Ca^{2+}-induced Ca^{2+} release.

In addition, the interior of the SR contains a low affinity, high capacity Ca^{2+} binding protein, calsequestrin, located predominantly in the terminal cisternae of the SR (Meissner 1975). This protein may be important in increasing Ca^{2+} buffering capacity of the SR. It has been estimated that the intra-SR Ca^{2+} is 9 ~ 14 mM and the free Ca^{2+} in the SR is only 1 mM, in other words, most of the intra-SR Ca^{2+} is bound (Bers 1991a).

B. The Dependence Of Force On SR Ca^{2+} Release

The contraction of individual myocytes is triggered by a transient increase in cytosolic free Ca^{2+}, which follows the depolarization of the sarcolemma. In mammalian cardiac muscle, a predominant fraction of the free Ca^{2+} is released from cytosolic Ca^{2+} stores in the SR. In muscle physiology, there is a recurring theme that skeletal muscle contraction depends critically and almost exclusively on Ca^{2+} released from the SR with quantitatively insignificant Ca^{2+} entry across the sarcolemma during

a normal twitch (Armstrong et al. 1972). Cardiac muscle contraction, on the other hand, depends on both Ca^{2+} entry across the sarcolemma and Ca^{2+} release from the SR (Rich et al. 1988). The relative importance of the SR Ca^{2+} release may vary in different animal species. Bers (1991b) gave a rough sequencing of cardiac muscle preparations from most to least dependence on the SR Ca^{2+} release in different animal species : adult rat V > dog V and ferret V > cat V > rabbit V and guinea pig V > frog V (V = ventricle). The different dependence of contraction on the SR Ca^{2+} between rat and rabbit ventricle was demonstrated by using ryanodine (depletion of SR Ca^{2+}) that decreased force in rat by 90% whereas in the rabbit, force was diminished by less than 10% (Rich et al. 1988). In guinea pig ventricle, full contractile force was maintained in the presence of ryanodine but the contraction was prolonged by 50% (Lewartowski et al. 1990). This indicates that one important function of the SR with its ability to amplify intracellular Ca^{2+} via Ca^{2+}-induced Ca^{2+} release was to increase the velocity of contraction (Langer 1992).

C. The Mechanism Of SR-Ca^{2+} Release

The cardiac muscle of all species, in contrast to skeletal muscle, has an absolute requirement for $[Ca^{2+}]_o$ in order to contract. If $[Ca^{2+}]_o$ is rapidly removed from around the cell, even within a single beat, there is no Ca^{2+} transient and therefore no contraction (Nabauer et al. 1990, Armstrong et al. 1972, Rich et al. 1988). This has strongly supported the early hypothesis of Ca^{2+} induced Ca^{2+} release (CICR) (Endo 1977), which holds that Ca^{2+} influx through the sarcolemma, in response to depolarization, triggers the release of additional Ca^{2+} from the SR. However, Leblanc et al. (1990) have proposed that a rapid rise in intracellular Na^+ during membrane

depolarization is sufficient to induce Ca^{2+} entry via the Na-Ca exchange and promotes CICR. At the present time, this hypothesis is not widely accepted (Stern et al. 1992) because the increase in bulk cytosolic Na^+ during a single depolarization is very small, and would require a confined space for coupling the sarcolemmal Na^+ influx to the Na-Ca exchanger. In an elegant series of studies, Fabiato (1985a,b,c) has extensively characterized CICR in mechanically skinned single cardiac myocytes. A remarkable feature of CICR is that the amount of Ca^{2+} released is graded with the amount of trigger Ca^{2+} (Fabiato 1985b). At higher trigger Ca^{2+} the amplitude of Ca^{2+} released by the SR is inhibited or inactivated. The CICR also appears to depend on the rate at which the Ca^{2+} changes around the SR with an increase in Ca^{2+} release at higher rate. CICR exhibits a refractory period where a second Ca^{2+} release could not be induced (Fabiato 1985b). To fit these results, Fabiato (1985b) proposed a model with two types of Ca^{2+} binding sites where the CICR occurs through a channel with time- and Ca^{2+}-dependent activation and inactivation. Ca^{2+} binds to an activating site with a high rate constant but low affinity and also binds to a second inactivating site which has a high affinity, but a slower rate constant. The Ca^{2+} release channel proceeds through at least four states: 1) when $[Ca^{2+}]_i$ used as a trigger rapidly increases the activation site is occupied and SR Ca^{2+} release occurs; 2) the large increase of free Ca^{2+} resulting from SR Ca^{2+} release will bind the inactivation site slowly and then turn off Ca^{2+} release; 3) refractory period at which Ca^{2+} dissociates from the both binding sites; and 4) the activatable period or resting state. Rapid application of very high Ca^{2+} can produce inactivation because binding to the inactivation site is expected to be proportional to the Ca^{2+} and the very high Ca^{2+} can partially overcome the limitation of the slow rate constant.

D. Characteristics Of The SR Ca^{2+} Release Channels

The open probability of the cardiac SR Ca^{2+} release channel is profoundly influenced by a number of ligands on the cytosolic side of the channel. The cardiac SR Ca^{2+} release channel can be activated by millimolar caffeine, milli molar ATP, submicromolar Ca^{2+} and inhibited by millimolar Mg^{2+}, micromolar ruthenium red, reduction of pH (Rousseau et al. 1986, 1989, Meissner et al. 1987). The ATP (mM) activated cardiac SR Ca^{2+} release channel functions only if Ca^{2+} is high enough to partially activate the channel (Rousseau et al. 1986). The recognition that ryanodine was a selective and specific ligand for this channel greatly accelerated the isolation and characteristic studies of the SR Ca^{2+} release channel. Lai et al. (1989) demonstrated that there was a maximum of one high affinity- and three additional low affinity-ryanodine binding sites per tetramer of the ryanodine receptor (Ca^{2+} release channel of the SR). At low concentrations (5 ~ 30 uM) ryanodine can open the cardiac SR Ca^{2+} release channel in either vesicle or bilayer (Meissner 1986). This probably corresponds to the occupation of the high affinity ryanodine sites (kd ~ 10 nM). At high concentrations (> 100 uM) the Ca^{2+} release channel appears to be locked in a closed state (Lai et al. 1989). This may result from ryanodine binding to low affinity sites (kd in the uM range).

E. The SR Ca-ATPase Pump

Following contraction, [Ca^{2+}]$_i$ must be removed from the cytosol to initiate relaxation. Most of the Ca^{2+} (depending on animal species) can be removed by the Ca-ATPase pump located in the SR membrane. The SR Ca^{2+} uptake is usually divided into two phases: initial and steady-state. The initial phase is rapid (~200 ms) and is

34

thought to represent the Ca^{2+} uptake during relaxation. The steady-state phase, on the other hand, represents the dynamic equilibrium between Ca^{2+} leakage from and uptake into the SR. The initial uptake has been estimated to be ~100 nmol Ca^{2+}/kg wet wt. in canine heart (McCollum et al. 1972). Solaro et al. (1974) reported that the maximal rate of Ca^{2+} uptake by the SR is about ~200 umol Ca^{2+}/kg wet wt/sec. The altered SR Ca-ATPase pump (increased or decreased) widely reported in hypertrophied myocardium, could modulate the relaxation phase. In thyrotoxic hypertrophy, the activity of SR Ca-ATPase was increased, with an accelerated uptake of Ca^{2+} by the SR (Conway et al. 1976). The SR Ca-ATPase pump mRNA and the pump density were both reduced in the hypertrophied rat heart 30 days after aortic constriction (Dela Bastie et al. 1990). In rabbit, aortic constriction was also associated with a significant reduction in isolated SR Ca^{2+} uptake and Ca^{2+}-stimulated ATPase activity (Lamers et al. 1979). In the rabbit pulmonary artery-banded model, the SR Ca-ATPase protein and mRNA were also reduced to 34% of the controls (Mirsky et al. 1980). The mRNA coding for phospholamban was also found to be depressed by the same amount as that for Ca-ATPase in rabbit pressure-overload model. These results indicate that a reduced density of SR Ca-ATPase pump sites may explain the reduced rate of Ca^{2+} sequestration, and the prolonged relaxation phase in pressure-overload hypertrophy.

(VI). THE MYOFILAMENTS

There has been increasing appreciation that other mechanisms in addition to changes in $[Ca^{2+}]_i$ may be important in modulating cardiac contractile performance (Morgan 1991). It is now known that changes in the responsiveness of the

myofilaments to Ca^{2+} can also regulate contractile force. Although, in general, the degree of activation of the myofilaments is directly related to the amount of Ca^{2+} binding to troponin C, the Ca^{2+} dependent force development may be substantially altered by pathophysiological states of myofillaments.

The myofilaments contain thick- and thin-filaments. The thick filament is composed largely of myosin but also contains some smaller proteins, such as C-protein. There are two subunits of cardiac MHC (α and β), sometimes referred to as fast (α) and slow (β) based on the myosin ATPase activity or shortening rate. So far, two types of myosin have been detected in the heart: ventricular and atrial. The two classes can be further subdivided into isomyosins: V_1, V_2, and V_3 in the ventricle, and A_1 and A_2 in the atrium. Myosin from the rat ventricle occurs in three isoforms that differ in MHC composition. The isoforms V_1 and V_3 are $\alpha\alpha$-MHC and $\beta\beta$-MHC homodimers, and the isozyme V_2 is an $\alpha\beta$-MHC heterodimer. The composition of MHC isoforms and the associated ATPase activity can contribute to the isotonic shortening velocity, and also can modulate the maximal rate of contraction. The isotonic shortening velocity measured during low mechanical load has been found to decrease in most models of pressure-overload hypertrophy (Capasso et al. 1986, Lecarpentier et al. 1987a, 1987b). The rate of ATP hydrolysis in various contractile protein preparations isolated from the myocardium of pressure-hypertrophied animals decreased compared to the controls (Henry et al. 1972). The MHC isoform profile in pressure-induced hypertrophy in rodents shifts from the V_1 to V_3 isoform (Capasso et al. 1986, Mercadier et al. 1981). The reduction in the isotonic shortening velocity in the pressure-overloaded rat cardiac muscle has been attributed to the shift in the contents of MHC isoforms and the concomitant reduction in ATPase activity (Lecarpentier et al. 1987a, 1987b). The

chronic effects of isoproterenol on cardiac isomyosin expression appear to be inconclusive, because it has been reported to cause an increase, decrease or no change in V_1 (Baldwin 1982, Bishop 1990). These variable results might be due to differences in experimental conditions including the dosage of the drug and the species of animals (Haddad et al. 1991). By using a concentration of isoproterenol similar to that employed in the present thesis, Baldwin et al.(1982) reported that myosin ATPase activity and composition of MHC isoforms did not change despite significant cardiac hypertrophy in rat.

The thin filament is composed of filamentous actin, tropomyosin and troponin. The thin-filament proteins are the principal regulatory unit that initiates striated muscle contraction. Cardiac troponin (cTn) is a complex of three proteins: TnC, TnI, and TnT. This complex confers Ca^{2+} sensitivity to myofibrillar activation. Cardiac TnC is the Ca^{2+}-binding subunit of the troponin complex. In the absence of TnC-bound Ca^{2+}, TnI subunit inhibits actin activation of myosin ATPase activity; hence, cTnI is termed the inhibitory subunit. In cardiac muscle, TnC has three sites that bind Ca^{2+}. Two sites that have a high affinity for Ca^{2+} and also competitively bind Mg are termed the Ca^{2+}-Mg sites. The third site, called the Ca^{2+}-specific site, binds Ca^{2+} exclusively, but at a lower affinity. The Ca^{2+}-specific site regulates the Ca^{2+}-dependent force development, because the cardiac Ca^{2+}-Mg^{2+} site is almost saturated (90% with Ca^{2+} and 7% with Mg) at resting $[Ca^{2+}]_i$ (75 ~ 200 nm) and intracellular Mg^{2+} (1mM) (Bers 1991b).

Interaction of the myofilaments with Ca^{2+} is modified by a large number of factors which will affect contraction. Several factors involved in this study will be discussed:

1). Temperature. Cooling (from 37 °C to 1 °C) decreases the Ca^{2+} sensitivitry of cardiac myofilaments, but increases the sensitivity of skeletal myofilaments. The

difference between the influence of temperature on cardiac and skeletal muscle could be attributed to the TnC type in the muscle, based on experiments in which rat ventricular TnC was extracted and replaced by rabbit skeletal TnC (Harrison et al. 1990).

2). Sarcomere length. Increases in the diastolic volume of the heart during its operation as a pump is associated with graded improvements in cardiac performance. The finding, that the force of contraction during ejection of blood is a function of the end-diastolic volume of the heart, was made nearly 100 years ago and is known as Frank-Starling's law of the heart (Babu et al. 1988). The fundamental assumption of the cardiac length-tension relationship is that the maximal force at any sarcomere length is determined by the degree of overlap of the thick and thin filaments. To seek the molecular explanation of this effect, a study of the effects of length on Ca^{2+} sensitivity in skeletal muscle by Kentish (1986) demonstrated that the Ca^{2+} sensitivity of the myofilaments was increased at longer sarcomere lengths. This effect appears to be specific for cardiac TnC, since Babu et al. (1988) found that when native cardiac TnC was extracted from isolated cardiac muscle and replaced with purified TnC from skeletal muscle, the sensitivity of the muscle to a length change was considerably reduced. This reduction offers a straightforward explanation for the difference in the responsiveness of skeletal and cardiac muscles, that is, the cardiac TnC moiety itself in the sarcomeric assembly is the transducer that adjusts the Ca^{2+} sensitivity of the myofilaments as a function of length. Babu et al. (1988) suggested that changes in cross bridge number is not the driving mechanism for the length-dependent effect on Ca^{2+} sensitivity below optimal length, but rather that the difference in the Ca^{2+}-TnC interaction modulates the number of cross-bridge attachments.

Thus the TnC subunit of the troponin complex that regulates the activation of actin filaments has intrinsic molecular properties that influence the length-induced autoregulation of myocardial performance. In addition to the myofilaments, the SR Ca^{2+} release is also increased (Fabiato 1980) at longer sarcomere length in intact muscle. Thus there are multiple factors which may contribute to the Frank-Starling's law of the heart.

3). TnI phosphorylation. Cyclic AMP-dependent phosphorylation of cardiac TnI can decrease Ca^{2+} sensitivity of myofilaments in intact ventricular muscle (Okazaki et al. 1990) in response to β-adrenergic stimulation (isoproterenol) and in skinned fibers which could be mimicked by cAMP. The decline in myofilament Ca^{2+} sensitivity due to cAMP-dependent phosphorylation of TnI can result in an increased off-rate of Ca^{2+} from TnC. This could contribute to the faster relaxation of contraction.

Therefore, in addition to changing the concentration of $[Ca^{2+}]_i$, altering the responsiveness of the myofilaments to Ca^{2+} is another important mechanism for the control of cardiac contractility.

CHAPTER 2

GENERAL METHODS

1. Experiment Model of Cardiac Hypertrophy

Adult female Wistar rats weighing 200~250g were housed individually in a temperature and light controlled room. In order to achieved a constant ratio of the heart weight/body weight, female rats were adopted in this study. All animals were provided with Purina rat chow and water ad libitum. Cardiac hypertrophy was induced following 12 days of daily subcutaneous injections of isoproterenol hydrochloride (0.3 mg/kg body weight) suspended in olive oil (Taylor et al. 1988). Control animals received an equal volume of olive oil only. To reduce sampling error it was necessary to remove aliquots while the isoproterenol and olive oil suspension were stirring. The control and experimental animals were matched by weight and age to reduce possible growth differences. In order to keep the constant ratio of heart/body weight, all animals were fasted and only given water 12 hours before dissection. Animals were used within 24 hours after the last injection.

2. Muscle Isolation

Rats were anaesthetized with ether and the abdominal cavity was opened by a mid-line incision. The rat was heparinized (200 units) by inferior vena cava injection and allowed to circulate for 30 seconds. After 30 seconds of heparin injection, the heart was rapidly removed, transferred to a dissection dish with ice-cold perfusate, and

cleaned free of connective tissue. The hearts were cannulated via the aorta and perfused by the Langendorff technique at room temperature. The perfusate contained 2,3-Butane Dione Monoxime (3.0 mg/ml) (BDM) to arrest contractions (Armstrong et al. 1991). The isolation and organ perfusion was accomplished within 2 – 3 minutes after ether anaesthetizing. Under a biocular microscope (Carl Zeiss, JENA, GDR), the right ventricle was opened along the interventricular septum toward the apex of the heart. The atrioventricular (A-V) ring was cut at the root of the aorta and the right atrium was reflected along the A-V ring. After cutting the attached papillary muscles, the exposed right ventricle was spread out. Trabeculae running between the fibrous A-V ring and the right ventricle free wall were easily seen. Usually, one or two suitable trabeculae could be found in approximately 50% of the hearts used in this study. Thin, free running trabeculae were dissected from the right ventricle between the A-V ring and the free ventricular wall. Extreme care was taken not to damage the tiny muscle during the dissection procedure.

3. General Experimental Set Up

Trabeculae were immediately transported from the dissection dish into a 0.6 ml perfusion bath. A schematic representation of the experimental set up is shown in Fig 4. The muscle bath was mounted on the stage of an inverted microscope (Photozoom, Japan). At one end of the bath, the block of the ventricular free wall was suspended in a cradle that was connected to a force transducer (AME, AE801, Sensonor Micro-electronics, Norway). At the other end, a tungsten wire hook was attached to a micromanipulator (Stoelting, Chicago, USA). A cradle made of stainless-steel wire was glued to a piece of carbon fibre (6 x 0.8 x 0.5 mm) (Fokker Aviation Industries, The
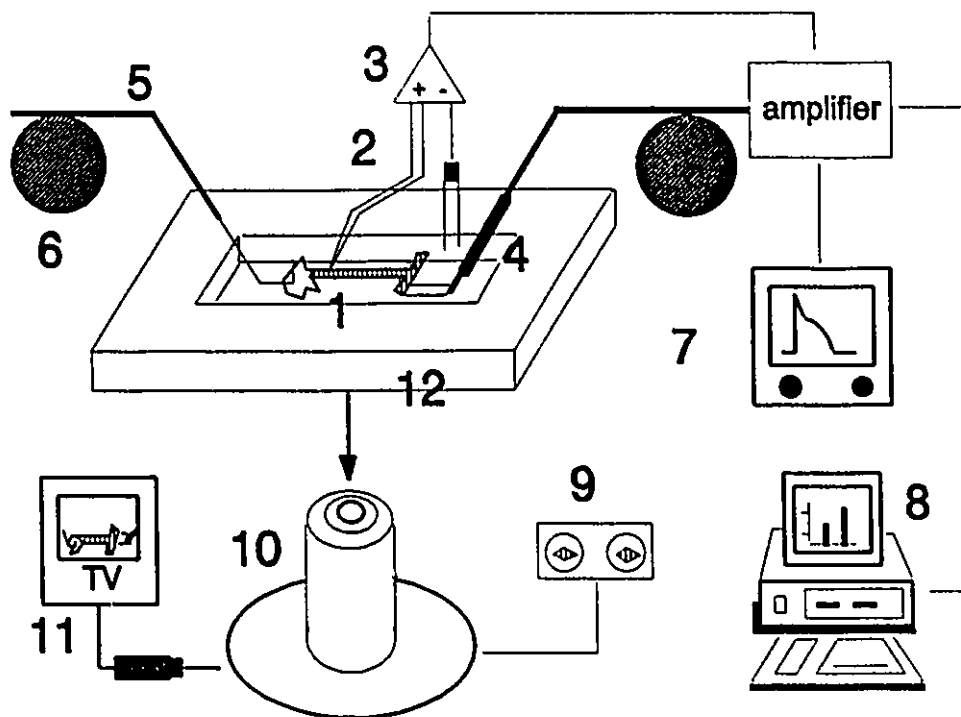
Figure 4. Experimental set up. 1, trabecular muscle. 2, stepped electrode. 3, electrometer. 4, force transducer. 5, metal hook. 6, micromanipulator. 7, oscilloscope. 8, microcomputer. 9, eye piece of microscope. 10, inverted microscope. 11, television. 12, muscle bath.

Netherlands) and the carbon fibre was glued to a force transducer. The transducer, carbon fibre and part of the cradle were covered by a thin layer of silicone elastomer (Dow Corning 170 A&B, Dow Corning Co. USA) to protect them from the salts in the perfusion buffer and to reduce any photo-electric effects from any visible light source. The transducer unit, composed of muscle cradle, carbon fibre and transducer, was

sensitive to force, insensitive to light, and resistant to buffer. The changes in transducer resistance induced by muscle contraction was converted to a voltage signal and amplified by a bridge amplifier (Model 7P122E, Grass, USA). The signals were displayed on a storage oscilloscope (Nicolet 3091, Nicolet Instrument Co. USA) and also digitized by a 12 bit A/D converter at a rate of 200 Hz. The muscle was observed by means of an inverted microscope (Photozoom, Japan) and a videocamera (Panasonic WV-1410, Japan) which was connected to a video monitor (Panasonic TR-930cb, Japan).

The trabecular muscle was mounted horizontally between the cradle, which was specially designed to hold the ventricular cube of the trabecula, and the tungsten wire hook that passed through the tricuspid valve at the opposite end of the trabecula. Thus, the trabecula itself was left relatively undamaged. An adequate preparation did not show any local spontaneous contractions and the active force production did not vary with increasing strength of stimulation above threshold voltage. The trabecular muscle was mounted such that all cell strands throughout the cross-section of the muscle had equal lengths at all muscle lengths; this was verified by inspection of the preparation through the microscope. Consequently, the preparation, which usually had the shape of a ribbon, did not twist in the horizontal plane during length changes or bend uniformly downward during a contraction. If necessary, the preparation was remounted to ensure uniform distribution of cell lengths throughout the central region of the muscle.

Before starting the experiment the muscle was equilibrated at 1 Hz at least one hour. The equilibration period itself was necessary to allow the muscle to recover from the surgery. Muscles were stretched to a length where the optimal active tension was

43

achieved without an appreciable increases in passive tension. The muscle was stimulated at 50% above threshold with a 4 millisecond pulse duration delivered through two platinum wire electrodes connected to a stimulator (Grass S6 C). The electrodes were located parallel to the long axis and on either side of the muscle. The stimulation voltage was determined by increasing the voltage until a contraction was observed then increasing the voltage by 50%. After the equilibration period the muscle was adjusted to a desired length by measuring sarcomere length via a video-camera system. The average sarcomere distance was determined by measuring several locations (at least 3). For each muscle, the cross-sectional area was estimated from width and thickness by means of an occular micrometer.

IV. Buffer

A modified Krebs-Henseleit (K-H) buffer of the following composition (in mM) was used: 117 NaCl, 5.0 KCl, 1.2 $MgCl_2$, 1.2 Na_2SO_4, 2.0 NaH_2PO_4, 27 $NaHCO_3$, and 10.0 Glucose. All solutions were made with deionized water. $[Ca^{2+}]_o$ was varied by adding amounts of 1 M $CaCl_2$ aqueous stock solution to Ca^{2+}-free solution. The perfusate was equilibrated with 95% O_2 and 5% CO_2. The temperature was kept at 26°C during the experiment and monitored by a thermocouple placed next to the muscle within the bath. It has been reported that the mechanical behaviour of cardiac muscle of the rat is more stable at this temperature than at 37°C (Taylor et al. 1988, Stone et al. 1990). The pH was adjusted to 7.35~7.45 with NaOH. The flow rate through the muscle bath was 14 ml/min. Under these conditions, stable responses were observed for experiments lasting about 8~10 hours.

CHAPTER 3.

CARDIAC HYPERTROPHY AND FUNCTIONAL CHARACTERISTICS INDUCED BY ISOPROTERENOL

INTRODUCTION

Catecholamines are important regulators of myocardial contractility and metabolism. However, excessive levels of plasma catecholamines can result in pathological alterations in cardiac structure and contractile failure. Chronic administration of low-doses of isoproterenol, a synthetic catecholamine (with an almost exclusively β-adrenergic effect on the heart), has been reported to produce cardiac enlargement with no visible evidence of tissue damage (left ventricle vs right ventricle) (Haddad et al. 1991, Allard et al. 1990, Taylor et al. 1988, Baldwin et al. 1982).

Conflicting reports exist regarding the regional development of isoproterenol-induced cardiac hypertrophy (Jalil et al. 1989, Collins et al. 1975, Kuribayashi et al. 1986) such that it is uncertain whether the degree of hypertrophy is uniform within both ventricles. The possibility exists that the degree of hypertrophy may be a variable that previously introduced inconsistant functional responses in this model of hypertrophy (Baldwin et al. 1982).

At the present time, the functional changes associated with this model of cardiac hypertrophy are inconclusive. It has been reported that a low-dose, long-term

45

administration of isoproterenol induces cardiac enlargement without altering the intrinsic functional properties, such as resting heart rate, left ventricular pressure, and the rate of pressure development (DP/dt) (Baldwin et al. 1982, Collins et al. 1975). However, other studies indicated that the stroke volume can be increased (Lin 1973) as well as the $+DT/dt$ and a reduced time to peak pressure (Taylor et al. 1988, Tang et al. 1987).

Based on these controversial results in contractile function, it was necessary to provide basic information about the functional characteristics of hypertrophied muscles.

The objectives of this section were: (1) to assess the degree of cardiac growth induced by chronic administration of isoproterenol; (2) to assess the regional development of this hypertrophy; (3) to assess the functional characteristics in this model of cardiac hypertrophy by using small intact preparations of right ventricular trabeculae.

METHODS

1. Tissue Sampling And Weighting

Following the isolation of right ventricular trabeculae, the large vessels, atria, and excess connective tissue were removed from the heart. The ventricles were divided into right ventricular free wall and the left ventricle plus septum. Tissue wet weight was measured for each portion. Dry weight was estimated after dehydrating the samples in an oven for 3 days at 60°C.

46

DT

+DT/dt

RT$_{1/2}$ ——→ -DT/dt

PT

TPT ——→
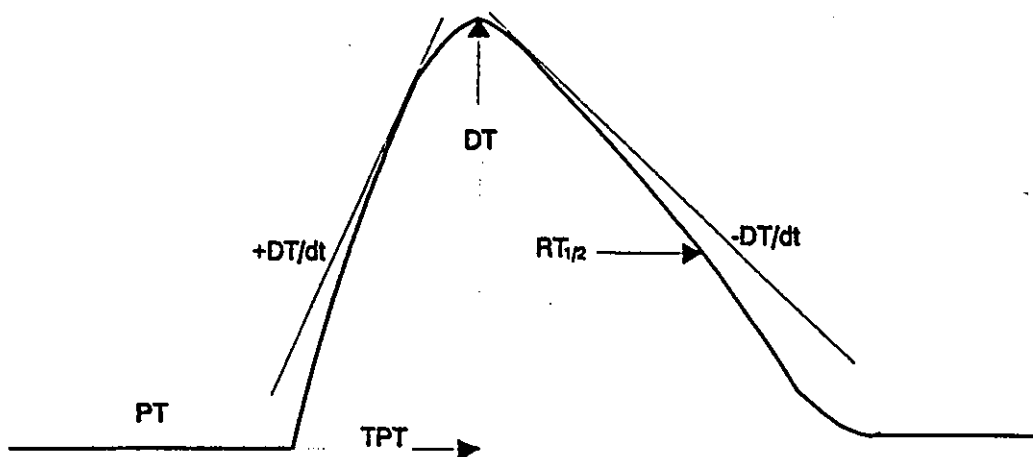
Figure 5. Schematic representation of a trabecular muscle contraction; PT, passive tension or baseline; DT, peak developed tension, +DT/dt, maximum rate of contraction; -DT/dt, maximum rate of relaxation; TPT, time to peak tension; RT$_{1/2}$, time to one-half of relaxation from DT.

2. Analysis Of Contractile Function Curve

Figure 5 displays a general twitch function curve for the right ventricular trabecular muscle and defines the various parameters used to characterize twitch function. During the diastolic interval, the muscle was adjusted to a given passive tension (PT). At the initiation of contraction, the force rises rapidly and smoothly from the baseline to a level of peak tension development. From this point, the muscle relaxes until the force returns to the baseline.

All parameters were obtained by digitizing the twitch curve through a data

47

acquisition computer programme (Unkel scope). The twitch force measurements were normalized by cross-sectional area and expressed as absolute developed tension (DT) (mN/mm²). The maximum rate of contraction (+ DT/dt) and relaxation (-DT/dt) represent maximum changes of DT per second. The time intervals (milliseconds) to characterize the contraction, relaxation phases were the time to peak tension (TPT) and the duration from peak tension to one half relaxation (RT$_{1/2}$).

The cross-sectional area for each muscle was estimated from width and thickness measured by means of an occular micrometer. At the end of each experiment the muscle was removed from the muscle bath and placed into a specially built chamber mounted on a microscope. The muscle could be measured in three-dimensions (length, width, and thickness). Assuming that the cross-section of a trabecular muscle is a rectangle, the area of cross-section was calibrated by:

Cross-sectional area (mm²) = width (mm) X thickness (mm)

RESULTS

1. Tissue Growth Induced by Isoproterenol

The growth response of the whole ventricle, left ventricle plus septum and right ventricular free wall is shown in Table 1. On a whole ventricular basis, both the ratio of ventricle/body weight and absolute dry weight significantly increased 35.7%. Regionally, the ratio of the right ventricle/body weight increased 46.9% while the left ventricle plus septum/body weight was enhanced 31.2% (p < 0.001). Since there was

Table 1. Effects of isoproterenol on tissue mass and percent water in different regions of ventricular muscle.

PARAMETER	CONTROL	HYPERTROPHY
NUMBER OF RATS	14	35
BODY WEIGHT (g)	219.5 ± 0.8	226.8 ± 0.5
WHOLE VENTRICLE:		
tissue dry weight (mg)	129.7 ± 0.7	182.5 ± 0.4*
ratio of WV/BW (mg/kg)	591.1 ± 3.3	802.3 ± 1.1*
% water	81.1 ± 0.2	80.4 ± 10.03
increase ratio (%)		35.7
LEFT VENTRICLE PLUS SEPTUM:		
ratio of LVPS/BW (mg/kg)	481.1 ± 1.9	631.3 ± 1.1*
% water	81.2 ± 0.1	80.6 ± 0.03
increase ratio (%)		31.2#
RIGHT VENTRICULAR FREE WALL:		
ratio of RVFW/BW (mg/kg)	118.3 ± 0.9	173.8 ± 0.5*
% water	79.0 ± 0.2	79.8 ± 0.03
increase ratio (%)		46.9

Note: Values were expressed as mean ± S.E. "*" Significant difference from corresponding control values at $p < 0.001$. "#" Significant difference from the increase ratio of right ventricular free wall at $p < 0.001$. BW, body weight. WV, whole ventricle. LVPS, left ventricle plus septum. RVFW, right ventricular free wall.

no evidence of increased tissue water content, these hearts were significantly hypertrophied. The right ventricle had a greater tissue enlargement than the left ventricle.

49

Table 2. Effects of isoproterenol on contractile parameters of rat myocardium.

Parameter	Control (n)	Hypertrophy (n)
Cross-section area of trabecula (mm^2)	0.026 ± 0.002 (16)	0.027 ± 0.006 (15)
Sarcomere length (um)	1.89 ± 0.005 (16)	1.87 ± 0.007 (15)
DT (mN/mm^2)	1.99 ± 0.21 (10)	4.18 ± 0.53 (5)*
+DT/dt ($mN/mm^2/s$)	69.5 ± 8.9 (8)	130.0 ± 11.3 (7)*
-DT/dt ($mN/mm^2/s$)	54.9 ± 7.9 (8)	103.8 ± 8.6 (7)*
TPT (ms)	106.6 ± 6.9 (8)	107.6 ± 7.4 (7)
$RT_{1/2}$ (ms)	74.4 ± 16.1 (8)	61.6 ± 4.1 (7)

Note: Values were expressed as mean $\pm$ S.E. "*" Significant difference from corresponding control values at $p < 0.001$. Data was from 0.2 Hz of stimulation rate and 0.5 mM $[Ca^{2+}]_o$. n, number of observations.

2. Contractile Characteristics

The contractile characteristics of right ventricular trabecular muscles are described in Table 2. The maximum rates of contraction (+DT/dt) and relaxation (-DT/dt) were increased in hypertrophied muscle. The time to peak tension (TPT) and to one-half of relaxation ($RT_{1/2}$) was unchanged compared to control muscles. It should be mentioned that the contractile characteristics in this study were from a short diastolic sarcomere length of 1.89 um to 1.87 um in control and hypertrophied muscles, respectively. A shorter diastolic sarcomere length was selected for a number of reasons : (1) Initial

studies with hypertrophied muscles showed a greater occurrence of spontaneous contraction at longer sarcomere lengths; (2) at a shorter diastolic sarcomere length, muscles could maintain stable twitch contractions for 8 – 10 hours, and (3) muscle could withstand repeated rapid cooling contractures with no evidence of loss in contractile function.

3. Effects Of Extracellular Calcium On Developed Tension

To determine the inotropic responsiveness of hypertrophied muscles to extracellular Ca^{2+}, the developed force at different extracellular Ca^{2+} concentrations was studied. $[Ca^{2+}]_o$ was varied by adding amounts of 1 M $CaCl_2$ stock solution to perfusate. The $[Ca^{2+}]_o$ was increased in several steps, at intervals of 5 – 10 minutes until a steady-state developed force was achieved, to a final concentration of 2.0 mM.

Figure 6 shows that there was a greater increase in steady-state developed force in hypertrophied muscles compared to the control at all $[Ca^{2+}]_o$ above 0.5 mM.

4. Effects Of Diastolic Sarcomere Length On Developed Tension

The influence of muscle length on contractile force in both control and hypertrophied muscles at $[Ca^{2+}]_o$ = 2.0 mM is illustrated in Figure 7. The relation between the average sarcomere length and peak tension showed that force increased with sarcomere length and this response was enhanced in hypertrophied muscles. In 9 control and 6 hypertrophied trabeculae, respectively, the optimal sarcomere length was 2.330 ± 0.013 um and 2.310 ± 0.012 um, and the slack length was 1.690 ± 0.004 um and 1.660 ± 0.010 um. These unchanged optimal and slack sarcomere lengths indicate that increased contractile function in the hypertrophied muscle was

51
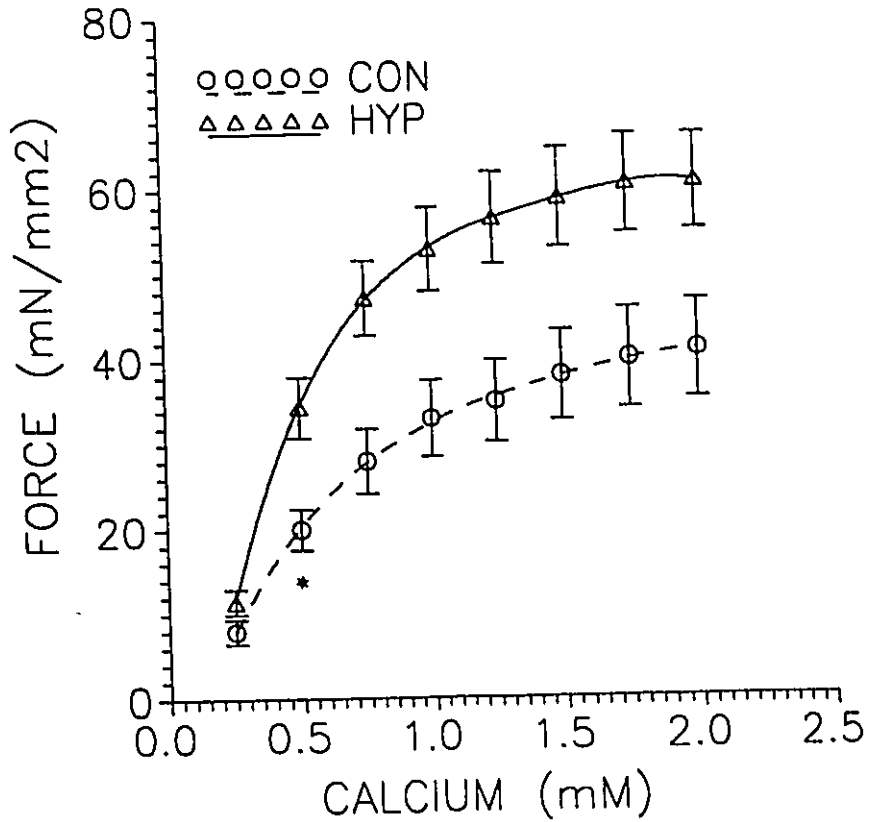
Figure 6. Influence of $[Ca^{2+}]_o$ on steady-state isometric force in both control (CON, n = 9) and hypertrophied (CON, n = 6) trabeculae. * Significant difference from hypertrophied muscle at p < 0.001. Muscles contracted at optimal length.

not related to a simple alteration in the average sarcomere spacing (shortening of slack

and optimal sarcomere length).

DISCUSSION

1. Effects Of Isoproterenol On Cardiac Mass
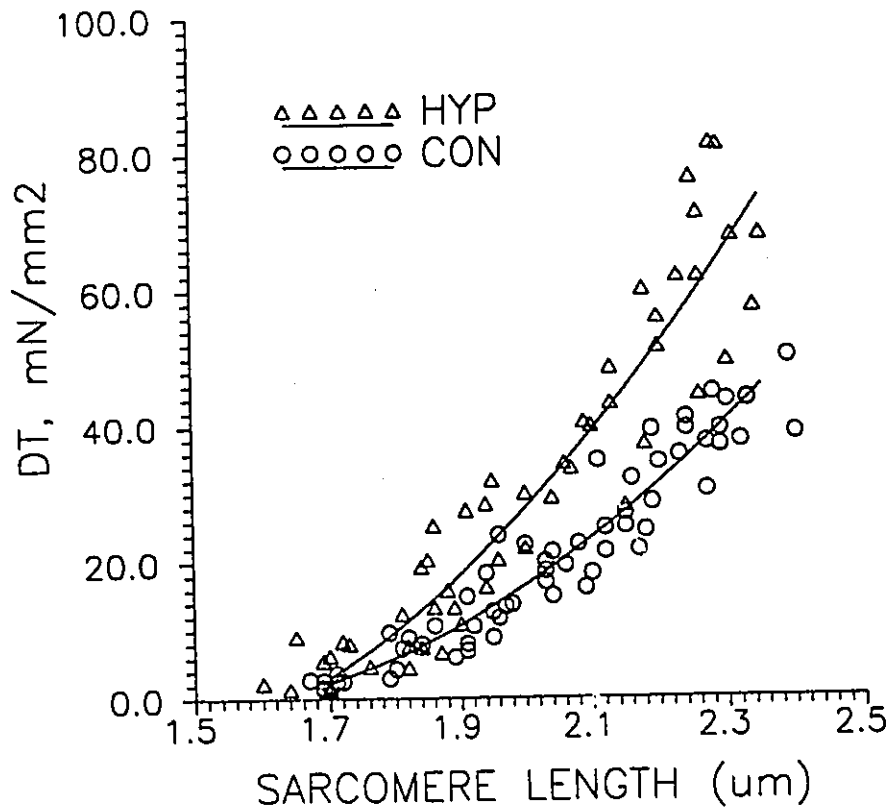
Figure 7. Fitted force-sarcomere length relation in both control (n = 9) and hypertrophied (n = 6) trabeculae. $[Ca^{2+}]_o$ = 2.0 mM.

This study showed that repeated injections of low doses of isoproterenol induced a significant degree of cardiac hypertrophy. The right ventricle achieved a greater hypertrophy than the left ventricle plus septum. Because it has been shown that this degree of cardiac hypertrophy induced by isoproterenol rarely produces evidence for substantial cell fibrosis and necrosis in the right ventricle (Allard et al. 1990), it is believed that any functional change in this model of hypertrophy does not result from

cell injury.

The mechanisms for the regional differences in the degree of cardiac hypertrophy are poorly understood, but may involve the following possibilities: (1) Regional differences in the responsiveness of cardiac adrenergic pathways. Because there is a coupling between isoproterenol-binding (β_1-adrenergic) receptor and the Ca^{2+} channel by adenylate cyclase system, any regional differences to isoproterenol stimuli in either β-adrenergic receptor sensitivity (or responsiveness) or intracellular signals such as cAMP and Ca^{2+} transient could result in a different degree of cardiac hypertrophy (Allard et al. 1990, Morgan 1991). (2). There may be a regional difference in tissue growth potency. Because the number of myocytes in the adult rat is constant, the increased weight of the ventricle can be accounted due to the increased myocyte volume (Schouten 1990). The smaller myocytes within the right ventricle compared to the left ventricle may have a greater potential for cellular enlargement (Allard et al. 1990).

2. Effects Of Isoproterenol On Contractile Characteristics

Enhanced maximal rate of contraction (+DT/dt) in hypertrophied muscle may indicate that either the amount of Ca^{2+} released from the SR to the myofilaments (Fabiato 1981, McIvor et al. 1988) or the myosin ATPase activity, or both, were increased. The effect of chronic administration of isoproterenol on the myosin ATPase activity is inconclusive and has been reported to be increased (Sreter et al. 1982), unchanged (Haddad et al. 1991, Baldwin et al. 1982), or decreased (Jasmin et al. 1986, Rupp et al. 1987). These variable results may be due to differences in experimental conditions, such as the doses of isoproterenol, the degree of hypertrophy,

and the animal species (Haddad et al. 1991). With a similar degree of cardiac hypertrophy induced by isoproterenol, Haddad et al. (1991) found no evidence of altered myosin ATPase activity. Because increased Ca^{2+} influx via L-type Ca^{2+} channel could augment the SR Ca^{2+} release (Fabiato 1985a), the possibility exists that the amounts of Ca^{2+} release per unit time from the SR in hypertrophied muscle may be increased. The possibly amplified Ca^{2+} release from the SR in hypertrophied muscle may explain the enhanced $+DT/dt$.

Twitch relaxation depends on the rapid removal of cytoplasmic Ca^{2+} mainly by the SR Ca-ATPase pump and sarcolemmal Na-Ca exchange (Schouten 1990). The enhanced Ca^{2+} removing mechanisms via either Na-Ca exchange or SR Ca-ATPase pump (see Chapter 8) in hypertrophied muscle could result in an enhanced $-DT/dt$ and unchanged $RT_{1/2}$.

It should be mentioned that basic twitch characteristics themselves cannot reveal specific mechanisms and would require additional study.

3. Effects Of Extracellular Calcium On Developed Force

One way to estimate the overall calcium movement in hypertrophied muscle is to determine the inotropic responsiveness of the tissue to changes in external calcium (Amrani et al. 1990). Several papers have addressed this question in other experimental models of cardiac hypertrophy. Gwathmey et al. (1985), using papillary muscle of the ferret in pressure overload hypertrophy, found that the isometric tension was depressed by increasing extracellular calcium. However, Amrani et al. (1990) showed that force development was enhanced in response to higher extracellular calcium (in a range of $0.25 \sim 3$ mM Ca^{2+}) in whole heart preparations from pressure-

overload hypertrophy. In contrast to the above two results, Raine et al. (1983) found that developed pressure, in whole heart preparations in spontaneously hypertensive rats, was reduced at high calcium concentrations, but greater at low calcium concentrations. In the present study, it was found that there was a significant increase in the contractile force in hypertrophied muscle at calcium concentration above 0.5 mM. High $[Ca^{2+}]_o$ enhances Ca^{2+} influx via L-type channels (Mitchell et al. 1985, Schouten 1990) and via the Na-Ca exchange (Sheu et al. 1986). The ensuing rise in intracellular Ca^{2+}, and storage in the sarcoplasmic reticulum (Orchard et al. 1985), explains the observed enhancement of steady-state peak force with increasing extracellular Ca^{2+}. The increased developed tension in hypertrophied muscle at various $[Ca^{2+}]_o$ could be due to more Ca^{2+} available for activation of myofilaments.

The possible involvement of altered Ca^{2+} sensitivity of contractile proteins in hypertrophied muscles could be excluded because (1) the increased Ca^{2+} transient in hypertrophied muscle was confirmed in the following chapters; and (2) the unchanged responsiveness of myofilaments to Ca^{2+} (force-pCa) was found in hypertrophied muscle by the study of skinned muscle (Chapter 4), which could strongly support that the enhanced Ca^{2+} concentration to myofilaments contributed to the increased developed tension.

4. Effects Of Diastolic Sarcomere Length On Developed Tension

The force-sarcomere length relation in this study indicated that force production increased more rapidly in hypertrophied muscles with increasing average sarcomere length. It has been widely reported that both Ca^{2+} release from the sarcoplasmic reticulum (Fabiato 1980) and Ca^{2+} binding by the myofilaments, especially troponin-C

(Babu et al. 1988), underlie the length dependence of force production. Although an adaptational change in myofilaments (decreased average sarcomere length or increased number of sarcomere) in other models of cardiac hypertrophy (Gwathmey et al. 1992) has been reported to be involved in the altered contractile performance. This factor may be excluded in this model based on the following: (1) The slack and optimal sarcomere length failed to reveal any difference between control and hypertrophy; and (2) The increase in sarcomere number can result in an enhanced absolute force development in hypertrophied muscle (Chien et al. 1991, Hajjar et al. 1991). The study on the force-pCa relation in skinned fibers clearly demonstrated that the increased force development in intact hypertrophied muscles (Fig 7), was not observed in skinned fibers (Fig 9), indicating that the probable increase of sarcomere number was not involved in the enhanced force production in this model of hypertrophy, while increased Ca^{2+} handling could contribute to the increased developed force with various sarcomere lengths in hypertrophied muscles.

From these studies it is found that contractile performance was enhanced in this model of hypertrophy. Based on the discussion above, it is reasonable to speculate that increased contractile function in hypertrophied muscle, probably involves pathways that control the delivering of Ca^{2+} to and from the myofilaments.

CHAPTER 4

MYOFILAMENT CALCIUM SENSITIVITY IN HYPERTROPHIED CARDIAC MUSCLE

INTRODUCTION

Abnormalities in E-C coupling due to alterations in intracellular Ca^{2+} availability and mobilization is a widely-held hypothesis to explain contractile dysfunction in many forms of pathological cardiac hypertrophy (Morgan 1991, Gwathmey et al. 1992, Hajjar et al. 1991, Lakatta 1993). However, other mechanisms in addition to changes in calcium handling may modulate contractile performance. Recent reports indicate changes in the responsiveness of contractile proteins to calcium in pathological hypertrophied human (Morgan 1991) and ferret hearts (Gwathmey et al. 1992).

It has been clearly demonstrated that normal Ca^{2+}-dependent regulation of force production is controlled at the thin filament level (troponin/tropomyosin complex) (Moss 1992). A direct role of troponin-I in the regulation of Ca^{2+}-dependent tension was recently confirmed by using protein extraction and reconstitution technology in permeabilized porcine ventricular trabecular muscle (Strauss et al. 1992). They found that calcium-dependent regulation of the force was eliminated through troponin I extraction because force was unchanged (approximately maximal force) in either calcium-free solution or high calcium (pCa 4.5) solution, while calcium-dependent force production was restored after reconstitution with troponin I. In hypertrophied

myocardium, Gwathmey et al. (1992) reported that adaptive changes at the level of the thin filaments can potentially alter the force-pCa relationship in idiopathic spontaneous cardiomyopathy. In isoproterenol induced cardiac hypertrophy, the responsiveness of myofilaments to Ca^{2+} has not been reported. Because acute isoproterenol administration can stimulate phosphorylation of troponin-I (Lakatta 1993), the altered developed force in this model of hypertrophy may result from a modulated sensitivity of contractile proteins to calcium.

In order to characterize the relationship between free calcium in the vicinity of the myofilaments and force development, I used a "skinned" muscle preparation in which the sarcolemma and the intracellular calcium compartments were chemically disrupted by Triton-100 (Kentish 1986). The sensitivity of myofilaments to calcium can be determined from the force-pCa relationship (i.e. Ca^{2+} required for 50% maximal activation of the myofilaments and the slope of the force-pCa activation curve). I was interested in determining: (1) the Ca^{2+}-sensitivity of myofilaments in skinned control and hypertrophied cardiac muscles; and (2) the maximal developed force in both control and hypertrophied muscle fibers.

METHODS

1. Solutions

The total salt concentration necessary for obtaining the desired pCa, pMg, pMgATP, and pH at a constant ionic strength as described by Kentish (1986), were calculated using a computer program. These solutions were prepared at a temperature of 25°C,

with an ionic strength of 0.2 M, and an ionic equivalence of 0.1745 M, and a pH of 7.1. The final concentration of these salts were: 10 mM EGTA, 10 mM phosphocreatine, 6.8 mM total ATP, and 1.05 mM free Mg^{2+}. Calcium was added as CaEGTA to the different activating solutions. The details of the preparation for each solution can be found in Appendix 2.

2. Muscle Skinning

In order to change the different pCa solutions, a special experimental set up was designed and built containing 8 switchable muscle baths with a constant temperature control system (Fig 8). Small, cylindrical trabecular muscle from the right ventricle (with diameter < 200 uM) was chosen for the study of muscle skinning. After one hour of equilibration at a stimulation frequency of 1 Hz in a modified Krebs-Henseleit buffer (see General Method), the muscle length was adjusted to L_{max}, the point at which there was no further increase in active twitch force. The stimulator was turned off and the muscle was transferred to a well containing a skinning solution with 1% (by volume) Triton X-100 dissolved in relaxing solution for 30 minutes. The criteria used to determine the adequacy of skinning included the following: (1) an even change of the muscle colour from dark red to light pink was observed; (2) force development occurred in response to submicromolar concentrations of calcium; (3) the level of force was reversibly controlled by changing the bathing fluid (calcium removal); and (4) no force development was observed when either caffeine or ryanodine was added to the relaxing solution.

After skinning, the muscle was moved to a new chamber containing fresh relaxing solution, and then maximally activated in activating solution with pCa of 4.5.
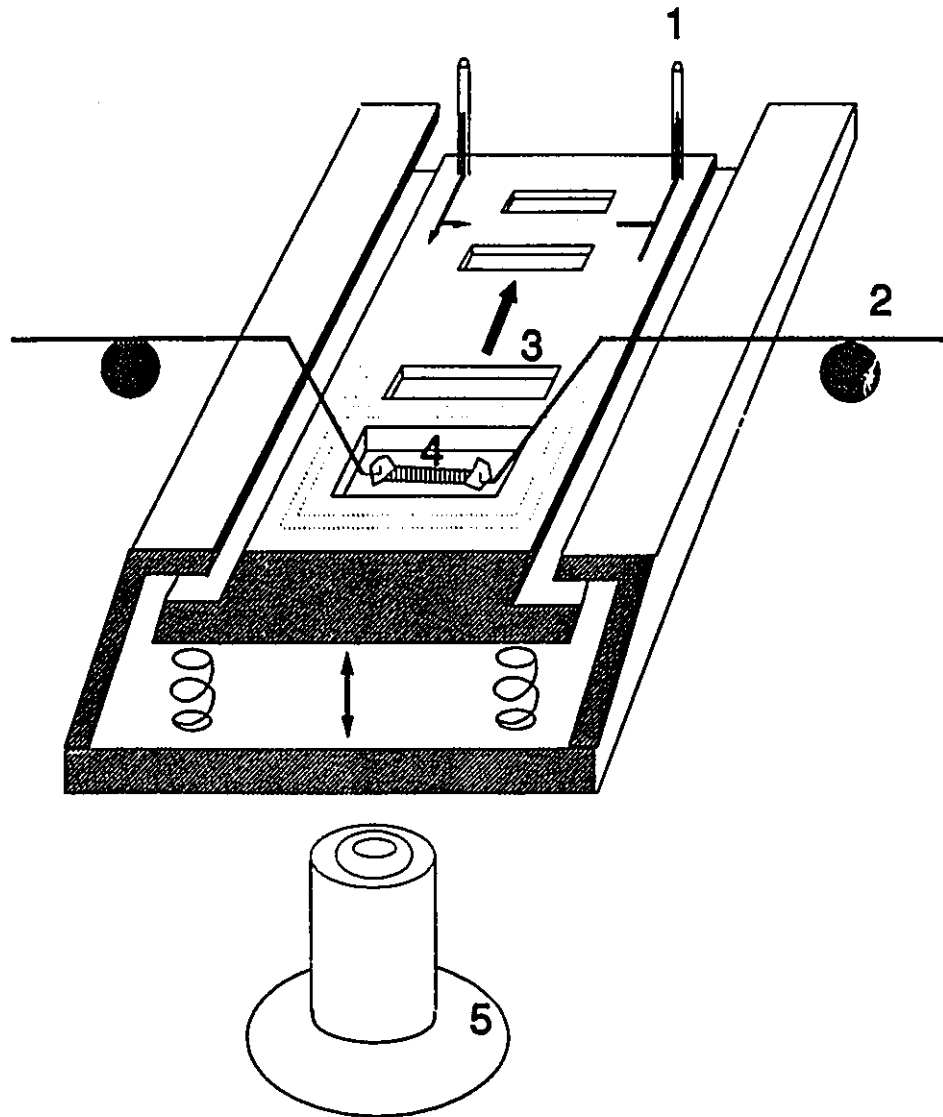
Figure 8. Experimental set up for muscle skinning. 1, temperature control system. 2, force transducer. 3, muscle chambers. 4, trabecular muscle. 5, inverted microscope.

Subsequently, the muscle was subjected to a series of contraction-relaxation cycles in different pCa solutions. After each activation at a given pCa, the muscle was switched to chamber containing a relaxing solution until complete relaxation was achieved. Before a new pCa solution was introduced, the muscle was exposed to a

preactivating solution. This did not induce a contraction, but it equilibrated the muscle with a very low concentration of EGTA (see Appendix 2) that resulted in a rapid activation when the muscle was exposed to a new pCa solution.

3. Force-[Ca^{2+}] Analysis

The force versus Ca^{2+} curves were fitted to a modified Hill relation:

$$F = F_{max} \frac{[Ca^{2+}]^n}{Kd^n + [Ca^{2+}]^n} 100\%$$

where F is developed force; F_{max} is the maximal force developed at pCa of 4.5; n is the Hill coefficient, which characterizes the steepness of the relation; and Kd is the Ca^{2+} concentration required for 50% maximal activation. The equation was solved for F, Kd and n by a computer modelling program (SigmaPlot-4.1) which employs a series of iterations to minimize the sum-of-squares value.

RESULTS

Fibers from control and hypertrophied hearts were skinned with Triton-100 as described in Methods and then activated with increasing Ca^{2+} concentrations. A typical example of the effect of various Ca^{2+} concentrations on force production is given in Figure 9. Note that a decrease in pCa resulted in a rapid increase in force and that
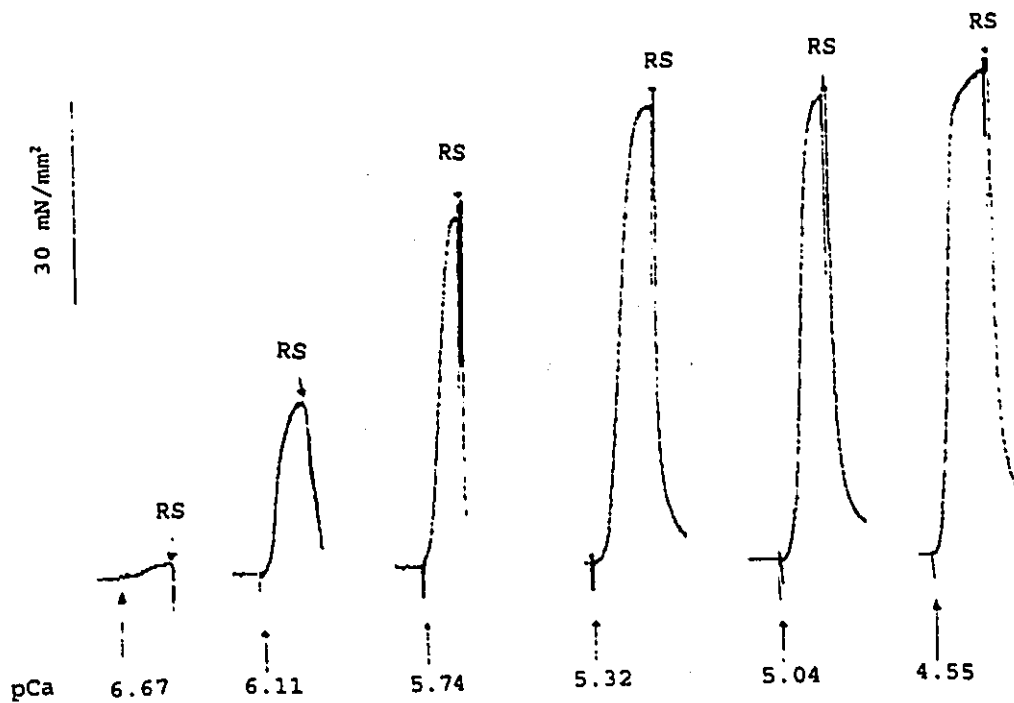
Figure 9. A typical example of the effect of altered pCa on force production in a Triton-100 skinned rat trabecular muscle. RS, relaxing solution. Muscle size was 0.029 mm^2.

returning the muscle to a relaxing solution (RS) caused a prompt dissipation of force,

indicating the adequency of the "skinning" procedure.

The effect of chronic administration of isoproterenol on the force-pCa relation is

given in Figure 10. Fibers from both control and hypertrophied groups were maximally

activated at a pCa of 4.5. The force-pCa curves were fitted using the Hill equation

as described in Methods. The absolute force-pCa relationship (Fig 10, A) from control

and hypertrophied muscle fibers showed no significant difference in either maximal

Table 3. Hill coefficients and pCa for 50% of force production.

Group	n	kd (uM)	#
Control	2.09 ± 0.30	1.23 ± 0.18	6
Hypertrophy	2.00 ± 0.52	1.52 ± 0.23	6

All data are expressed as means ± S.E. "#", number of experimental preparation. n, Hill coefficient. kd (or $pCa_{50\%}$), Ca^{2+} required for 50% activation.

Ca^{2+}-activated force or the shape of the curve. In the lower panel (B), the force in each preparation was normalized to its maximum value. Note that in both groups, the normalized force-pCa relationship was steep and that the shape of the relative force-pCa curve was not significantly different. A typical result of the curve fitting procedure to define the shape of the force-pCa relation is depicted in Fig 10 (C). The derived average Hill coefficients (n) for the force-pCa relationship and $pCa_{50\%}$ are given in Table 3. There were no differences in either calcium required for 50% activation of the myofilaments (kd), or the Hill coefficients (n).

DISCUSSION

Hypertrophied hearts have different structural and functional properties. When compared to the control muscles, the hypertrophied hearts show significant differences in contractile characteristics, electrophysiological activity, and calcium handling, as

64

65
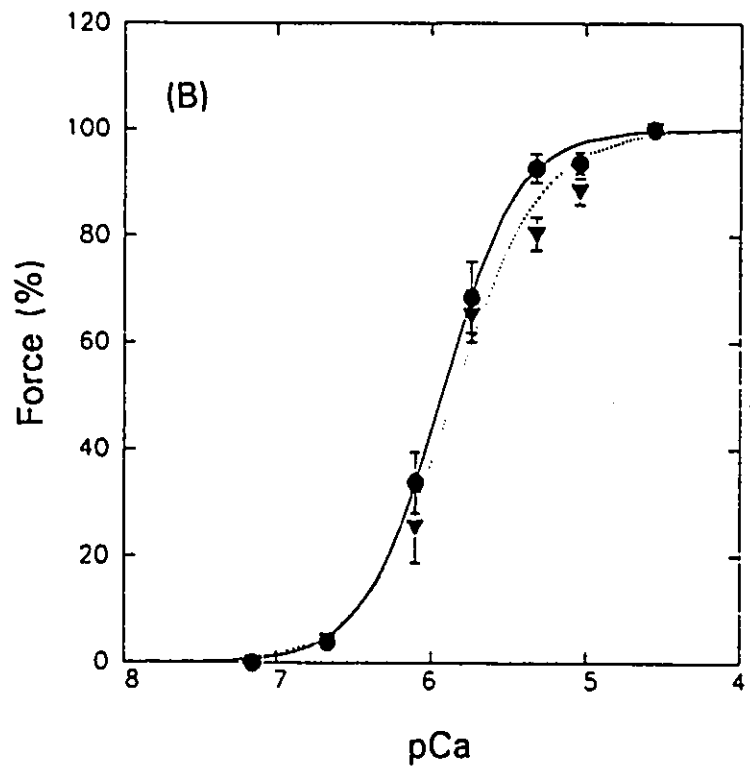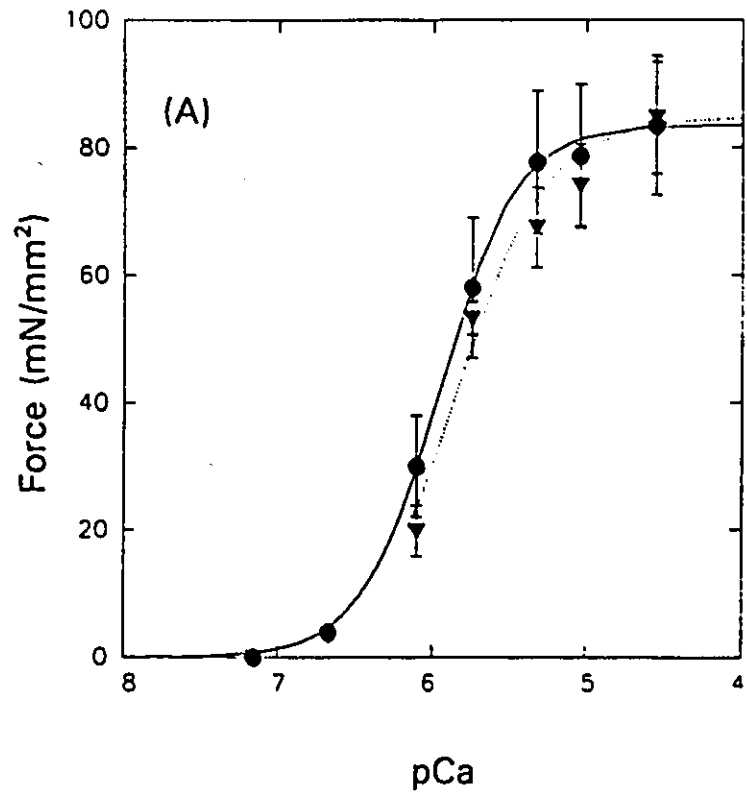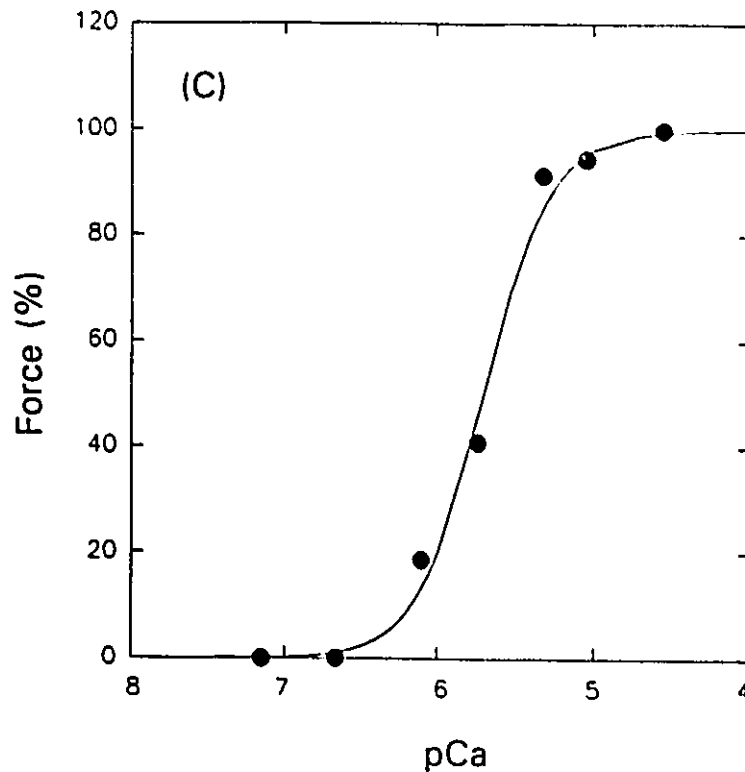
Figure 10. Force-pCa relationship expressed in absolute force (A) and relative force (B) for control and hypertrophied muscles. (C) a typical example of curve fitting for the force-pCa relation. Solid lines with filled circle represent control group. Dashed line with filled triangle represents the hypertrophied muscle. Each curve presents mean values ± S.E. for 6 control and 6 hypertrophied muscle fibers. The curves are approximated with the Hill relationship.

confirmed in other chapters. These differences have been attributed to alterations in Ca^{2+} handling. Because changes in Ca^{2+} responsiveness at the level of the myofilaments can affect peak twitch force, it was important to distinguish whether the increased contractile force in intact hypertrophied muscles results from the altered Ca^{2+} handling or possibly from altered Ca^{2+} activation of the myofilaments.

In these muscle preparations of right ventricular trabeculae, no difference was

detected in the sensitivity of the myofilaments to Ca^{2+}, as shown in either unchanged Hill coefficients or $pCa_{50\%}$. These results suggest that the increased contractile force in intact hypertrophied muscle preparation with different $[Ca^{2+}]_o$ (Fig 6) or sarcomere lengths (Fig 7), does not reside at the level of the myofilaments. These findings are similar to most models of cardiac hypertrophy, i.e. rat (Perreault et al. 1990), guinea pig (Siri et al. 1991), rabbit (Maughan et al. 1975), ferret (Hajjar et al. 1991, Baudet et al. 1990), and especially in human myocardium (Morano et al. 1991) which demonstrated similar force-pCa relationship, (e.g. unchanged myofilament calcium responsiveness).

It has been suggested that an increased number of sarcomeres in the hypertrophied muscle could result in an enhanced Ca^{2+}-activated force (Hajjar et al. 1991). However, this study failed to reveal any difference in absolute force development in skinned muscle fibers between control and hypertrophy, indicating that the increased absolute force production found in intact hypertrophied muscles with either different $[Ca^{2+}]_o$ or sarcomere lengths (Fig 6, 7) could result from the enhanced Ca^{2+} availability of myofilaments.

The present results strongly indicate that in this model of cardiac hypertrophy the increased force development in intact trabecular muscle under different loading conditions ($[Ca^{2+}]_o$ or sarcomere length) could be attributed to the enhanced intracellular Ca^{2+} transient.

CHAPTER 5

THE FORCE-INTERVAL RELATIONSHIP IN HYPERTROPHIED MYOCARDIUM

INTRODUCTION

The magnitude of force development in cardiac muscle can be altered by two factors: (1) the availability of calcium to activate myofilaments upon excitation; and (2) the responsiveness of the myofilaments to cytoplasmic free calcium. Since there was no identified change in the sensitivity of myofilaments to calcium, then changes in calcium handling may contribute to the enhanced contractile function in this model of hypertrophy. In rat cardiac muscle, most of the calcium (about 90%) which activates the contractile apparatus originates from the SR. Obviously, the SR plays a dominant role in delivering calcium to the myofilaments, and controlling the magnitude of contractile force. The ability of the SR to release calcium can be modulated by: 1) the content of calcium within the SR; 2) calcium influx through the L-type Ca^{2+} channel which triggers calcium release from the SR; and 3) the capacity of SR release channels to recover from an inactivated (closed) state to an activated (open) state.

Accumulating evidence has showed that many properties of cardiac excitation-contraction coupling are altered in cardiac hypertrophy. The lengthened duration of action potential in hypertensive hypertrophied rat hearts may indicate enhanced influx of calcium (Capasso et al. 1986), which can amplify SR Ca^{2+} release (Fabiato 1983,

68

Banijamali et al. 1991). Decreased abundance and/or function of the SR Ca-ATPase pump may lead to a reduction in the amount of SR Ca^{2+} content and also may impair relaxation (Kimara et al. 1989). However, reduced activities of the Na-K-ATPase may cause intracellular accumulation of sodium in hypertensive hypertrophy (Whitmer et al. 1986), which in turn inhibits calcium extrusion via the Na-Ca exchange, and possibly favors the SR calcium accumulation. However, it is unclear whether these alterations exist and affect the SR calcium release in isoproterenol-induced hypertrophied heart.

It is well known that force production by the heart is influenced by the interval between beats (Banijamali et al. 1991, Schouten et al. 1987, 1990, Ragnarsdottir et al. 1982, Taylor et al. 1988). The phenomenon, in which a premature beat will cause a weak contraction and a longer interval produces a greater force of contraction, is referred to as force-interval relation. In the rat, this interval dependent force recovery process has been extensively studied and has showed a remarkable and reproducible recovery pattern. Since the magnitude of an electrically stimulated twitch is predicted by the SR calcium release in rat (Schouten 1990, Banijamali et al. 1991), the force-interval relation has been used to demonstrated the time-dependent characteristics of the SR calcium release channels.

A typical force-interval curve is depicted in Figure 11 (A) and a model developed by us to explain the force-interval relationship (B). In rat myocardium, the force-interval relationship is characterized by three phases: alpha, beta and gamma.

The early recovery (alpha) phase, in which the small magnitude of force at short intervals below 10 seconds rapidly increases to a steady state level, can be explained by insufficient time for the SR calcium release channel to recover from inactivation.

The second phase (beta) shows a slower increase of twitch force to a maximum at
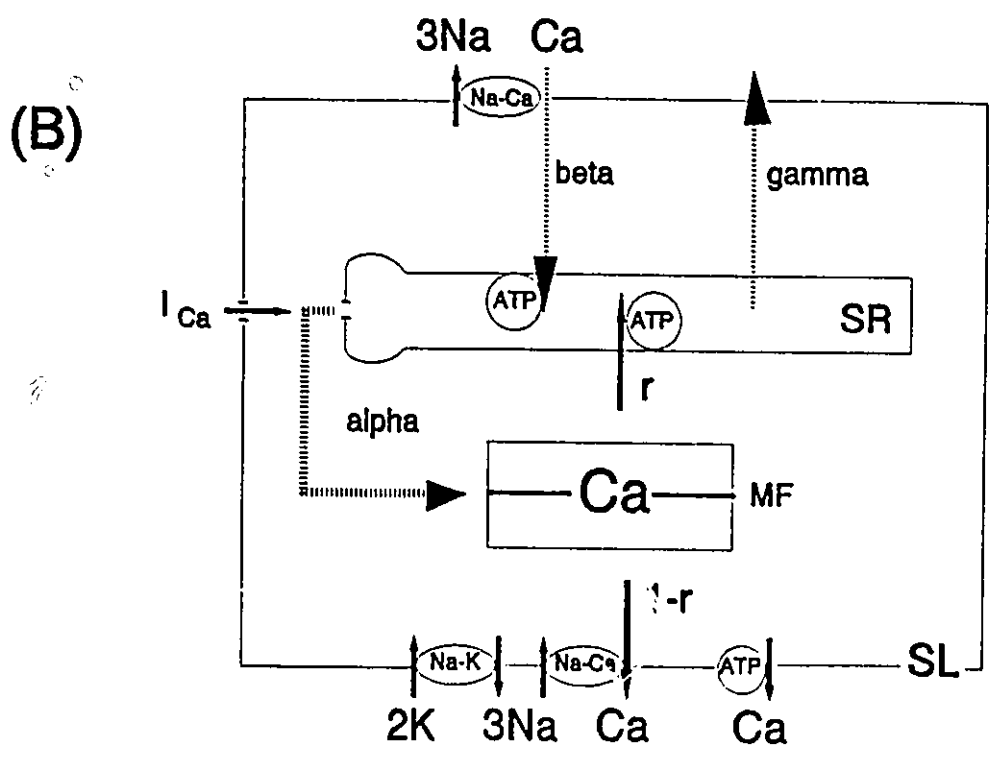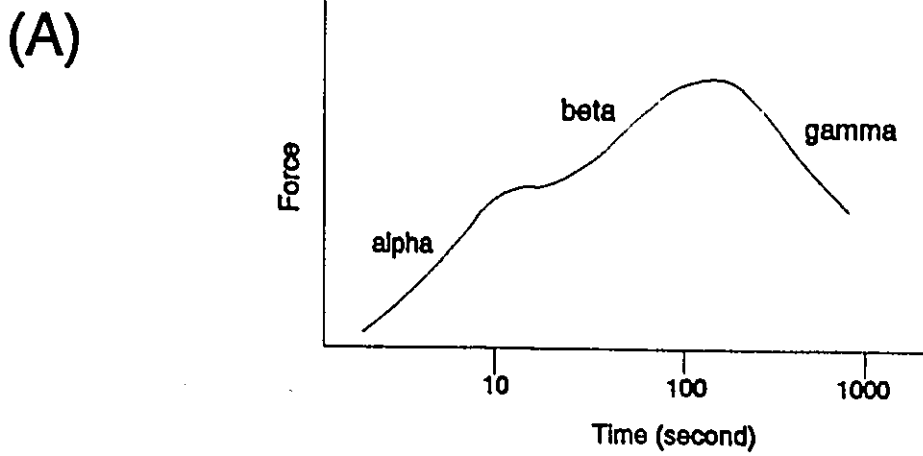
Figure 11. Panel A: Typical force-interval curve. Panel B: Model illustrating the force interval relationship of rat myocardium. r = fraction of recirculated Ca^{2+} by SR with each beat. 1 - r = fraction of Ca^{2+} efflux from cell with each beat.
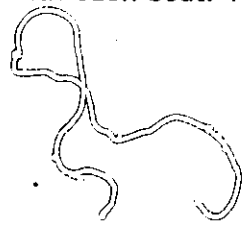
rest interval of about 120 seconds (rest potentiation). The physiological explanation for the rest potentiation is a gain in SR calcium due to a net calcium influx into the cell via Na-Ca exchange during diastole, and that this calcium is then taken up by the SR. Subsequently, during the following contraction, the increased SR calcium content and the greater time available for recovery from inactivation of the SR calcium release channel, will result in a greater fraction of SR calcium release, and a potentiated contraction.

The third phase (gamma) represents a decrease in twitch force at diastolic intervals > 120 seconds (rest depression). The rest depression can be interpreted as a reduction in the SR calcium content due to calcium leakage out of the SR and leaving the cell by calcium extrusion mechanisms at a longer diastolic interval.

Although acute application of isoproterenol can modulate cardiac E-C coupling (Lakatta 1993), the chronic effects of isoproterenol on intracellular Ca^{2+} handling, especially on sarcolemmal Na-Ca exchange and SR Ca^{2+} release channels, are unclear. The purpose of this study was to: (1) determine the chronic influence of isoproterenol on the force-interval relationship in conjunction with mathematic modelling procedures; (2) infer changes in intracellular Ca^{2+} handling associated with E-C coupling, especially the Na-Ca exchange and SR Ca^{2+} release, from an altered force-interval relationship.

METHODS

1. Experimental Protocol

After the equilibration period, the muscle was paced at 0.2 Hz and the sarcomere

length was visualized through a video camera system (see General Methods) and adjusted to 1.9 uM. Twenty four test (rest) intervals were used (0.40, 0.54, 0.73, 0.99, 1.34, 1.81, 2.44, 3.33, 4.46, 6.02, 8.13, 10.47, 14.81, 20.00, 27.00, 36.45, 49.21, 66.44, 89.70, 121.00, 130.00, 135.00, 150.00, 163.00 seconds) to generate the force-interval data. These rest intervals were chosen to allow full examination of both force generating phases (alpha and beta) of the force interval relationship. To reduce the potential error in developed tension at various test intervals, the stimulator was controlled through a data acquisition and control software (Unkel Software, Lexington MA). This allowed precise control over the off-on cycle of the stimulator and the activation of the A/D converter. Diastolic test intervals (0.4 ~ 160 seconds) were programmed to be interposed between the control pacing at 0.2 Hz (Fig 12). Following each rest interval the developed force was allowed to stabilize before a new test interval was interposed.

The beat immediately prior to the test interval was collected as the control beat (Fc) while the first beat following the test interval was recorded as the test contraction (Ft) (Fig 12). The force-interval curves were then generated by plotting the developed force of the test contraction normalized by the developed force of the last control beat as a function of the test interval. This method was selected because it was less affected by a reduction in force over time since the developed force of test contraction was normalized by the control force developed on the beat immediately prior to the rest interval.

2. Data Recording

Force signals generated by the transducer were amplified by a Grass preamplifer

72
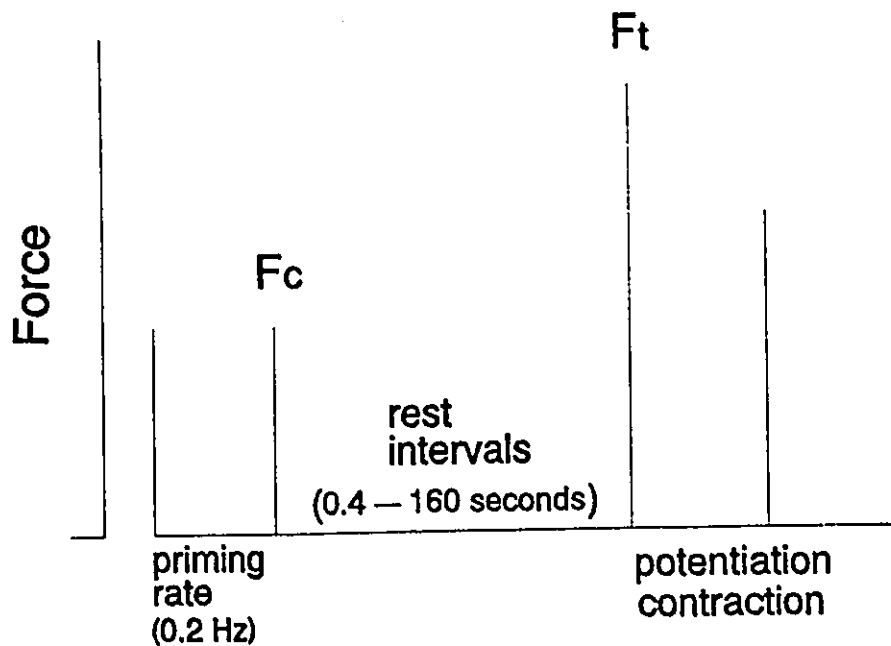
$$\text{Potentiation (force)} = \frac{F_t}{F_c}$$

Figure 12. Experimental protocol used to generate the force-interval data. F_t = test contraction, F_c = last control contraction.

(Model 7p 1222D) powered by a Grass power supply (RPD 107E). This signal was then converted to digital form using a 12 bit analogue-digital (A-D) converter. The force signal was sampled at 200 Hz and each twitch curve contained 250 data points. These data were stored on floppy discs and used for subsequent analysis.

3. Data Analysis

The force-interval curve was constructed by plotting peak force of the test contraction as a ratio of the last control contraction versus the test time (Fig 13). To describe the exponential characteristics of the ascending limb during the interval-dependent force recovery, the curves were fitted by a mathematical model that used a nonlinear, recursive, least squares analysis employing the steepest descent method for the fit parameters (Taylor et al. 1988).

The mathematical model used a linear combination of terms in the general form, $A_i(1-\exp(-a_i t))$, where "A_i" is the amplitude or force parameter, "a_i" is the inverse time constant of the particular process, and "t" is the length of the test interval. Thus in the analysis of the force-interval relationship two terms were utilized to evaluate two simultaneously occurring phases as follows:

$$F(t) = F_{end} \cdot [1 - M \cdot \exp(-\alpha t) - (1 - M) \cdot \exp(-\beta t)]$$

where "F_{end}" is the final and maximal force of the ascending limb of the restitution curve, "M" describes the fractional contribution of the alpha phase to the total curve. The parameters used to fit data are F_{end}, M, α, and β. It was therefore possible to separate and graphically illustrate the overall process and the two underlying individual alpha and beta processes (Taylor et al. 1988).

4. Statistical Analysis

A one-way analysis of variance (ANOVA) was performed to determine overall statistical significance between control and experimental groups. A t-test was

supplemented to determine if mean difference also existed between groups. p < 0.05

was considered as significant difference.

RESULTS

Figure 13 shows the force-interval relationship for control and hypertrophied
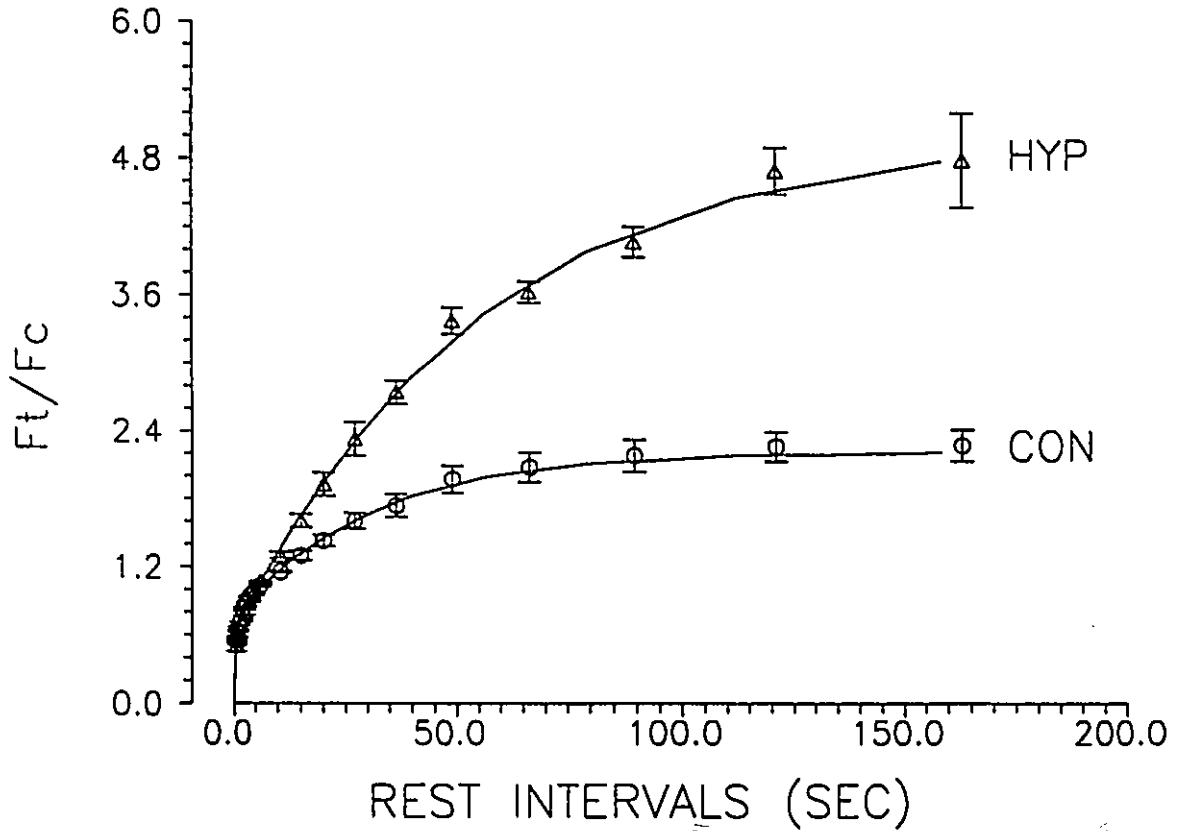
Figure 13. Raw data (symbols) and fitted curves of the force-interval relationship plotted on a linear X-axis in control (CON, n=7) and hypertrophied (HYP, n=5) muscles. $[Ca^{2+}]_o = 1.0$ mM.

muscles. The force-interval curves were constructed by plotting the developed force of the test contraction (Ft) normalized by the last control force (Fc) as a function of the rest interval. In order to insure that the fitted parameters reflected the raw datu, Figure 13 compares the experimental derived raw data with the fitted curves in control and hypertrophied muscles. These data clearly show that the fitted curves generated by the mathematical parameters correspond extremely well with the raw data in both groups.
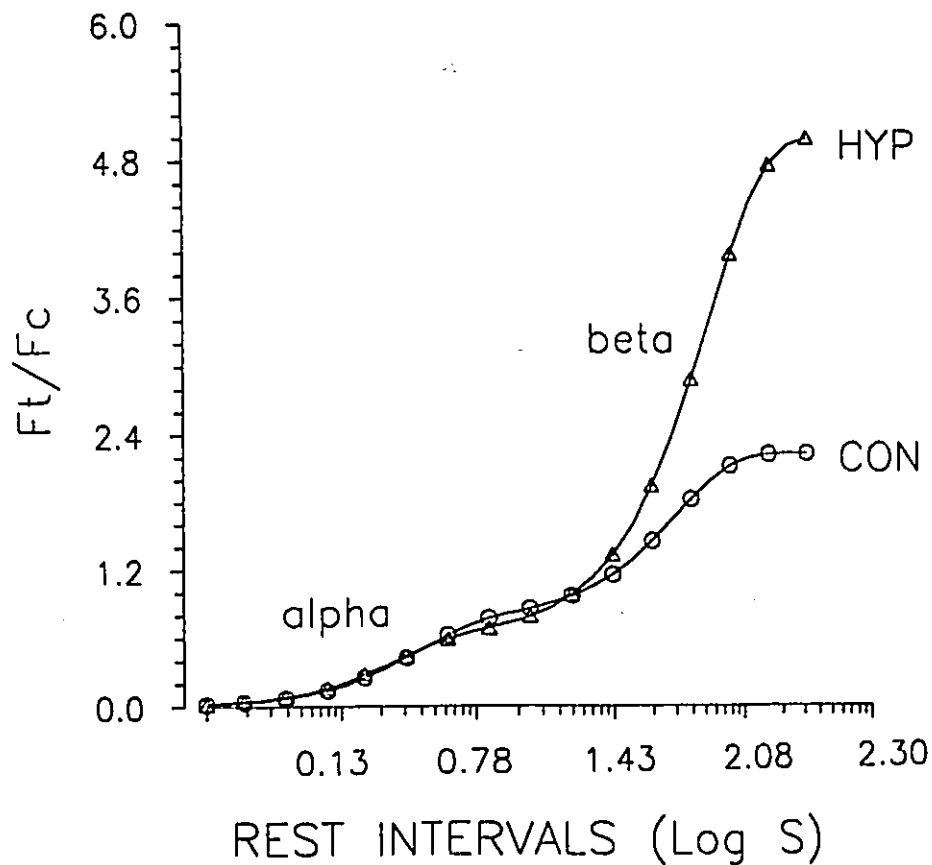
Figure 14. A composite of fitted force-interval data plotted on a logarithmic X-axis in control and hypertrophied muscle.

To present more clearly the characteristics of the force-interval relation, the fitted curves were plotted as a logarithmic function of rest interval (Fig 14). These results clearly show a biphasic process (alpha and beta) in the time dependent force recovery (mechanical restitution) in both control and hypertrophied groups. The alpha phase, occurring at rest intervals up to approximately 10 seconds, did not show any difference between control and hypertrophied muscles. In contrast, the beta phase, occurring at rest intervals up to approximately 160 seconds, became significantly amplified in the hypertrophied muscles.

To understand more precisely how cardiac hypertrophy affects these recovery processes, each phase was mathematically isolated from the compound force-interval curve and plotted on the same logarithmic scaled time axis (Fig 15). This isolation procedure makes it possible to compare graphically the contribution of each process to the whole curve. Obviously, during short rest intervals it can be observed that the fundamental alpha process dominates earlier than the beta components in both groups. With prolonged rest, and as the alpha process has essentially completed its contribution, the developed force continues to gain an additional and ongoing contribution from the beta process. The beta phase in hypertrophied muscles significantly dominates the whole force-interval curve.

Figure 16 shows the comparison of each phase (alpha and beta) between control and hypertrophied muscles. Chronic administration of isoproterenol had little effect on the alpha phase (Fig 16, A). However, isoproterenol treatment not only increased the amplitude of the beta phase, but also altered the early activation (leftward shift) of this process.
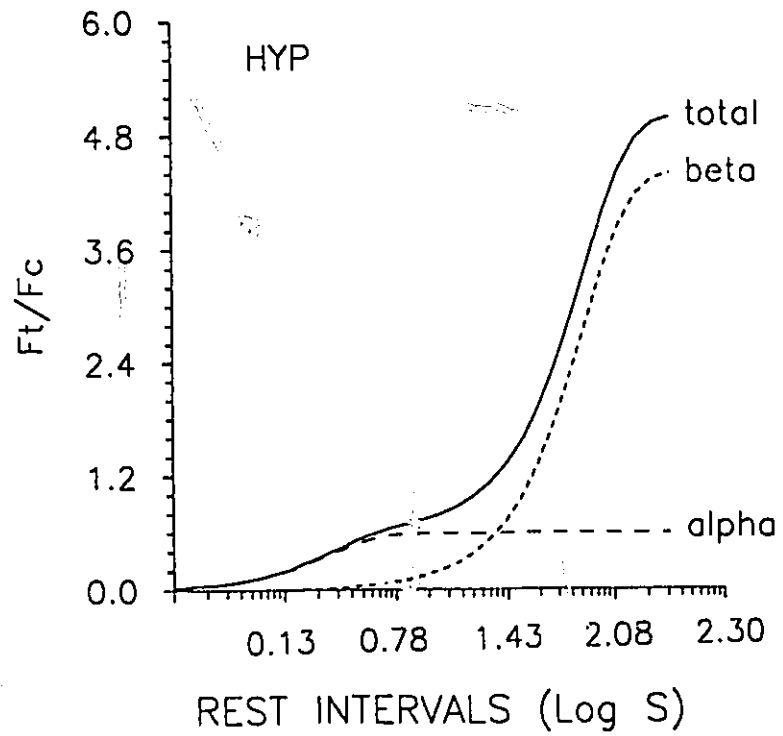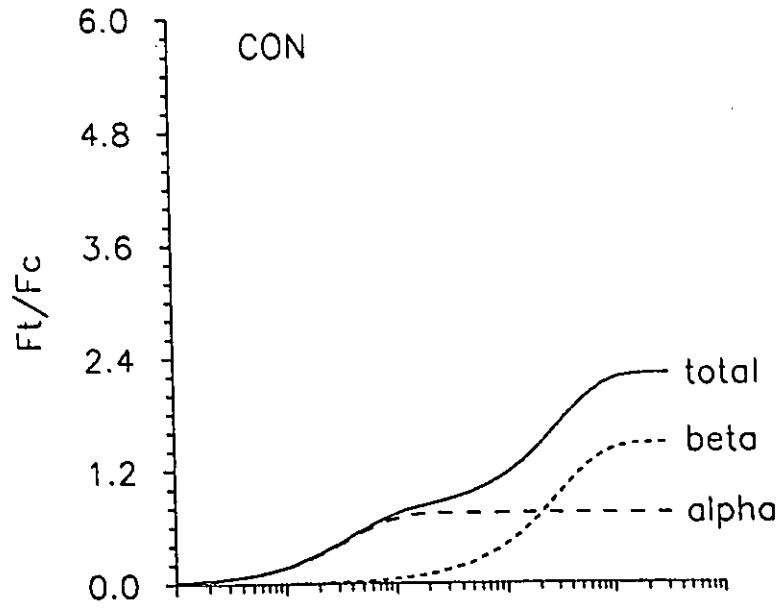
Figure 15. Force-interval curves from control (A) and hypertrophied (B) muscles with isolated alpha and beta phases.
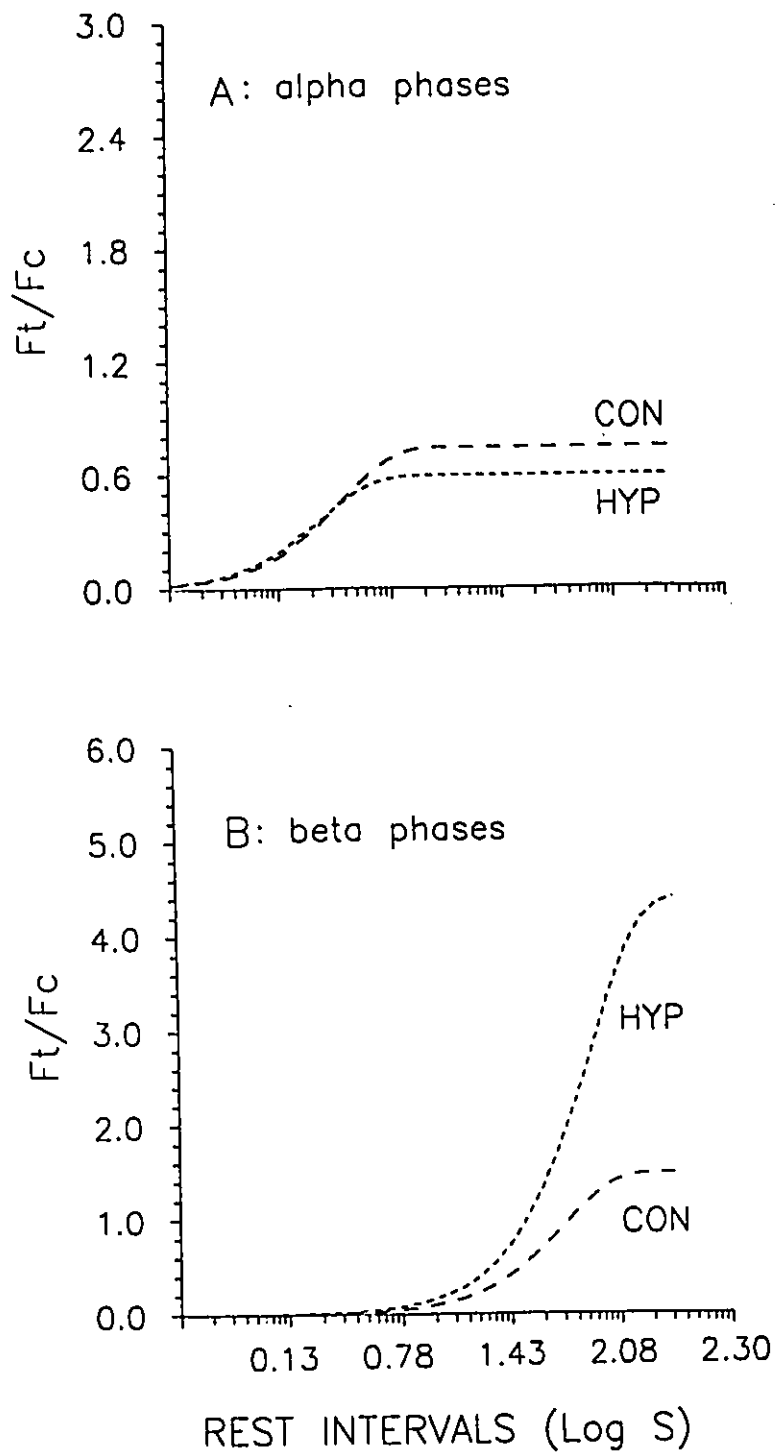
Figure 16. Mathematically isolated alpha (A) and beta (B) phases overlaid from control and hypertrophied muscles plotted on a logarithmic time axis.

Table 4. Mathematically derived parameters of alpha and beta phases in control and hypertrophied muscle.

Parameters	Control	Hypertrophy	%Change
Time Constant (s)			
Alpha	0.389	0.258	- 33.53
Beta	30.89	54.59	+ 79.64
% Contribution			
Alpha	33.36	11.88	- 64.37
Beta	66.63	88.11	+ 32.23
Maximal Rate (U/mSec)			
Alpha	748.1	726.1	- 2.930
Beta	29.04	58.04	+ 99.86

Note that these parameters were calculated from the fitted data illustrated in Figure 16. U/mSec, unit per millisecond.

To analyze quantitatively the force-interval curves, the percentage contribution, maximum rate and time constant of each phase were mathematically calculated and presented in Table 4. By definition, the time constant reflects the time required to progress through 66.6% of each phase. In the hypertrophied muscle there was a 79.64% increase in the time constant of beta phase with a 33.53% decrease in alpha phase. The decreased time constant of alpha phase in hypertrophied muscles was due to a lower amplitude in alpha phase which can be found in Figure 16 (A). These

80

altered time constants were consistent with the increase ($+32.23\%$) and decrease (-64.37%) of the percentage contribution of beta and alpha phases of the hypertrophied muscles to the total curves. These changes are also clearly illustrated in Figure 15 where the total curve and each of the isolated phases, alpha and beta, are depicted on a single graph for each experimental group. The parameter of maximal rate was used to indicate the slope of ascending limb for each phase, which can reflect the sensitivity of developed force to the altered rest intervals. There appeared to be no change in the maximal rate of the alpha phase between the two groups, while the maximal rate of beta phase was faster in hypertrophied muscles.

DISCUSSION

The force-interval relationship in rat myocardium clearly shows that the time interval between contractions can alter the cardiac contractile state and has been extensively used to reflect intracellular Ca^{2+} handling (Ragnarsdottir et al. 1982, Schouten et al. 1987, Schouten 1990, Banijamali et al. 1991). The mechanisms of force-interval relationship can be explained by the current model of cardiac mechanical restitution (Fig 11). The Ca^{2+} influx upon membrane excitation triggers Ca^{2+} release from the SR Ca^{2+} release channels. The released Ca^{2+} from the SR activates contraction. After contraction, most but not all of the Ca^{2+} can be resequestered by the SR Ca-ATPase pump while the remaining Ca^{2+} is extruded from the cell via the sarcolemmal Na-Ca exchange. The time-dependent recovery in the SR Ca^{2+} release channels has been widely reported in skinned cardiac muscles (Fabiato 1981, 1983), and intact

81

preparations (Banijamali et al. 1991, Schouten et al. 1991). In rat myocardium, the small magnitude in twitch contraction seen at short rest intervals is due to the finite time required by the SR Ca^{2+} release channels to fully recovery after a contraction. Thus, the alpha phase of mechanical restitution is characterized as a time-dependent recovery of the SR Ca^{2+} release channels from inactivation following SR Ca^{2+} release.

In contrast to many other species that exhibit a characteristic rest decay when subjected to long diastolic interval (Arlock et al. 1988), the rat myocardium has a unique rest potentiated contraction, which consists of the beta phase of the force interval relationship. The explanation of the rest potentiation in rat cardiac muscles may be attributed to either: (1) diastolic net sarcolemmal influx of Ca^{2+} via reversed Na-Ca exchange (Fig 11), which gradually fills the SR (Schouten 1990). It is possible that Ca^{2+} will enter the cell via the reversed Na-Ca exchange during diastole. The direction of net Ca^{2+} movement depends on the transsarcolemmal Na^+ gradients (Bers et al. 1989). The resting intracellular Na^+ concentration in rat is 12.7 mM and is high enough that Ca^{2+} entry via Na-Ca exchange could be slightly favoured during diastole (Bers et al. 1989). (2) Relatively avid SR Ca^{2+} loading with virtually no diastolic Ca^{2+} leak or (3) longer time for full recovery of the SR Ca^{2+} release channel from inactivation. These unique characteristics of rat myocardium result in greater SR Ca^{2+} accumulation, which contributes to more SR releasable Ca^{2+} and thus a potentiated contraction at longer rest intervals. Based on the current E-C coupling model, the beta phase of the force-interval relation has been interpreted to reflect the activity of sarcolemmal Na-Ca exchange, the dominant contributor to rest potentiation.

Examination of the force-interval relationship in control and hypertrophied rat hearts revealed a biphasic response (Fig 14), similar to that reported in the literature for

control (Ragnarsdottir et al. 1982, Schouten et al. 1987, Schouten 1990, Banijamali et al. 1991), hypothyroid (Pogessi et al. 1987) and hypertrophied hearts (Taylor et al. 1988, Crozatier et al. 1987). These results (Fig 15) indicate that the fundamental characteristics of the force-interval relationship still exist in hypertrophied muscles.

The force-interval relation from raw data in the present study was fitted to a general two compartment model. This was useful because each compartment (alpha and beta) could be mathematically isolated from the total force-interval curve, and analyzed to determine if alterations in each process were independent or a simple amplification or depression in the total force-interval response.

Figure 14 shows that hypertrophied muscles significantly modulated the shape of the force-interval curve. Specifically, the beta process was more dominant while the alpha phase remained unchanged.

The shape of ascending limb of the alpha process (Fig 16, A) did not change, but the amplitude was slightly lower in the hypertrophied muscles. The quantitative data presented in Table 4 indicated that both the decreased time constant and percent contribution to total force recovery coupled with an unchanged maximal rate in the hypertrophied muscles are consistent with lower amplitude and the unchanged shape of alpha process in Figure 16 (A). These results suggest that the alpha phase tends to disappear early (or early occurance of the potentiated contraction, i.e. beta phase) in hypertrophied muscles, although there was no alteration in the rate of early force recovery.

In terms of intracellular Ca^{2+} handling, these results suggest that chronic administration of isoproterenol does not affect the characteristics of SR Ca^{2+} release delay at short rest intervals. There are two possible explanations for the unchanged

kinetics of SR Ca^{2+} release in hypertrophied muscle. First, chronic treatment of isoproterenol may not affect the mechanisms of the SR Ca^{2+} release; Second, the function of the SR Ca_{2+} release channel may be decreased while other cellular pathways (i.e., sarcolemmal Ca^{2+} influx and SR Ca^{2+} content) can compensate for the altered characteristics of SR Ca^{2+} release in hypertrophied muscle. Based on the following evidence, the second possibility seems to be a reasonable explanation. (1) There was an enhanced Ca^{2+} influx in hypertrophied muscles (see Chapter 6) and (2) the total SR Ca^{2+} content was increased in this experiment model (see Chapter 6). (3) Early activation of the beta phase (or early disapearance of the alpha phase) suggests that the uncompensated release of the SR Ca^{2+} occurs with further accumulation of the SR Ca^{2+} due to the early involvement of Ca^{2+} influx via Na-Ca exchange.

Taken together, the compensated mechanisms seem to contribute to the unchanged characteristics of SR Ca^{2+} release during the phase in early force recovery in hypertrophied muscles.

The beta phase (Fig 16, B) showed that not only the amplitude increased, but also an early activation (leftward shift) and an increased slope of the ascending limb of this process. The quantitative information indicated an enhanced percentage contribution, a prolonged time constant, and an enhanced maximal rate. These results suggest that increased force generation at longer rest intervals significantly dominates the total force restitution, which results in an increased potentiated contraction in hypertrophied muscles.

In the current E-C coupling model, the explanation for the beta phase is highly dependent upon sarcolemmal Na-Ca exchange activity. The enhanced beta process in hypertrophied muscle would suggest an increased influx of Ca^{2+} via the Na-Ca

exchange during longer rest intervals. Because the direction of net Ca^{2+} movement mainly depends on the intracellular Na^+ concentration, the reversed Na-Ca exchange seems to imply a high intracellular Na^+ concentration, which may result from either an increased Na^+ influx or/and decreased Na^+ efflux in hypertrophied muscles. Although there is no evidence to show an increased Na^+ influx in this study, the reduced activity of sarcolemmal Na-K-ATPase pump, which is the main pathway of Na^+ efflux, has been reported in hypertrophied myocardium induced by hypertension (Clough et al. 1983, Whitmer et al. 1986).

In summary, based on the mathematic modelling of the force-interval relation, this study suggests that the characteristics of the SR Ca^{2+} release were not altered during the early phase of force recovery. However, the SR Ca^{2+} release was significantly increased at longer rest intervals (beta phase) which may be partially explained by enhanced Ca^{2+} influx via a reversal in Na-Ca exchange in hypertrophied muscles. The increased Ca^{2+} influx may compensate for the SR Ca^{2+} release delay at short rest intervals, which results in early occurance of potentiation contraction in hypertrophied muscle.

CHAPTER 6

FORCE-FREQUENCY RELATIONSHIP OF HYPERTROPHIED RAT HEART

INTRODUCTION

In mammalian cardiac muscle, increased stimulation frequency has been shown to lead to an increased contractile force in a wide variety of animal species, for example, in sheep, cat, rabbit, guinea pig (Schouten 1985). However, the force-frequency relationship is a controversial issue in rat myocardium with a negative response in papillary muscle (Orchard et al. 1985, Stemmer et al. 1986, Schouten 1985, Bouchard et al. 1989), a biphasic rate staircase in thin ventricular trabeculae (Schouten et al. 1991) and single myocyte (Borzak et al. 1991). It is generally agreed that the positive force-frequency response results from more intracellular Ca^{2+} available for the activation of the myofilaments. Borzak et al. (1991) support the Na^+-lag hypothesis in which an increased stimulation rate results in a higher steady-state intracellular Na^+ due to more action potentials per unit time. The elevated intracellular Na^+ inhibits Ca^{2+} extrusion from the myocyte, and possibly even favours net Ca^{2+} entry (Shattock et al. 1989, Simon 1989), via the Na-Ca exchange mechanism. Recent work by Schouten et al. (1991) indicated that the positive force frequency relation is partially supported by a frequency-dependent inward Ca^{2+} current (I_{Ca}) in intact rat myocardium.

Because the force-frequency response is still a controversial issue in the rat heart,

the first aim of this study was to identify this relationship in thin trabecular muscle and to clarify the contribution of the sarcolemma and sarcoplasmic reticulum to frequency dependent force development.

Because chronic administration of isoproterenol results in cardiac hypertrophy and increased peak force development, the second aim of this study was to determine if the force-frequency response was maintained in the hypertrophied state and if the contribution of the sarcolemma and sarcoplasmic reticulum pathways was changed in this model of cardiomegaly.

METHODS

1. Experimental stimulation Protocol

After the muscle was equilibrated for 60 minutes, the tissue was stimulated with the following series of test frequencies: 0.1, 0.3, 0.5, 1.0, 1.5, 2.0, and 2.5 Hz. At each stimulation frequency the muscle was allowed to reach a new steady-state developed tension before the force signal was digitized. Each test frequency was separated by a control stimulation frequency of 0.2 Hz. Contractile force at a stimulation frequency of 0.2 Hz was used as a control before giving a new test frequency, in order to minimize errors (Schouten 1985) due to variations in peak force during the prolonged time course of the experiment. The force-frequency curves were derived by plotting developed tension normalized by peak force at 0.2 Hz as a function of the test frequency series.

2. Calcium Modulation Experiment

The effect of extracellular calcium concentration ($[Ca^{2+}]_o$ = 0.5, 1.0, 2.0 mM) on developed force was achieved by adding appropriate amounts from a 1 M $CaCl_2$ stock solution.

The Ca^{2+} channel blocker, nifedipine, was solubilized in 95% ethanol to provide a 1 mM stock solution. Samples were added directly from this stock solution to the perfusate to give a final 0.1 uM nifedipine solution. The addition of nifedipine resulted in 0.01% (v/v) ethanol in the perfusate and had no effect on contractile force (Post et al. 1991). During the experiments, the muscle and perfusate were protected from room light to avoid possible photodegradation of nifedipine (Lynch 1991).

Ryanodine, a pharmacological modulator of the SR, was added from 1 mM stock aqueous solution to give a final 0.1 uM concentration in the perfusate.

After the addition of these drugs (nifedipine, ryanodine), muscles were equilibrated for 30 minutes at 0.2 Hz before proceeding with the stimulation protocols. This equilibration period was adequate to provide a stable pharmacological effect on contractile force.

3. Rapid Cooling Contractures (RCCs)

Rapid cooling was achieved by switching the perfusion solution using a pair of solenoid valves (Cole Parmer) located close to the inlet of the muscle bath. One valve was in the normally open configuration while the other was normally closed. The solenoids were externally triggered with a 12 DC supply and controlled the flow of a bypass system (either cold or warm) to the muscle bath (Banijamali et al. 1991, Bers et al. 1990). The exchange of warm buffer (26° C) to cold (0 ~ 0.5 °C) was typically

completed in less than 0.4 seconds as measured by a thermocouple at the surface of the muscle. The RCC was initiated following the last steady state contraction. The interval between the last twitch contraction and RCC was the same as that test frequency studied.

4. Statistic Analysis

Data were expressed as means ± standard error (S.E.). All comparisons were performed by calculating the two-sided probabilities with the t-test for paired observations.

RESULTS

1. Effects Of Stimulation Frequency On Contractile Force

The initial experiments of stimulation frequency on contractile force were studied at 0.5 mM $[Ca^{2+}]_o$. An increase in contraction rate caused a biphasic force frequency response in both control and hypertrophied muscles (Fig 17). The force frequency curves were derived by plotting the developed tension normalized by the peak force at 0.2 Hz as a function of the test frequency series. A stepped increase in frequency from 0.1 to either 0.5 (control) or 0.3 Hz (hypertrophy) resulted in a decrease of contractile force, i.e., the negative phase of the force-frequency response.

At frequencies above 0.5 Hz, there was a clear and significant increase in developed tension, i.e., the positive phase of the force-frequency relationship. In hypertrophied muscles, the magnitude of the positive staircase was significantly
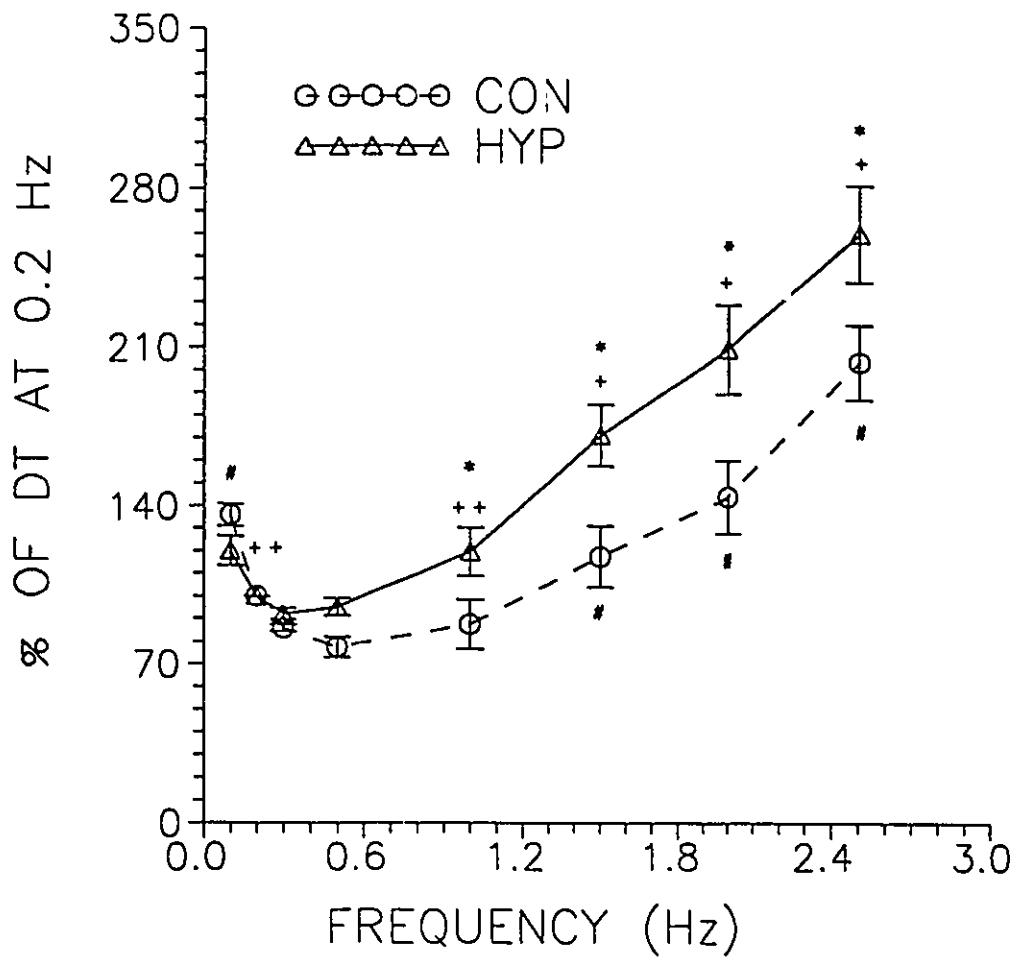
Figure 17. Influence of stimulation rate on steady state developed tension (DT) shown in relative scales. Significant differences were shown: "#" from 0.5 Hz in control (CON, n = 10, p<0.001); "+" from 0.3 Hz in hypertrophy (HYP, n = 6, "++" p<0.05, "+" p<0.001); "*", between hypertrophy and control at same test frequency (p<0.05). $[Ca^{2+}]_o$ = 0.5 mM.

greater than the controls.

These results are contrary to prevailing notions in which the rat possesses a unique negative force-frequency relationship (Orchard et al. 1985, Stemmer et al. 1986, Bouchard et al. 1989). However, my results are consistent with the recent reports that a biphasic rate staircase was revealed in isolated rat ventricular myocytes (Borzak et

al. 1991) and ventricular trabeculae (Schouten et al. 1991).

The biphasic force-frequency response suggests that two different mechanisms may contribute to frequency dependent force development in the rat. The mechanism (s) that contributes to the positive phase was enhanced in hypertrophied muscles.

2. Effects Of $[Ca^{2+}]_o$ On The Biphasic Rate Staircase

It has been reported that in thin trabeculae peak force was almost independent of stimulation frequency in 2.5 mM $[Ca^{2+}]_o$ (Schouten 1985). Probably, at this calcium concentration at least one transport pathway became saturated, i.e., peak force was nearly maximal at different stimulation frequencies. Previous results (Taylor et al. 1988) indicate that 2.5 mM $[Ca^{2+}]_o$ was close to Ca^{2+} saturating conditions in rat trabeculae. In this study, three non-saturating $[Ca^{2+}]_o$ concentrations (below 2.5 mM) were chosen to determine the effects of $[Ca^{2+}]_o$ on the biphasic force-frequency relationship.

When $[Ca^{2+}]_o$ was increased from 0.5 to 1.0 mM, the positive phase of the force-frequency relationship was significantly decreased in hypertrophied muscles (Fig 18). However, this $[Ca^{2+}]_o$ did not significantly modulate the positive force frequency response in the control group. When the extracellular calcium was increased from 1.0 to 2.0 mM the biphasic force-frequency response was similar in both the control and hypertrophied muscles. With higher $[Ca^{2+}]_o$ concentration (2.0 mM), changes in the stimulation frequency had little effect on developed tension in both groups. The general effect of increasing $[Ca^{2+}]_o$ was to flatten the positive phase of force frequency response. The hypertrophied muscles were more sensitive to changes in extracellular calcium (from 0.5 to 1.0 mM) than the controls.
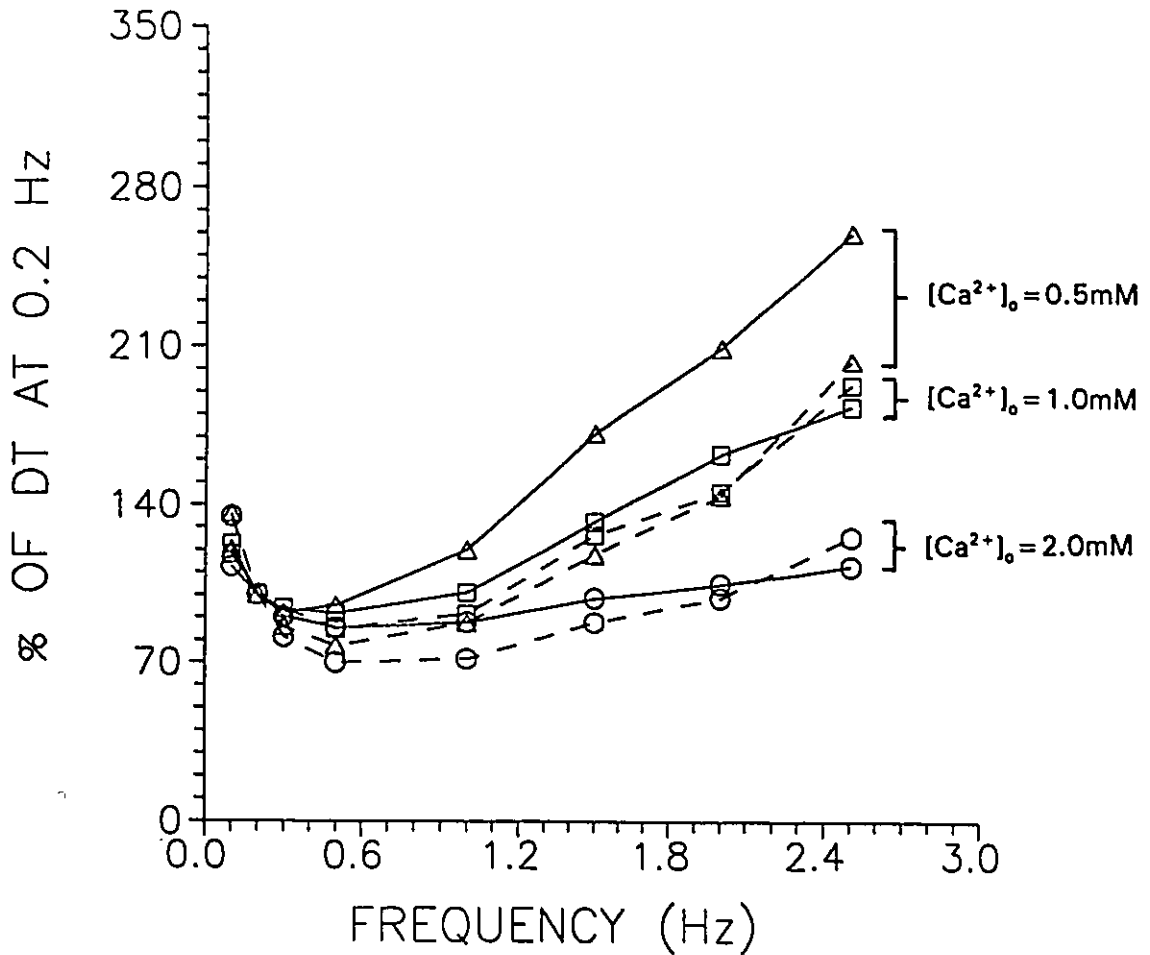
Figure 18. Effects of different $[Ca^{2+}]_o$ on the biphasic force frequency relationship in control and hypertrophied muscles. Solid (—) and dashed (- -) lines, respectively, represent hypertrophied and control group. The numbers of preparations are shown in Appendix 4 (Table 13, 14, 15).

3. Effect Of Stimulation Rates On The SR Ca^{2+} Content

Calcium released from the SR induced by rapid cooling of the muscle (to near 0°C) activates a contracture, the amplitude of which is indicative of the SR Ca^{2+} content (Banijamali et al. 1991, Bers et al. 1990). To assess the relationship between the SR Ca^{2+} content available for contraction and the steady-state twitch force following

different test frequencies, rapid cooling contractures were initiated following the last steady-state stimulated contraction with the same rest interval as that test frequency. Figure 19 shows that increasing the frequency of stimulation, there was a parallel increase in twitch force and the SR Ca^{2+} content in both the control and hypertrophied muscles. There was a more sensitive enhancement of the SR Ca^{2+} content in hypertrophied muscles than the controls at higher stimulation frequency. These results suggested that (1) the releasable SR Ca^{2+} content is proportional to the twitch tension, and (2) there was a higher capacity of the Ca^{2+} handling in this model of hypertrophy, which could contribute to a greater SR Ca^{2+} content with increasing frequency of stimulation.

4. Effects of E-C Coupling Modulators (Ryanodine, Nifedipine) On Force-Rate Staircase

Ryanodine, which binds specifically to the SR Ca^{2+} release channel of the terminal cisternae in cardiac muscle, has been used in various studies to estimate the magnitude of the SR Ca^{2+} release (Lynch 1991, Banijamali et al. 1991). It has been widely reported that ryanodine can induce a Ca^{2+} leak from the SR during the interstimulus interval, resulting in a lower amount of SR Ca^{2+} to be released with each action potential (Lynch 1991, Banijamali et al. 1991).

The contributions of SR Ca^{2+} loading on the biphasic force frequency relationship between control and hypertrophied muscles were explored by using 0.1 uM ryanodine. At this concentration, ryanodine can induce SR Ca^{2+} leakage, but still permits Ca^{2+} reuptake and release during electrical stimulation (Borzak et al. 1991). Previous reports have indicated that the negative force frequency response in rat ventricular cells (Borzak et al. 1991), trabeculae (Schouten et al. 1991) and papillary muscles (Orchard
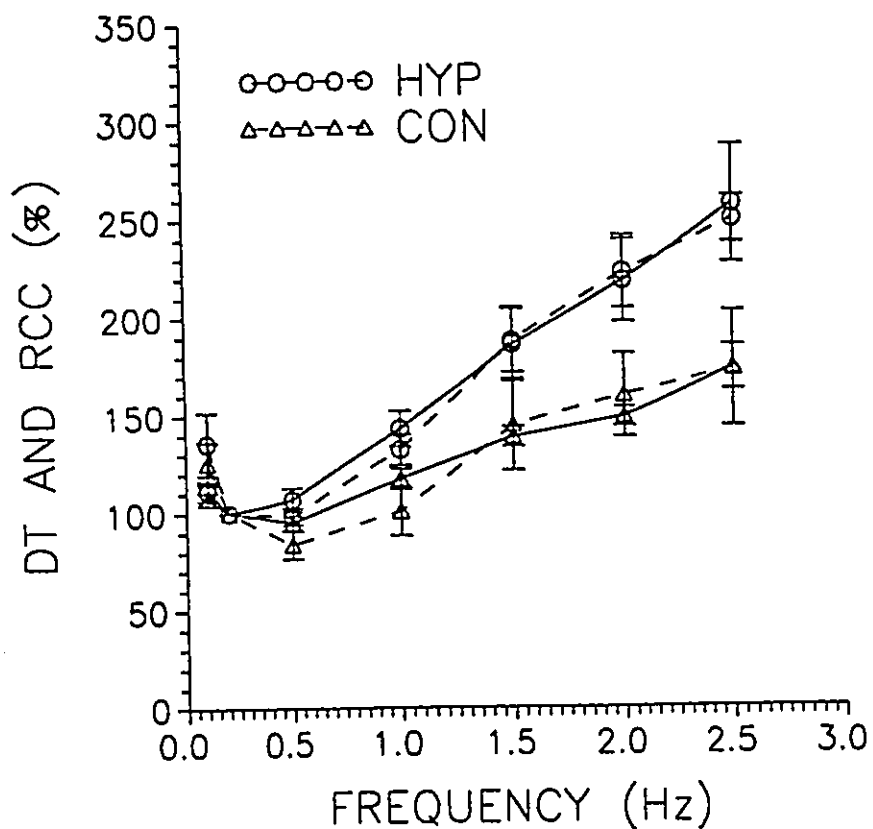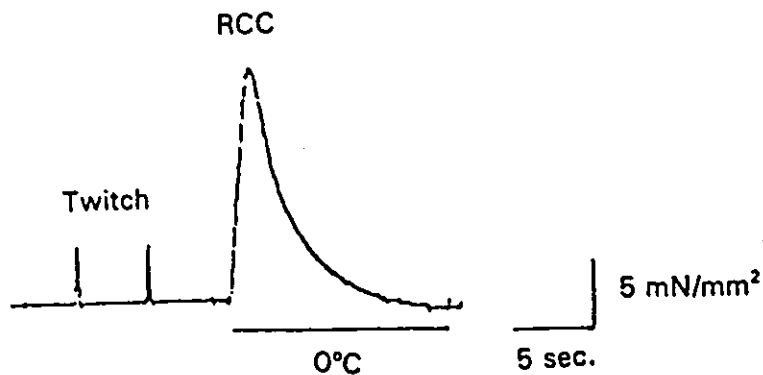
Figure 19. Effects of frequency on RCC and DT in both control and hypertrophied muscles. The top panel shows an original recording of a RCC induced after an interval of 5 seconds. $[Ca^{2+}]_o$ = 0.5 mM. All values (low panel) of RCC and DT were normalized by the respective RCC and DT at 0.2 Hz. Solid (—) and dashed (- -) lines, respectively, represent RCC and DT in control (DT, n=5; RCC, n=6) and hypertrophied (DT, n=10; RCC, n=10).

et al. 1985) was reversed following ryanodine treatment and was confirmed in the present study for both control and hypertrophied rat trabeculae (Fig 20).

In the negative phase, ryanodine transformed this response into a positive relation in both control (Fig 20, A) and hypertrophied (Fig 20, B) muscles. At stimulation frequencies above 0.5 Hz, ryanodine had no effect on the force of contraction in either control (Fig 20, A) and hypertrophied (Fig 20, B) muscles. In the presence of ryanodine, hypertrophied muscles developed a greater contractile force than the controls in the whole range of test frequencies studied (Fig 20, C).

These results suggest that SR Ca^{2+} loading dominates contractile force at low frequencies of stimulation. Because the contractile force was greater at lower frequencies of stimulation in hypertrophied muscles, this suggests an enhanced SR Ca^{2+} loading.

To determine the contribution of Ca^{2+} influx via sarcolemmal L-type Ca^{2+} channel on the biphasic force frequency relationship, the muscles were exposed to 0.1 uM nifedipine, which is known to block L-type Ca^{2+} channel (Borzak et al. 19, Schouten et al. 1991).

In contrast to ryanodine, which converted the negative response into a positive one at low frequencies of stimulation, nifedipine had little effect at low stimulation rate (0.1 – 0.3 Hz) (Fig 21). However, at frequencies above 0.5 Hz, nifedipine significantly inhibited contractile force and transformed the positive response to a negative relation in both control (Fig 21, A) and hypertrophied (Fig 21, B) muscles. Even though nifedipine eleminated the positive phase, muscles were still capable of developing twitch force. Careful examination of Fig 21 (C) indicates that hypertrophied muscles were able to develop a greater twitch force than the controls at frequencies below
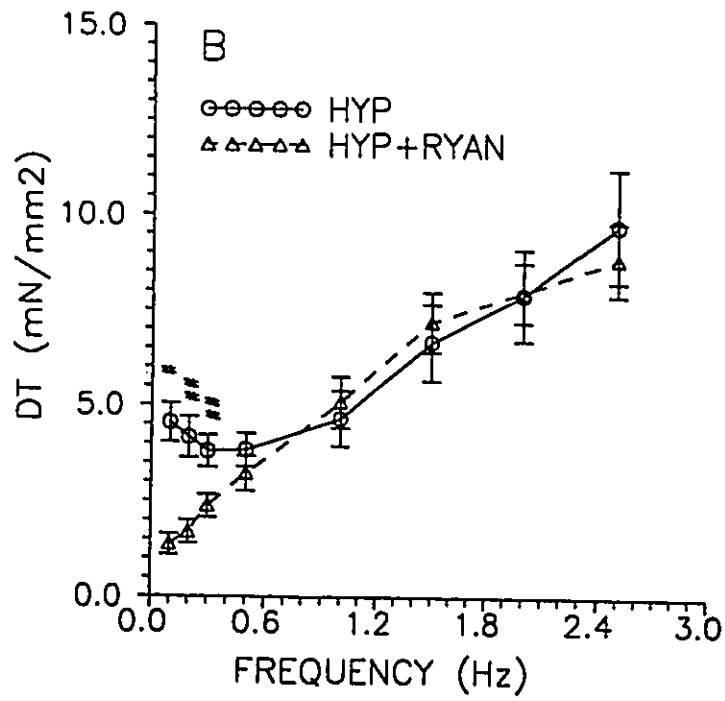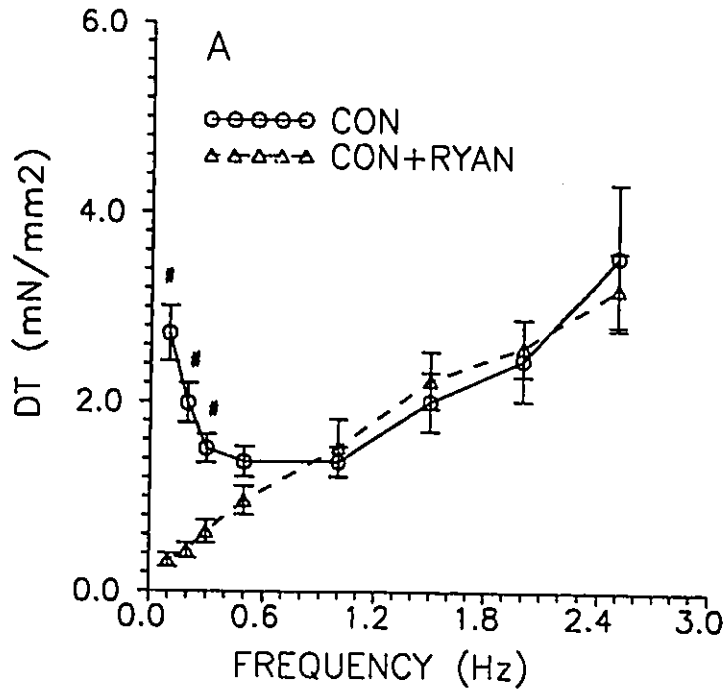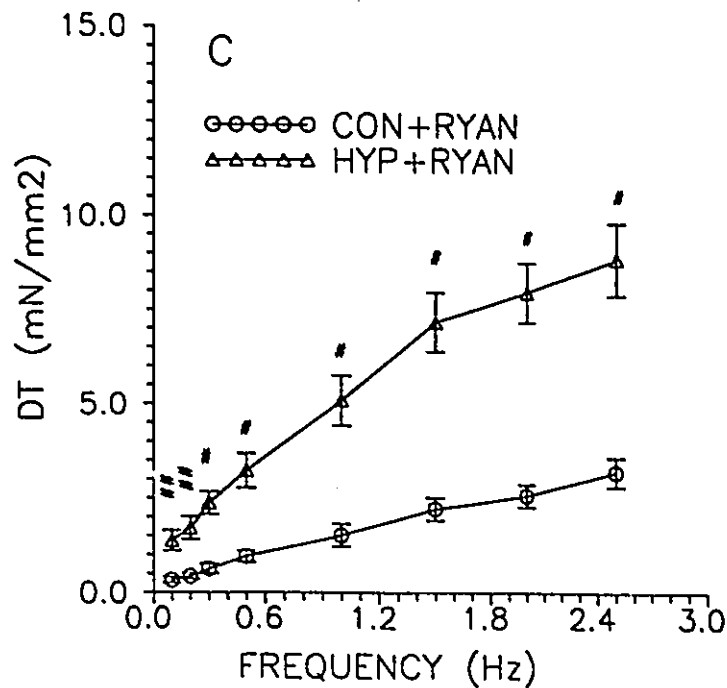
Figure 20. Effects of ryanodine on the biphasic force frequency relationship in both control (A) and hypertrophied (B) muscles. (C) showed a comparison between ryanodine treated control and hypertrophied muscles from (A) and (B). Significant difference (##p<0.05, #p<0.001) from corresponding value observed in the absence of ryanodine at the same test frequency. CON: control (n=10); CON+RYAN: ryanodine-treated control (n=6); HYP: hypertrophy (n=5); HYP+RYAN: ryanodine-treated hypertrophy (n=7). $[Ca^{2+}]_o = 0.5$ mM.

2.0 Hz. Consequently, nifedipine modulated the developed force only at higher stimulation rates and produced a monotonically negative response through the whole range of frequencies, in contrast to ryanodine that acted only at lower frequencies and produced a positive staircase in both control and hypertrophied muscles.

These results indicate that in the rat Ca^{2+} influx via sarcolemmal L-type Ca^{2+} channels plays a dominant role in developed tension at higher frequencies of

A

○○○○○ CON
△ △ △ △ △ CON+NIF

B

○○○○○ HYP
△ △ △ △ △ HYP+NIF

98
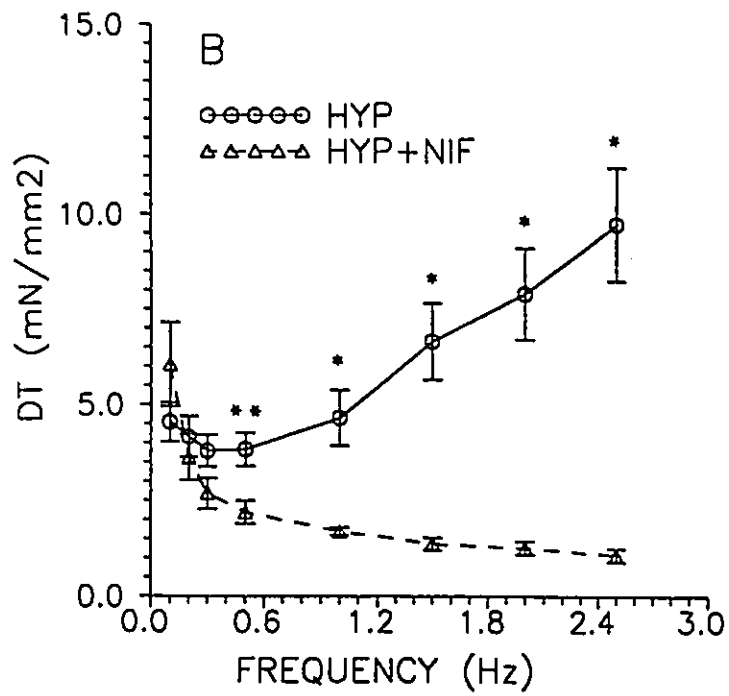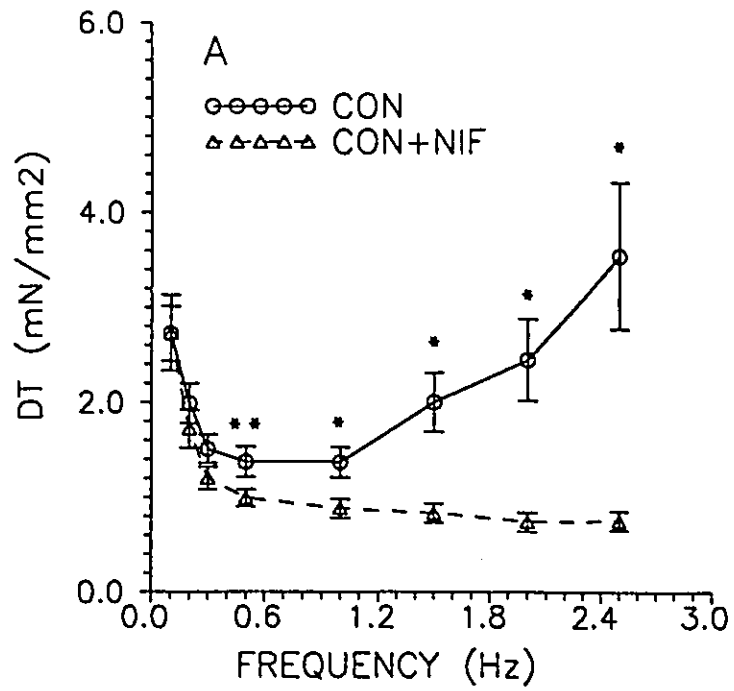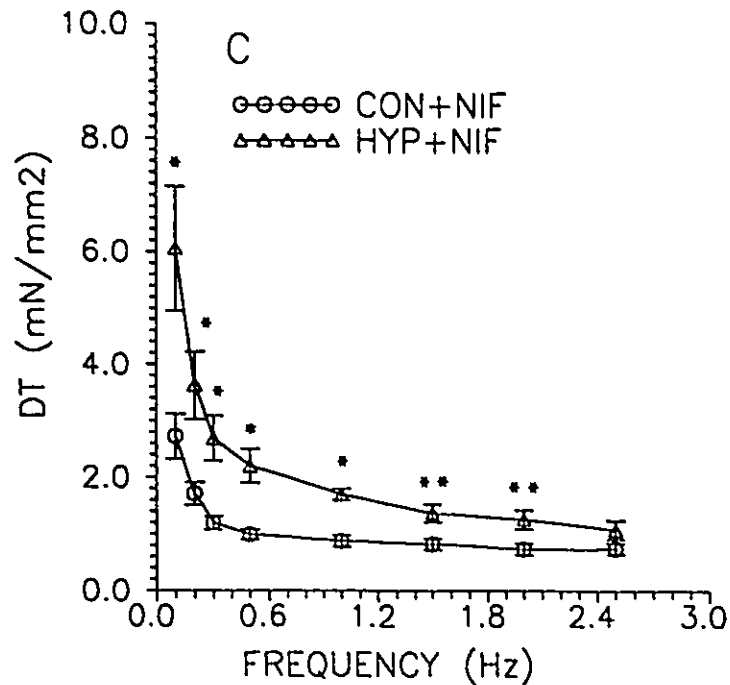
Figure 21. Effects of nifedipine on the biphasic force frequency relation in both control (A) and hypertrophy (B). (C) showed a comparison between nifedipine treated control and hypertrophy from (A) and (B). Significant difference (** p<0.05, * p<0.001) from corresponding value observed at the same test frequency. CON (n = 10); HYP (n = 5); CON + NIFED (n = 7); HYP + NIFED (n = 6). NIFED = nifedipine. $[Ca^{2+}]_o$ = 0.5 mM.

stimulation. The ability of hypertrophied muscle to maintain higher levels of contractile force than controls suggests a significant increase in Ca^{2+} influx during electrical stimulation in hypertrophied muscles.

DISCUSSION

1. The Biphasic Force Frequency Relationship In Rat Heart

99

In rat cardiac muscle the force frequency relationship is controversial because it is often found that contractile force decreases with increment in stimulation frequency, which is contrary to other mammals that exhibit a positive force frequency response (Schouten 1985, Stemmer et al. 1986, Shattock et al. 1989, Borzak et al. 1991).

Two main proposals have been suggested to account for the negative force frequency relationship in rat cardiac muscle. One is ischemia or diffusion limitation of metabolic substrates in intact cardiac muscle (Borzak et al. 1991, Schouten et al. 1991, Orchard et al. 1985). This factor was not believed to be involved in this study because at high frequencies and high $[Ca^{2+}]_o$, which may require a high rate of energy consumption (Schouten et al. 1991), an increase in contractile force was achieved. Also, evidence suggests that isolated trabeculae from the right ventricle of the rat having a "critical thickness" of $\leq$ 0.2 mm did not exhibit ischemia in the core cells of the muscle (Schouten 1985, Stemmer et al. 1986). In attempt to avoid the effect of muscle size, the thickness of the muscles used in the present investigation was less than 0.2 mm. Another factor that may contribute to a negative force frequency response is the time-dependent cycling of the SR Ca^{2+} (Orchard et al. 1985). It has been reported (Orchard et al. 1985) that at high stimulation rates there is less time for SR Ca^{2+} recycling, in which the stores of releasable SR Ca^{2+} would be expected to decline further and result in a decrease in the developed tension. Obviously, this cannot explain the increase in steady-state developed tension and the parallel increase in the RCCs at high frequencies of stimulation.

This study showed a biphasic force frequency relationship in rat trabecular muscles in 0.5, 1.0, and 2.0 mM $[Ca^{2+}]_o$. High extracellular Ca^{2+} has been reported to increase the SR Ca^{2+} loading and flatten negative rate staircase of rat heart (Orchard et al.

1985). This study confirmed that high extracellular Ca^{2+} inhibited the biphasic force frequency relationship, indicating that the SR Ca^{2+} loading can significantly modulate the force frequency relationship.

Rapid cooling contracture (RCC) in mammalian cardiac muscles provides valuable information about the relative SR Ca^{2+} content available for release. Recent studies have shown that rapid cooling of cardiac muscle to $0°C$ rapidly "freezes" the SR Ca^{2+} release channels in an open state, which allows a large and possibly complete release of Ca^{2+} from the SR (Bers et al. 1989). Rapid cooling is neither accompanied by an action potential nor by a depolarization of sufficient magnitude to cause gated Ca^{2+} entry into the cell (Bridge 1986). The amount of Ca^{2+} released by the SR in response to cooling is probably determined by the SR Ca^{2+} content, as has been shown by atomic absorption spectrophotometry (Bridge 1986). Experiments by Dani et al. (1979) on isolated myocytes showed that SR-related Ca^{2+} sequestration amounted to about 300 umol/kg wet weight. Bridge (1986) has shown that nearly all of this Ca^{2+} was lost from the tissue during a rapid cooling contracture (i.e., about 260 umol/kg wet wt). In the same study, a strong correlation between the magnitude of the rapid cooling contracture and the Ca^{2+} content was documented. Although part of the Ca^{2+} released may have some other origin, the similarity between SR Ca^{2+} sequestration in isolated myocytes and the amount of Ca^{2+} that was lost with cooling suggests that cooling causes a near complete Ca^{2+} release from the SR. Therefore, the measurement of amplitude of the contracture induced by rapid cooling was used to reflect the relative SR Ca^{2+} content in this study.

A parallel change in twitch force and the RCC in response to an increase in stimulation frequencies were achieved (Fig 19). The RCC data support two concepts:

101

(1) there was a greater SR Ca^{2+} loading at higher stimulation rates, and (2) the content of the SR Ca^{2+} changes with different frequencies and determines the amounts of Ca^{2+} released from the SR, thus the magnitude of twitch force.

Ryanodine binds with high specificity to the Ca^{2+} release channel proteins within the SR in cardiac muscle. This pharmacological treatment depresses twitch force without influencing other E-C coupling mechanism such as myofilament Ca^{2+} sensitivity, Na-Ca exchange and Ca^{2+} influx via L-type channel (Sutko et al. 1983). In the intact muscle preparation it has been shown that ryanodine at nanomolar concentrations exerts only one effect, that is, to convert the SR Ca^{2+} release channel to an opened low conductance state, which permits Ca^{2+} to leak out of the SR, decreasing the store of SR Ca^{2+} available for release (Banijamali et al. 1991, Lynch 1991).

In this study, it was found that ryanodine significantly decreased the steady state developed tension at lower stimulation frequencies and the negative force frequency response was converted to a positive phase. These results suggest that SR Ca^{2+} loading plays a major role in contractile force at the lower frequencies of stimulation. At high frequencies, ryanodine had little effect on the positive phase which is consistent with the time dependent leak of the SR Ca^{2+} induced by ryanodine.

However, sarcolemmal L-type Ca^{2+} channel blocker, nifedipine, significantly decreased contractile force at high frequencies of stimulation, which indicates that Ca^{2+} influx via L-type Ca^{2+} channel dominates the contractile force at high frequencies of stimulation.

Taken together, these results indicate that $[Ca^{2+}]_o$ concentration plays an important role in SR Ca^{2+} loading and the biphasic force frequency relationship. The amount of

the SR Ca^{2+} loading changes with different frequencies and determines the amounts of Ca^{2+} released from the SR, thus twitch force as confirmed by the studies of RCC. At low frequencies of stimulation, relatively avid SR Ca^{2+} loading could contribute to the negative phase of the biphasic relation; while at high frequencies, Ca^{2+} influx via L-type Ca^{2+} channel dominates the SR Ca^{2+} content. Therefore, the possible mechanisms that could differentially alter the amount of the SR Ca^{2+} in response to different frequencies of stimulation in both control and hypertrophied muscles will be discussed.

2. Contribution Of L-Type Ca^{2+} Channel On The Rate Staircase

There are two major extracellular sources of the SR Ca^{2+} in rat myocardium, the Ca^{2+} influx via L-type channels (I_{ca}) and the Na-Ca exchange (Bers 1991a). It seems unlikely that I_{ca} was the major source of the SR Ca^{2+} at low frequencies of stimulation, since nifedipine had no effect on developed tension in the present study. This phenomenon was comparable with others (Stemmer et al. 1986, Borzak et al. 1991). The I_{ca}, however, can significantly contribute to the developed tension at high frequencies of stimulation because nifedipine converted the positive phase into a negative one. These results indicate a frequency induced increase in Ca^{2+} influx and SR Ca^{2+} loading in intact rat heart, which results in a positive force frequency relationship at high frequencies of stimulation. In addition, there was a significantly greater positive force frequency behaviour in hypertrophied muscle, which might suggest that Ca^{2+} influx via L-type Ca^{2+} channels was increased. The increased I_{ca} may account for the greater developed tension, RCC and a more sensitive response to altered extracellular Ca^{2+} (Fig 18) in hypertrophied muscles.

103

3. The Role Of Na-Ca Exchange In The Force Frequency Relation

The Na-Ca exchange can transport Ca^{2+} into or out of the myocytes. The direction of net Ca^{2+} movement depends on the transsarcolemmal Na^+ gradients (Fozzard et al. 1986, Bers et al. 1989). Based on the following reasons, it is assumed that Ca^{2+} influx via Na-Ca exchange is a major extracellular source for SR Ca^{2+} at low frequencies of stimulation.

First, the resting intracellular Na^+ concentration in rat (12.7 mM) was high enough that Ca^{2+} entry via Na-Ca exchange may be slightly favoured at rest (Bers et al. 1990). Second, calcium sensitive microelectrode data clearly shows a rest induced transsarcolemma calcium influx (Shattock et al. 1989). The unique rest potentiated contraction in rat heart strongly supports the Ca^{2+} influx by the reversed Na-Ca exchange at longer rest intervals. Third, the I_{cn} is small because there are fewer membrane depolarizations per unit time coupled with the characteristically short action potential duration in rat heart (Schouten 1985). However, this study showed that the SR Ca^{2+} increased with decreasing frequencies of stimulation below 0.5 Hz. Fourth, because of the lack of nifedipine effect at low frequency of stimulation this suggests that the SR Ca^{2+} loading was not due to Ca^{2+} influx via L-type channels.

The hypertrophied muscles produced a greater steady-state contractile force compared to the controls, while exposing the tissue to nifedipine (Fig 21, C). If the reversed Na-Ca exchange contributes to the Ca^{2+} influx at low frequencies of stimulation, the greater contractile force (Fig 21, C) suggests that this pathway (Na-Ca exchange) was more active in the hypertrophied state, which more favoured the Ca^{2+} influx at low frequencies of stimulation. This is consistent with the force-interval study where a significant increase in the beta phase was observed in the hypertrophied

muscles, suggesting that sarcolemmal Na-Ca exchange was amplified to act as a net Ca^{2+} influx pathway at longer rest interval.

It needs to be mentioned that the results with nifedipine (Fig 21, C) do not support the Na-pump lag hypothesis which suggests that high stimulation rates can result in intracellular Na^+ accumulation due to more action potential per unit time. Intracellular Na^+ accumulation causes an elevated intracellular Ca^{2+} level via Na-Ca exchange, and thus a positive rate staircase (Borzak et al. 1991). Fig 21 (C) showed that developed tension did not increase in both groups with nifedipine treatment at high frequencies of stimulation (>0.5 Hz), suggesting that Ca^{2+} influx via Na-Ca exchange is not important. These data (Fig 21, C) further support the notion that Ca^{2+} influx via L-type channels plays a critical role in developed tension at high frequencies of stimulation.

At high rates of stimulation, there was a greater developed tension in hypertrophied muscles compared to controls (Fig 21, C) under treatment of nifedipine which is consistent with an enhanced Na-Ca exchange in hypertrophied state. However, the involvement of the Ca^{2+} entry via Na-Ca exchange declined with increasing rate of stimulation and, finally, did not show any difference between the two groups at 2.5 Hz (Fig 21, C). These data suggested there was a decreasing domination of Na-Ca exchange to elevate intracellular Ca^{2+}, and the Ca^{2+} influx via L-type channels shifted to the primary source of SR Ca^{2+} with increasing rates of stimulation.

The enhanced activity of the Na-Ca exchange in hypertrophy may also be explained by the results of ryanodine treated muscles. Figure 20 (C) shows a greater contractile force at low frequencies, while exposing the hypertrophied muscles to ryanodine. Because the ability of ryanodine to deplete SR Ca^{2+} depends critically on the ability of other transport systems (principally the Na-Ca exchange) to remove Ca^{2+} from the

105

cytoplasm under conditions where Ca^{2+} extrusion via Na-Ca exchange is limited, the SR Ca-pump can requestrate a large fraction of the SR Ca^{2+} lost by the ryanodine induced leak (Bers et al. 1989). Under hypertrophied conditions, it is possible that there was more Ca^{2+} in the SR, while exposing the muscle to ryanodine since the enhanced Na-Ca exchange mechanism could decrease Ca^{2+} efflux at low frequencies of stimulation.

There are two possible explanations for increased activity of reversed Na-Ca exchange (i.e., increased Ca^{2+} influx or decreased Ca^{2+} efflux) in hypertrophied muscle: (1) There may be a higher intracellular Na^+ in hypertrophied muscle. Simon (1989) reported that hypertrophied myocardium (spontaneous hypertensive rat)) has a higher intracellular sodium concentration in comparison to the controls. In isoproterenol induced cardiac hypertrophy, there was an enhanced Ca^{2+} influx via L-type channel (see Chapter 7). In order to balance steady-state intracellular Ca^{2+} homeostasis, Ca^{2+} efflux must be increased during relaxation. Because the stoichiometry of one intracellular Ca^{2+} is transported out of cell in exchange for the influx of three extracellular Na^+, the elevated intracellular Ca^{2+} extrusion can lead to an higher intracellular sodium (Fozzard et al. 1986). (2) There may be a reduced Na-K pump activity. Reduced activity of the Na-pump can cause intracellular Na^+ accumulation. Although we have not found any report about the altered Na-pump activity in isoproterenol induced cardiac hypertrophy, it has been reported that the Na-pump is less active in hypertrophied myocardium induced by hypertension (Clough et al. 1983, Whitmer et al. 1986).

In summary, there was a biphasic force frequency relationship in rat ventricular trabeculae. The SR Ca^{2+} content determines the steady-state twitch force. Both the

106

diastolic Ca^{2+} influx via Na-Ca exchange and the relatively avid SR Ca^{2+} loading contribute to the negative rate staircase at low frequencies of stimulation. The positive force frequency response is dominated by Ca^{2+} influx via L-type channels at high stimulation rates. The increased functioning of L-type Ca^{2+} channel and Na-Ca exchange may attribute to the higher intracellular Ca^{2+} in hypertrophied state.

CHAPTER 7

ELECTROPHYSIOLOGICAL CHANGES IN HYPERTROPHIED RAT HEART

INTRODUCTION

Calcium influx via sarcolemmal L-type channel (I_{ca}) represents the major source of external calcium for cardiac myocytes (Ten Eick et al. 1992). In hypertrophied myocardium the most consistent electrophysiological alteration is an increased duration in the transmembrane action potential (Bouron et al. 1992, Aronson 1980, Keung et al. 1981, Scamps et al. 1990, Nordin et al. 1989, Kleiman et al. 1988). The prolonged action potential in hypertrophied rat heart has been explained by an enhanced influx of calcium during action potential (Gulch et al. 1979, Aronson 1980, Capasso et al. 1986).

Binding studies with radioactive dihydropyridine clearly showed that the total number of L-type Ca^{2+} channels per left ventricle increased in pressure overload hypertrophy (Mayoux et al. 1988). Even though, the total number of calcium channels increased, the channel density remained constant. Recently, Scamps et al. (1990), by using whole cell patch-clamp to measure the activity of calcium channels, reported that the intensity of the calcium current per cell was increased, but the current density normalized per unit of membrane surface area remained unchanged, suggesting that the quantity of functionally active calcium channels increased with the degree of

hypertrophy.

The study on the force-frequency relationship (Chapter 6) led to the suggestion that calcium influx, in this model of cardiac hypertrophy, and especially at high stimulation rates may be one pathway that was enhanced. However, studies have reported that at short rest intervals (high frequency) in normal myocytes, the calcium current decreased, which is inconsistent with the notion of increased calcium influx with increasing frequencies of stimulation (See Chapter 6). These studies of calcium current were carried under voltage-clamp conditions with a holding potential of -60 to -40 mV in isolated rat (Mitchell et al. 1985) and guinea pig myocytes (Fedida et al. 1988). If the holding potential was close to the normal resting membrane potential (-80 mV) calcium current increased with frequency in isolated frog trabeculae (Noble et al. 1981) and myocytes (Argibay et al. 1988, Schouten et al. 1991). It has been suggested that results from enzymatically isolated cells, perfused with an artificial intracellular solution from the patch-electrode are not necessarily representative for intact heart muscle (Schouten et al. 1991).

Since the short, early plateau of the action potential (APD_{50}) in general is a good indicator for calcium influx (Mitchell et al. 1985, Schouten et al. 1985), the APD_{50} was used to:

(1). identify a possible frequency-induced increase in calcium influx (APD_{50}) in normal intact myocardium of the rat;

(2). identify if this calcium influx pathway becomes more dominant in the isoproterenol model of cardiac hypertrophy.

METHODS

1. Electrode Fabrication

A vertical pipette puller (Model 720, David KopF Inst. Calif.) with a parallel platinum strip heater filaments was used. Electrodes were drawn using WPI glass capillaries (Cat. No. IB100F-3; WPI). This type of glass capillary tube has a filament that aids in electrode filling. The electrodes were made in two stages (illustrated in Figure 22). First, a long-shanked straight electrode (2.5 ~ 3 cm) was drawn which tapered gradually from the electrode shoulder. In order to produce the required shank length in a single pull, the heater and solenoid of the puller were adjusted to 11.0 A and 1.4, respectively. Before the second stage fabricating, microscope inspection of all tips was carried out to ensure a final thinning of the electrode in the distal part (~ 100 um) with a sharp angle and an open tip. The second stage involved the bending of the electrode shank portion. The straight electrode was positioned at an angle of 70 ~ 80°C to the vertical shaft, while holding the electrode by hand. The electrode shank was bent downward between the filaments by using a lower heat setting (~ 6A). The final bend at the tip of the electrode (~ 5 mm) was fabricated by holding the electrode (tip downward) at an angle of 70 ~ 80 °C to the vertical shaft. The bent shank was positioned between the filaments and the heater briefly energized (heated). The final 5 mm of the electrode tip was bent downward by the heat and gravity of the electrode tip. To enable the heater to function during the manufacturing of the final bend, the lower chuck was raised from the rest position to inactivate the heating element when the electrode tip was bending downwards.
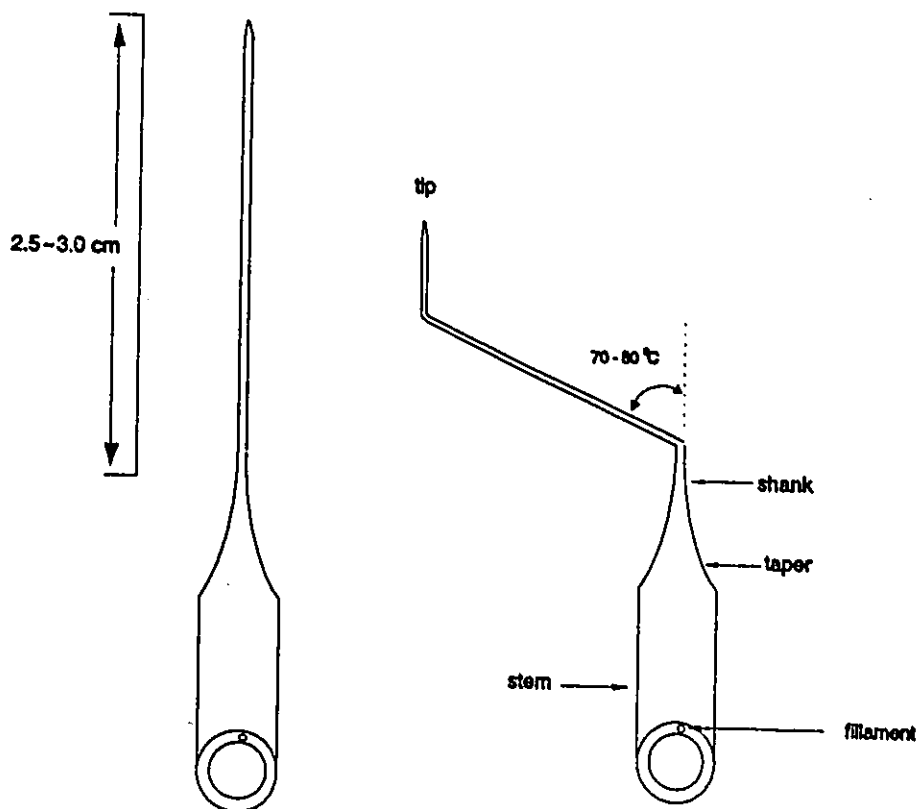
Figure 22. A schematic presentation of the stepped electrode.

The production of a long electrode shank resulted in a gradual taper throughout the 2.5 ~ 3 cm length with two steeper tapers toward the tip of the microelectrode. Fedida et al. (1990) reported that, by using the same fabrication technique, the final taper of the tip of the electrode was <0.5 um in length and the tip openning varied from 0.15 to 0.5 um. The presence of the final taper was examined for every electrode under the light microscope (Magnification = 500 Diameters, CAS Olympus TOKYO).

2. Electrode Filling And Set Up

The electrode was filled with 3 M KCl. The KCl solution was filtered through a glass bottle-top millipore filtration with a pore size of 0.45 uM. Because this electrode is long and stepped, it was difficult to fill the electrode by injecting KCl into the electrode capillary. Two steps were followed to fill the electrode. First, KCl was injected into the capillary by using a syringe with a long needle (PS 30). Small unfilled parts at the angles and tip can be observed under microscope. Second, in a sealed bottle (500 ml) containing ∼300 ml of 3 M KCl solution, the electrode was held at a vertical position (tip downward) and immersed in the KCL solution. A negative pressure was provided to the bottle by attaching a vacuum line. After 24∼48 hours, the electrodes were inspected under a microscope for complete filling. Normally, 20% of the electrodes were filled after 48 hours and the unfilled electrodes were discarded. The filled electrodes were kept in refrigerator (∼4 °C), immersed in KCl and reused.

The electrode was held in a right angle holder which plugged into the headstage of an electrometer (Electra 705, WPI). The output of the electrometer was connected to a preamplifier (10 times). The output signal of the preamplifier was digitized with a 12 bit A/D converter sampled at a rate of 2 kHz and stored on floppy discs. The signal was also simultaneously visualized with a digital storage oscilloscope. The resistance of the electrodes, filled with 3 M KCL, was 30∼50 megohm. Frequently, single cell impalement lasted up to 5∼6 hours even if the preparation contracted vigorously at different frequencies of stimulation. The action potential shape and resting membrane potential remained unchanged during the whole experiment. This stepped electrode design also allowed the headstage of the electrometer and the electrode holder to be more easily placed out of the optical pathway used to visualize the muscle. In order
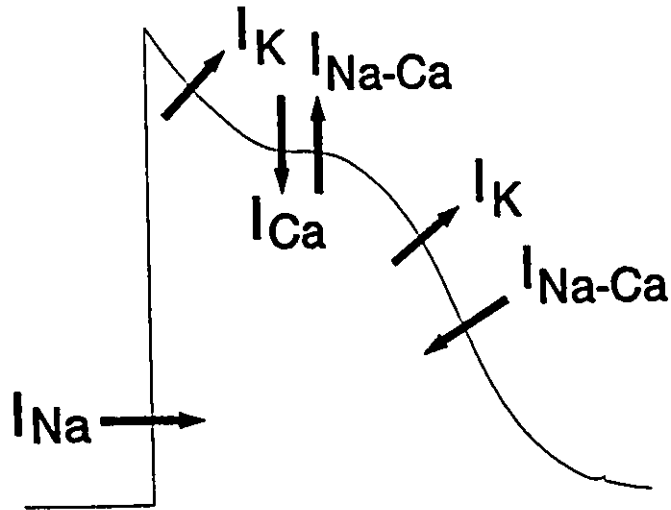
Figure 23. A typical membrane action potential. I_{Na}, fast inward sodium current. I_{Ca}, L-type calcium current. I_K, potassium current. I_{Na-Ca}, Na-Ca exchange current. The directions of the arrows for I_{Na-Ca} indicate the Na^+ flow.

to prevent mechanical disturbances in the electrical signal and contractile force, the micromanipulator and the microelectrode were supported on a heavy metal base which was fixed to the surface of an antivibration table.

3. Measurements of 50% Action Potential (APD_{50})

Figure 23 illustrates a typical membrane action potential and the associated phase changes. The action potential consists of a spike, due to the fast inward Na^+ current,

followed by a short plateau generated by the inward Ca^{2+} current, and the slow final phase of repolarization that is due to electrogenic Na-Ca exchange (Mitchell et al. 1985, Schouten et al. 1991). In this study, the duration of action potential at 50% of amplitude was focused on, which was primarily composed of the plateau phase. This plateau region is associated with voltage-dependent calcium channel function. The APD_{50} was used to reflect the contribution of calcium influx via L-type calcium channels (I_{ca}) during membrane excitation.

The action potential was recorded at a rate of 2 kHz. A computer programme (Unkelscope) was used to measure the duration of the action potential at 50% of its amplitude (APD_{50}). Based on the following reasons, APD_{50} was considered as an appropriate measurement of the plateau phase: (1) 50% repolarization is at -30 to -20 mV so that APD_{50} covers the period of calcium influx; and (2) 50% repolarization was about midway between the plateau and the slow final phase, i.e., variations in the amplitude of the slow phase of repolarization would have a minimal effect on the duration of the plateau (Schouten et al. 1991, Ten Eick et al. 1992).

4. Experimental Protocols

The experiments were initiated after an equilibration period of one hour at a stimulation frequency of 1 Hz in a modified Krebs-Henseleit buffer (see General Method). Stimulus pulses of 4 ms duration were derived from a stimulator connected to a stimulus isolator (Isostim A320 WPI). The membrane action potential was measured at the following stimulation frequencies: 0.2, 0.5, 1.0, 1.5, 2.0, 2.5, and 3.0 Hz. Each test frequency was separated by periods of a few minutes at the control frequency of 0.2 Hz.

114

1. Membrane Potential Characteristics

During stable impalements using the stepped flexible electrode it was possible to record membrane potentials continuously for 5 ~ 6 hours even during vigorous muscle contraction. Figure 24 shows a typical simultaneous recording of membrane potential and contractile force at low (0.2 Hz) and high (3.0 Hz) stimulation rates with 0.5 mM extracellular calcium. At the higher frequencies, contractile force increased. Careful examination of the action potentials clearly indicates that the duration was prolonged.

Table 5 summarizes changes in membrane potential under low (0.2 Hz) and high (3.0 Hz) stimulation rates between control and hypertrophied muscles. The resting (diastolic) membrane potentials were -78.4 mv and -74.5 mv, respectively, in control and hypertrophied muscles. At a low stimulation rate (0.2 Hz) peak membrane voltage in hypertrophied muscles was slightly but not significantly lower than the controls (106 mv vs 97 mv). At the higher stimulation rate (3.0 Hz) the peak of the action potential was significantly reduced compared to the value at 0.2 Hz in each group. The resting potential was slightly depolarized with increasing frequency from 0.2 Hz to 3.0 Hz in both the control and hypertrophied muscles (5 ~ 8 mv).

2. Effect Of Stimulation Rate On APD_{50}

In the rat, the action potential duration is relatively short compared to other animal species (Schouten et al. 1985). In hypertrophied rat myocardium the duration of the action potential was not affected by the amplitude of the signal since peak membrane voltage was not significantly changed. This suggests that components of

action potential
at 0.2 Hz

action potential
at 3 Hz

force at 3 Hz

0 mV

force at 0.2 Hz

-81 mV

100 ms
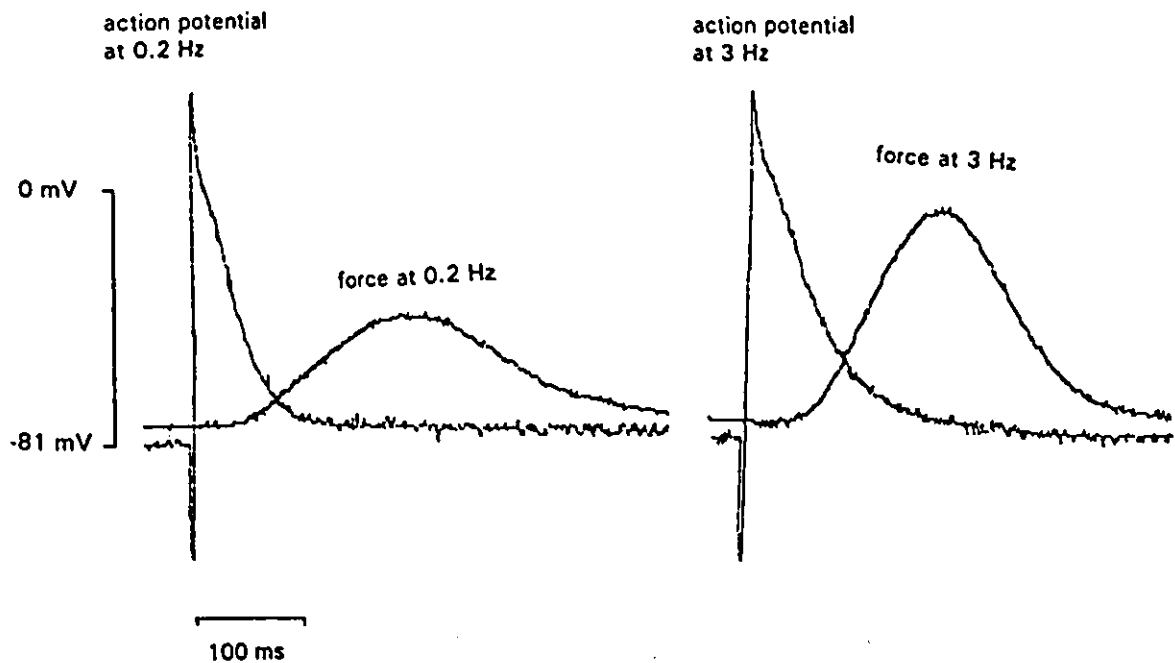
Figure 24. Comparison of frequency-dependent changes in the time course of the action potential and the associated contractile force from original records of control muscle.

the signal following the peak of the action potential must be modified. Figure 25 (top panel) compares a typical action potential from original recordings between control and hypertrophied muscles. The lower panel shows the response of the APD_{50} as a function of stimulation frequencies. In both control and hypertrophied muscles the APD_{50} lengthens with increasing stimulation frequency. The absolute value of steady state APD_{50} in the hypertrophied muscles was significantly enhanced compared with the control ones at all frequencies of stimulation studied (Fig 25).

116

Table 5. Characteristics of the action potei.tial of control and hypertrophied trabeculae.

	$APA_{0.2Hz}$ (mv)	$APA_{3.0Hz}$ (mv)	RP (mv)	$DRP_{0.2-3.0Hz}$ (mv)
CON	106.4 ± 6.0	$91.2 \pm 2.4^{\#}$	-78.4 ± 1.8	5 ± 2.1
HYP·	97.41 ± 5.1	$83.7 \pm 3.4^{*}$	-74.5 ± 2.4	8 ± 2.1

Values are mean $\pm$ S.E. for six preparations in each case. $APA_{0.2Hz}$ and $APA_{3.0Hz}$ represent action potential amplitude at 0.2 Hz and 3.0 Hz, respectively. RP, resting membrane potential. $DRP_{0.2-3.0Hz}$, depolarizing rest potential with increasing frequency from 0.2 to 3.0 Hz. * $p < 0.05$ compared with $APA_{0.2Hz}$ of the hypertrophied (HYP) muscles. # $p < 0.05$ compared with $APA_{0.2Hz}$ of the control (CON) group.

DISCUSSION

Action potentials were measured in thin ventricular trabeculae from control and hypertrophied rat heart and the plateau phase was isolated and analyzed as an index of calcium influx. The present investigation demonstrated that the APD_{50} was significantly prolonged in hypertrophied muscles at all series of stimulation frequencies studied. The lengthened action potential duration is consistent with previous reports of hypertrophied myocardium in different animal models (Bassett et al. 1973, Kleiman et al. 1988, Scamps et al. 1990, Aronson 1980, Thollon et al. 1989). Since I_{ca} (Ca^{2+} influx through L-type Ca^{2+} channels) is thought to play a major role in producing the
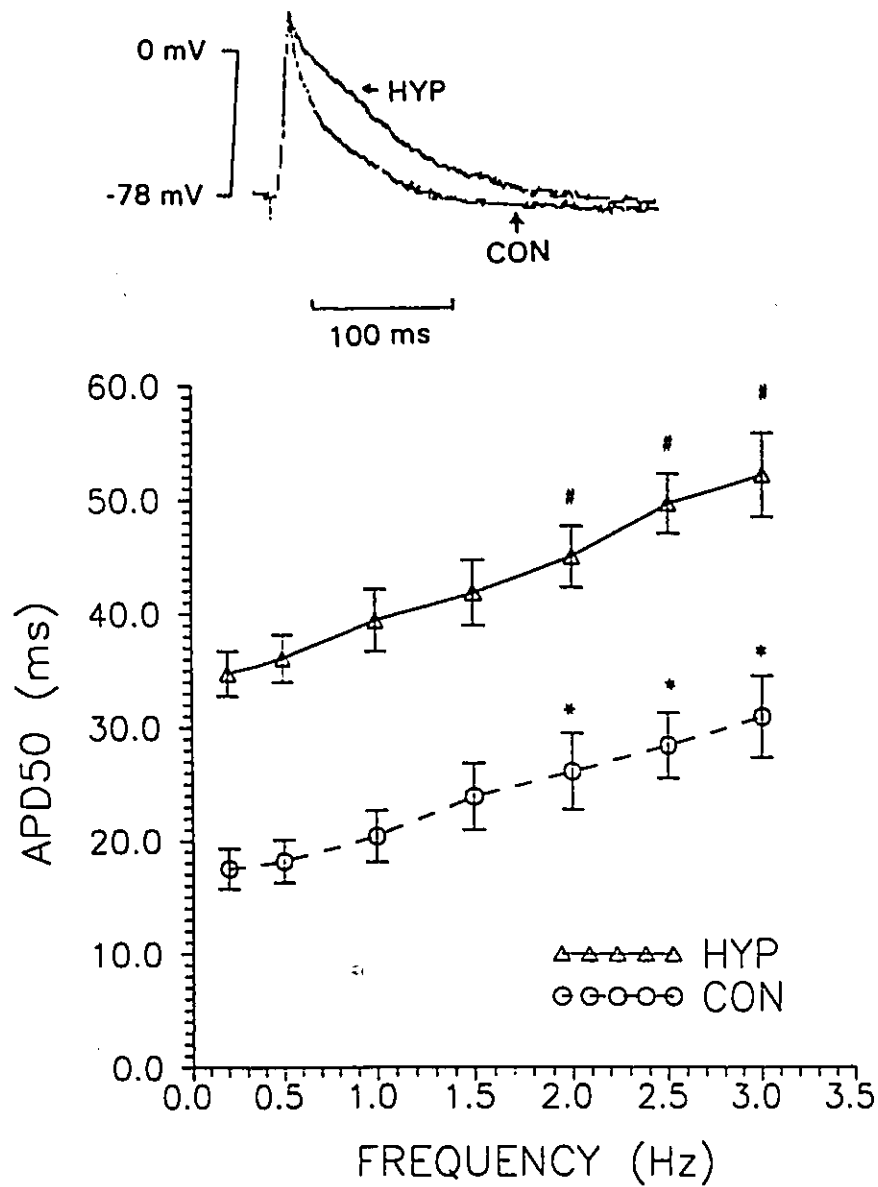
Figure 25. Comparison of APD_{50} in control and hypertrophied muscles at different frequencies of stimulation in 0.5 mM $[Ca^{2+}]_o$. The top panel shows the original records from control and hypertrophied muscle at 1 Hz. "*" and "#", respectively, represents the significant difference (p<0.05) from the value at 0.2 Hz in control (CON, n=6) and hypertrophy (HYP, n=6). The significant difference of the APD_{50} between CON and HYP at all series of frequency was not labelled.

118

prolonged plateau phase of the action potential in mammalian ventricular myocardium (Kleiman et al. 1988, Schouten et al. 1991, Scamps et al. 1990, Ten Eick et al. 1992), these data suggest that the transsarcolemmal Ca^{2+} influx was amplified in this model of cardiac hypertrophy, and persisted throughout a broad range of stimulation frequencies.

The mechanisms responsible for the prolonged duration of the action potential at present are not completely understood. However, Kleiman et al. (1988) and Keung (1989), using the whole cell patch clamp technique, found that a combination of: (1) an increase in peak net inward current and (2) a decrease in the rate of inactivation of I_{ca} appeared to contribute to the prolonged APD_{50} in hypertrophied myocardium. The early experiments of Aronson (1980), using a multicellular muscle preparation, also attributed the prolonged APD_{50} to a slower inactivation of the slow inward current. Recent data by Keung (1989) and Kleiman et al. (1988) clearly showed that the time constant of inactivation of I_{ca} was prolonged in hypertrophied myocytes. In addition, the peak inward current was increased 2.5-fold in Goldblatt renovascular hypertensive rats (Kleiman et al. 1988). On the other hand, Kleiman et al. (1988) showed no change in I_{ca} density (total calcium current normalized by membrane surface area), suggesting that the net inward membrane current was increased due to the increased membrane surface area of myocytes.

The inactivation of I_{ca} is thought to be controlled by Ca^{2+} influx through the Ca^{2+} channel and/or by changes in cytosolic free Ca^{2+} (Lee et al. 1980). Kleiman et al. (1988) has argued that the slower inactivation of I_{ca} in cardiac hypertrophy is somehow associated with a diminished sensitivity of the calcium channels to increases in cytosolic free Ca^{2+}.

119

The present study found that an increase in stimulation frequency leads to a consistent lengthening of the plateau phase of the action potential in both control and hypertrophied muscles, suggesting a frequency-induced enhancement of calcium influx. To date, both a negative and positive staircase of I_{ca} have been reported with increasing frequency in patch clamp studies by using isolated myocyte (Mitchell et al. 1985, Charnet et al. 1988) when membrane potential was held at -40 mv and -90 mv, respectively. These controversial patch clamp results have been attributed to different membrane holding potentials (Schouten et al. 1991). In thin ventricular trabeculae from rat heart, a positive APD_{50}-frequency relationship was found by Schouten et al. (1991), which is in agreement with the present results.

The result from the study of force-frequency relationship (Chapter 6) indicated two possible mechanisms with opposite frequency dependencies were involved: (1) the negative staircase at low stimulation rates was due to a strong dependence of SR Ca^{2+} stores filled by the diastolic influx of Ca^{2+}, and possibly via Na-Ca exchange, and (2) the positive staircase at higher rates was mediated by increased Ca^{2+} entry through the L-type Ca^{2+} channel that either reloads the SR with Ca^{2+} or contributes directly to myofilament activation. The consistent prolongation of APD_{50} in this study supports the contribution of I_{ca} to the positive staircase of force frequency response at higher stimulation rates. The physiological significance of this response probably amplifies the Ca^{2+} release by the SR ,or contributes to the direct activation to myofilaments, or both. The increased I_{ca} of hypertrophied muscles at different frequencies supports the amplified positive phase of force frequency relationship in hypertrophied muscles compared to control ones.

In the lower frequency range, APD_{50} consistently increased in this study (Fig 23),

whereas the force-frequency response (Chapter 6) showed that peak force decreased with increasing frequency (Fig 17), i.e., negative phase of force-frequency relationship in both groups. This response is not controversial because the I_{ca} plays little effect on the peak force at lower rates of stimulation, as manifested as no effect of I_{ca} blockage (nifedipine) on contractile force at lower frequency (Fig 21, A, B).

There was a significant decrease in the amplitude of action potential with increasing frequency of stimulation (0.2 Hz vs 3.0 Hz) (Table 5) in both control and hypertrophied muscles. Since the fast inward Na^+ current depolarizes the membrane, the amplitude of the action potential is more or less dependent upon Na^+ influx. A decrease in the density of the Na^+ current is expected to reduce the amplitude and the maximum upstroke velocity of action potential (Ten Eick et al. 1992). An increase of stimulation frequency may result in a higher steady-state intracellular Na^+ concentration due to more action potentials per unit time (Borzak et al. 1991). It is possible that higher intracellular Na^+ may inhibit the Na^+ entry during depolarization, and result in the decreased amplitude of the action potential with increasing frequency.

The slight depolarization of the resting potential with increasing frequency can be explained by the accumulation of K in the interstitium. Assuming a more or less constant K efflux per action potential, then the efflux averaged over time increases with frequency. In the steady state, the efflux of K is balanced by the accelerated Na-K pump and the interstitial K concentration and resting membrane potential maintained at the normal values (Ten Eick et al. 1992). The slight depolarization in the resting membrane potential in hypertrophy (8 ± 2.1 mv) compared with controls (5 ± 2.1 mv) may suggest a decreased functioning of the Na-K pump in the state of hypertrophy.

121

CHAPTER 8

RECIRCULATION FRACTION OF THE SARCOPLASMIC RETICULUM CALCIUM

INTRODUCTION

A key aspect of excitation-contraction coupling in mammalian myocardium is the presence of the sarcoplasmic reticulum (Bers et al. 1989). This compartment accumulates Ca^{2+} by an active process (SR Ca-ATPase pump), and releases Ca^{2+} upon Ca^{2+} influx into the cell during the ac on potential as a result of Ca^{2+} induced Ca^{2+} release.

The removal of the relatively large quantities of cytoplasmic Ca^{2+} following a contraction depends mainly on two mechanisms: the Ca-ATPase pump in the SR and the Na-Ca exchange in the sarcolemma. The rate of transport by the mitochondria and sarcolemmal Ca-pump appears to be too slow to significantly contribute to the beat to beat systolic and diastolic Ca^{2+} oscillations (Hryshko et al. 1989, Bers et al. 1989).

It is generally assumed that the SR Ca-ATPase pump is the principal pathway to remove cytoplasmic Ca^{2+}. Physiological estimates from post-extrasystolic potentiation studies (Schouten 1985, 1990) indicated that the SR removes $60-80\%$ of cytosolic Ca^{2+} following a contraction (recirculation fraction) while the remaining Ca^{2+} $(20-40\%)$ is extruded through the sarcolemma Na-Ca exchange pathway (Bers et al. 1990). On a beat to beat basis, the resting diastolic Ca^{2+} is determined primarily by

the competition of these two pathways: (1) the SR Ca^{2+} resequestration (recirculation) and (2) the sarcolemmal Ca^{2+} extrusion. Information on the recirculating fraction of the SR Ca^{2+} can be used to reflect the competition between the SR Ca^{2+} reuptake and Ca^{2+} extrusion through the sarcolemmal Na-Ca exchange.

In the hypertrophied heart, decreased abundance and/or function of the SR Ca-ATPase pump may lead to a reduction of the amount in Ca^{2+} recirculated by the SR (Lamers et al. 1979, Rupp et al. 1988, Kimara et al. 1989). However, the reported reduced activity of the Na-K-ATPase pump (Clough et al. 1983, Whitmer et al. 1986) in hypertrophied heart may cause intracellular accumulation of Na^+, which in turn inhibits Ca^{2+} extrusion via Na-Ca exchange and thus favours the Ca^{2+} reuptake by the SR Ca-ATPase pump. It is difficult to predict the outcome of the concerted effects of these pathways on Ca^{2+} transport, especially in isoproterenol induced cardiac hypertrophy, in which little information is available for the function of the SR Ca-ATPase pump and the sarcolemmal Na-K-ATPase pump.

The objective of this section was to investigate the relative physiological contributions of the SR Ca-ATPase pump and sarcolemmal Na-Ca exchange pathways to remove cytoplasmic Ca^{2+} during relaxation in control and hypertrophied muscles.

METHODS

Experimental Protocols

1. Post-Rest-Potentiation-Decay: Post rest potentiation decay was used to analyze beat-dependent recirculation of intracellular Ca^{2+} by the SR. Figure 26 shows the

123
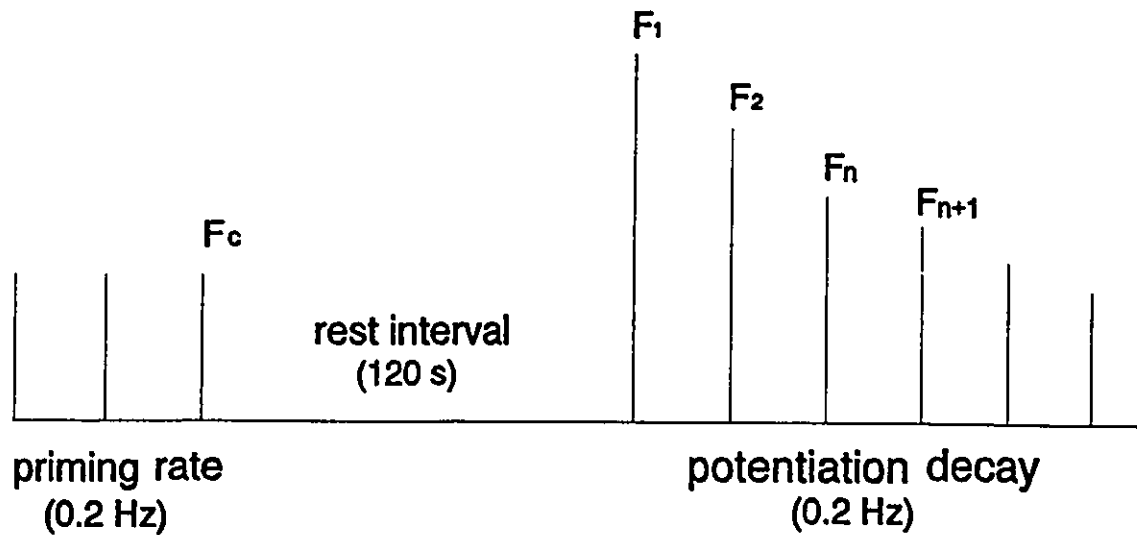
Figure 26. Experimental protocol of rest-post-potentiation-decay. F_c was the last steady-state contraction at a priming frequency of 0.2 Hz. F_1 was the potentiation contraction following a rest interval of 120 seconds. The remaining beats represent the decay from potentiation to steady-state force development.

stimulation protocol. The preparations were paced at a priming frequency of 0.2 Hz until the steady state was reached. One potentiated beat was initiated by interposing a long rest interval (120 seconds). This rest interval was chosen because it produced near maximal amplitude of contraction in both control and hypertrophied muscles. This high degree of the potentiated contraction (F_1) is important for accurate determinations of the recirculation fraction (Schouten et al. 1987). Following the potentiated contraction, contractile force decays over 6 beats were used to determine the beat to beat recirculation fraction of Ca^{2+} by the SR.

The post rest potentiation protocol is illustrated in Figure 26. Assuming that the

amount of Ca^{2+} taken up by the SR following the potentiated beat is constant, i.e., the recirculation fraction (r), then the loss of force with each beat should reflect the beat to beat Ca^{2+} extrusion (1-r) from the cell (Morad et al. 1973). The data for each muscle was linearized by plotting the force (F_{n+1}/F_c) for a given contraction after a rest interval as a function of the force of previous beat (F_n/F_c) as shown in Figure 28. This relation has been defined by the following equation (Schouten et al. 1987):

$$F_{(n+1)}/F_c = r.F_{(n)}/F_c + constant \quad .... \quad (1)$$

where $F_{(n)}$ is peak force of the nth beat after the rest interval. F_c is the force at the priming frequency. Thus, the recirculation fraction (r) is the slope of the linear regression of $F_{(n+1)}/F_c$ on $F_{(n)}/F_c$ calculated with the least squares method (Wohlfart et al. 1982, Schouten et al. 1987).

2. Paired Rapid Cooling Contractures (RCCs). Rapid cooling was achieved by switching the perfusate solutions using solenoid valves located close to the inlet ports of the muscle chamber. A bypass system allowed two separate solutions (independently temperature controlled at 26 °C and 0 °C) to circulate continuously. During cooling of the muscle, a rapid contracture (Fig 27) can be induced due to a large amount of Ca^{2+} released from the SR. Rewarming the muscle induces relaxation which occurs presumably due to reactivation mechanisms responsible for lowering intracellular Ca^{2+}. These would mainly include the Ca^{2+} removal by the SR and

125

extrusion by sarcolemmal Na-Ca exchange. Invoking a second RCC immediately after the first RCC should provide a relative index of the amount of Ca^{2+} resequestered by the SR during relaxation from the first RCC (Bers et al. 1986). This second RCC indicates the initial SR Ca^{2+} minus that amount of Ca^{2+} extruded during relaxation.

Figure 27 shows the experimental protocol of the paired RCCs. Different priming frequencies were used to determine the dependence of SR Ca^{2+} resequestration on the stimulation frequency. The series of priming frequencies were 0.1, 0.2, 0.5, 1.0, 1.5, 2.0, 2.5 Hz. The first RCC (RCC_1) was initiated at a same time interval as the priming frequency. The second RCC was initiated immediately after the RCC_1 was rewarmed and returned to baseline levels.

RESULTS

1. Recirculation Fraction From Post Rest Potentiation Decay Analysis

The recirculation fraction (r) was analyzed by calculating the slope of potentiation decay, as defined by equation (1). Figure 28 shows the potentiation decay response for both control and hypertrophied muscles. The slope (recirculation fraction) of this relation was slightly decreased in the hypertrophied muscles. However, this reduction was statistically non-significant (0.51 vs 0.46, p=0.35). The lower value of "r" represents a more rapid decay from the potentiation state, which reflects less Ca^{2+} was resequestered by the SR or more Ca^{2+} was extruded from the cell probably via sarcolemmal Na-Ca exchange.
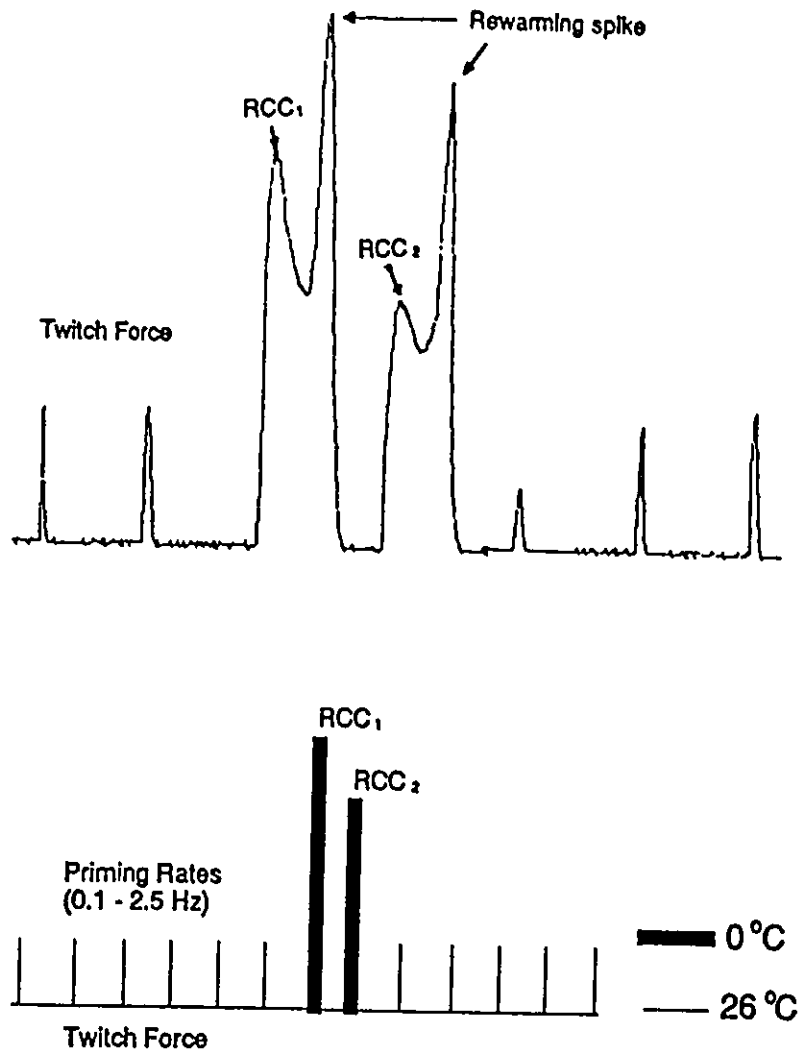
Figure 27. Experimental protocols (bottom) for paired rapid cooling contractures where a muscle was cooled (RCC_1), rewarmed, then recooled (RCC_2), and rewarmed again. RCC_1 was induced at the same time intervals as that priming frequency. Upper panel shows an example of raw data at a priming frequency of 0.2 Hz in control muscle. $[Ca^{2+}]_o = 0.5$ mM.
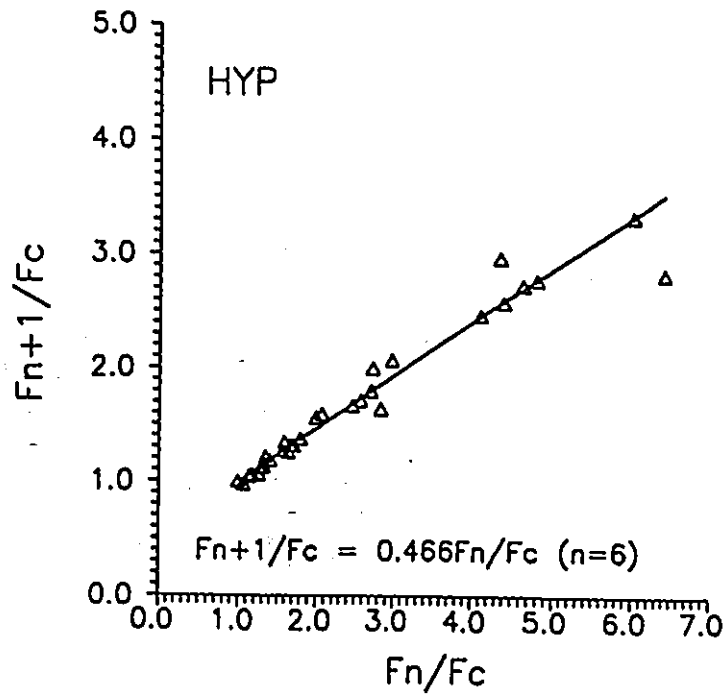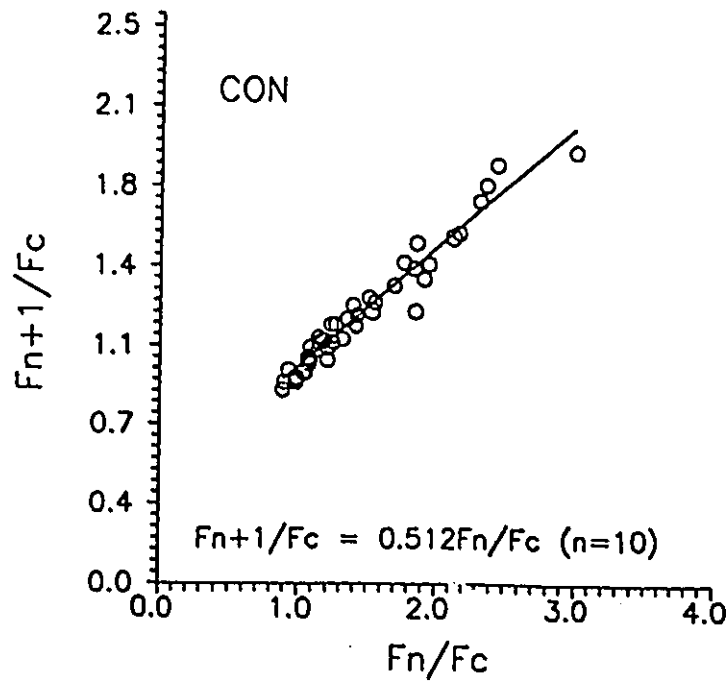
Figure 28. Plot of linearized potentiation decay in control and hypertrophied muscles. The F_n/F_c = force[nth] normalized by force at the priming frequency. F_{n+1}/F_c = force[(n+1)th] normalized by F_c. The experimental protocol can be seen in Figure 26. The linear best fit lines yielded the equations shown in above Figures.

2. Recirculation Fraction From Paired RCCs

Figure 27 shows a typical recording of paired rapid cooling contractures from control muscle at a priming frequency of 0.2 Hz (Upper panel). Rapid cooling of trabecula to $0 - 0.5°C$ in a 5.0 second interval following last twitch contraction induced SR Ca^{2+} release to the cytoplasm and subsequently activated a rapid contracture (RCC_1). The second RCC (RCC_2) was induced immediately after RCC_1 was rewarmed and force returned to baseline. The rapid cooling is neither accompanied by an action potential nor by a depolarization of sufficient magnitude to cause gated Ca^{2+} entry into the cell (Bridge 1986). The peak of the RCC has been used as a relative index of SR Ca^{2+} content that is available for release (Bers et al. 1989). Rewarming after a RCC leads to a transient increase of force (rewarming spike) that has been attributed to an increase in myofilament calcium sensitivity at higher temperatures while intracellular Ca^{2+} concentration is still elevated (Harrison et al. 1990). Rewarming also reactivates mechanisms responsible for relaxation, such as the SR Ca-ATPase pump and Na-Ca exchange, which were previously inhibited by the cold. Thus, the relaxation upon rewarming of RCC_1 from the "rewarming spike" to the baseline (complete relaxation) reflects the removal of calcium from the cytoplasm via either SR Ca-ATPase pump or Na-Ca exchange. The ratio of RCC_2/RCC_1 should provide a relative index of the amount of Ca^{2+} resequestered by the SR during recovery from the RCC_1.

Figure 29 shows the response of the SR recirculation fraction as a function of stimulation frequency as analyzed by paired RCC in both control and hypertrophied muscles. These curves were constructed by plotting the ratio of RCC_2/RCC_1 as a function of the different priming frequencies. The priming period was maintained long enough to establish an new steady-state contraction before RCC_1 was induced.
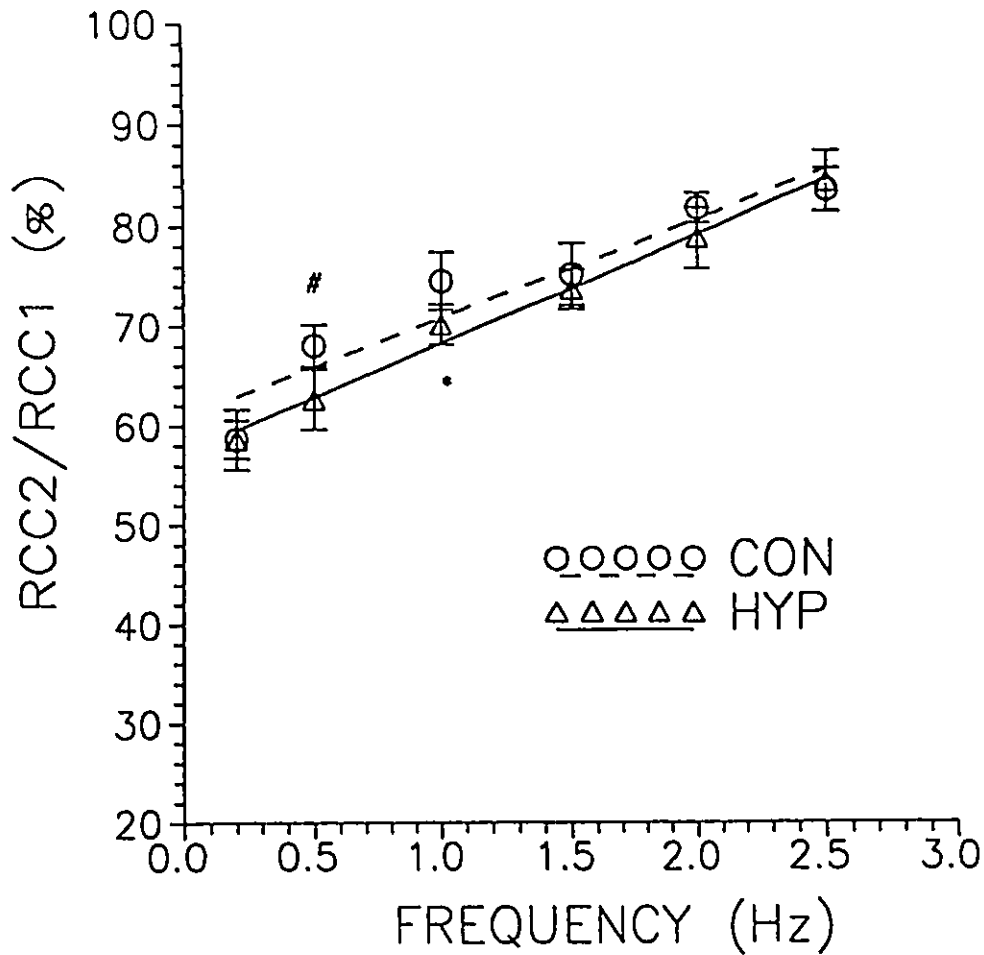
Figure 29. Rapid cooling contracture determination of the recirculation fraction of SR Ca^{2+} at different priming frequencies of stimulation in control and hypertrophied muscles. The recirculated Ca^{2+} of SR (r) was evaluated by the ratio of RCC_2/RCC_1 as shown in Fig 27. Each symbol represents the mean $\pm$ S.E. of both control (n = 7) and hypertrophied (n = 6) muscles. The lines were the least squares linear fit to the data. "#" and " * ", respectively, represents significant difference (p < 0.05) from control and hypertrophy at 0.2 Hz. $[Ca^{2+}]_o = 0.5$ mM.

Analysis of the RCC ratios indicated that there was no difference in the recirculated Ca^{2+} fraction by the SR between control and hypertrophied muscles. Most of the Ca^{2+}

released at the first RCC was resequestered by the SR, because the second RCC produced amplitudes of 58.64% ~ 83.4% and 58.6 ~ 84.2% (Figure 29, values shown in Appendix 6) of that of the RCC_1, respectively, in control and in hypertrophied muscles at different priming frequencies of stimulation. However, the recirculation fraction was sensitive to stimulation frequency and was significantly enhanced above 0.5 Hz in controls and 1.0 Hz in hypertrophied muscles.

DISCUSSION

In this study, two approaches were used to determine the SR Ca^{2+} recirculation fraction, i.e., the classical beat-dependent decay from the potentiated state (Morad et al. 1973, Schouten et al. 1990) and a novel application of paired RCCs (Bers et al. 1990). The slope of the regression analysis from potentiation decay studied attempts to estimate the fraction of Ca^{2+} resequestered by the SR during electrical stimulation. The technique of paired RCCs was used to maximally unload the SR Ca^{2+}. The second RCC following the rewarming (recovery) phase of the first RCC maximally unloads that fraction of SR Ca^{2+} that was resequestered during rewarming phase of the first RCC.

Figure 30 illustrated the main physiological pathways of cytoplasmic Ca^{2+} removal following a contraction in control (a) and hypertrophied muscles (b). Myocardial relaxation results from the lowering of cytoplasmic Ca^{2+} by two pathways: (1) Ca^{2+} sequestration of the fraction "r" by the SR and (2) Ca^{2+} extrusion of the fraction "1-r" via Na-Ca exchange. The fractional contribution of each mechanism depends upon the competition between the SR Ca-ATPase pump and the sarcolemmal Na-Ca exchange

(Bers et al. 1989). In this study, I did not find any difference in the recirculating fraction (r) of the SR Ca^{2+} between control and hypertrophied muscles using either potentiation decay or paired RCCs analysis, indicating an unchanged relative proportion of SR Ca^{2+} accumulation. By inference that fraction of Ca^{2+} that was extruded (1-r) via Na-Ca exchange was also unchanged. Because the total intracellular Ca^{2+} transient (or SR Ca^{2+} release) is enhanced during contraction as manifested as an increased twitch force in hypertrophied muscles, the unchanged proportion of "r" suggests that

ICa   SR   ATP   r   Ca   MF   1-r   Na-Ca

(a). Normal

ICa   SR   ATP   r   Ca   MF   1-r   Na-Ca
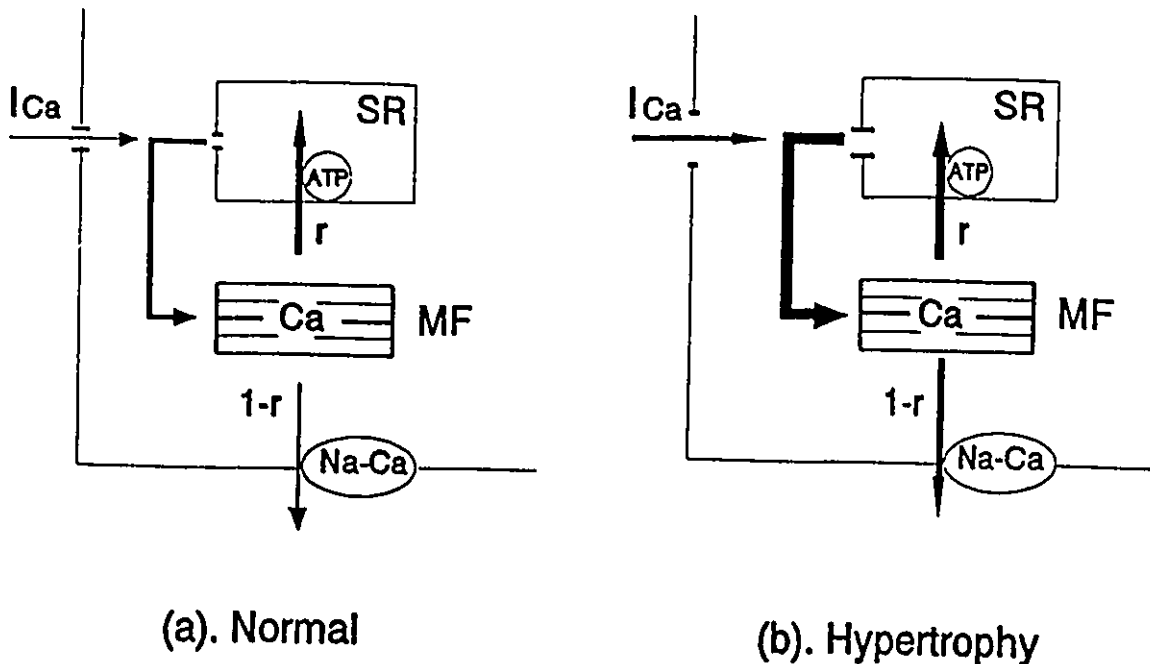
(b). Hypertrophy

Figure 30. Relative contribution of cytoplasmic Ca^{2+} removing mechanisms. Ca^{2+} is removed from the cytoplasm via the SR Ca-pump (r) and via Na-Ca exchange (1-r). In normal myocardium (a) most of the Ca^{2+} recirculates via the SR. In hypertrophied muscle (b) an unchanged fraction of "r" or "1-r" indicates an increase of absolute amount of Ca^{2+} removal by each mechanism (as expressed by the width of the arrows) due to higher $[Ca^{2+}]_i$ transient.

there was an increase of absolute amount of either SR Ca^{2+} uptake or Ca^{2+} extrusion

via Na-Ca exchange in the hypertrophied state (Fig 30, b). The fraction "1-r" of

released Ca^{2+} is extruded via the Na-Ca^{2+} exchange mechanism and in the steady-state

the extruded amount is equal to the influx per beat. The increased extrusion of the

absolute amount of Ca^{2+} via Na-Ca exchange is consistent with the amplified Ca^{2+}

influx by L-type channels (see Chapter 7) in hypertrophied muscles.

The paired RCCs also showed that there was a significant dependence of the SR

Ca^{2+} uptake on the priming frequency in both control and hypertrophied muscles. This

behaviour can be explained on the basis of a competitive mechanism for cytoplasmic

Ca^{2+} removal between the SR Ca-ATPase pump and sarcolemmal Na-Ca exchange.

Normally, there is an increase in intracellular Na^+ concentration with increasing

frequency of stimulation due to more action potentials per unit time (Borzak et al.

1991, Schouten 1985). An increase in intracellular Na^+ would inhibit Ca^{2+} efflux via

Na-Ca exchange. The increase of "r" with increasing priming frequency is probably due

to inhibition of Ca^{2+} efflux via Na-Ca exchange, which results in a reduction of the

extruded fraction (1-r) and thus favours the competition of the SR Ca-pump.

The post-rest-potentiation-decay was adopted to study the recirculating fraction of

SR Ca^{2+} because: (1) the "r" from paired RCCs was estimated by investigating the SR

Ca^{2+} content from the RCC_2 under conditions, which depleted almost all of SR Ca^{2+}

from RCC_1. This depleted SR Ca^{2+} may not represent the state of twitch contraction

and thus may modulate the SR Ca^{2+} reuptake in the rewarming phase of RCC_1; and (2)

the study of "r" from post-rest-potentiation-decay reflected Ca^{2+} reuptake from

undepleted SR, which occurs during normal twitch contraction. This study of post-rest-

potentiation-decay did not show any difference in "r" between the control and

hypertrophied muscles, which is consistent with the result of paired RCCs. Because the Ca^{2+} influx is in exchange for Na^+ efflux via the Na-Ca exchange during the long rest interval (120 second), the slightly lowered values of "r" in the post-rest-potentiation-decay in both groups was probably associated with lower intracellular Na^+, which favours Ca^{2+} extrusion (1-r) via Na-Ca exchange system.

OVERVIEW

Cardiac hypertrophy associated with pathological alterations of structure and function can be the result of excessive levels of plasma catecholamines. Experimentally, isoproterenol, a synthetic catecholamine, was used to induce cardiac hypertrophy by daily subcutaneous injection (0.3 mg/kg. body weight) for 12 consecutive days. Whole ventricular weight was significantly increased (35.7%) with no evidence of tissue edema. Regionally, the right ventricle produced a greater degree of hypertrophy than the left ventricle (46.9% vs 31.2%).

The contractile characteristics were studied by using small right ventricular trabecular muscle. There was a significant increase of contractile force at various concentrations of extracellular calcium and sarcomere lengths. These data indicate that contractile performance was enhanced in isoproterenol induced cardiac hypertrophy, suggesting that either the responsiveness of myofilaments to calcium and/or the availability of intracellular calcium was increased.

The responsiveness of contractile proteins to intracellular calcium was investigated using Triton-100 skinned trabecular muscles. The calcium sensitivity of myofilaments was determined from the force-pCa relationship (i.e., Ca^{2+} required for 50% maximal activation of the myofilaments and the slope of the force-pCa curve). The force-pCa relationship showed no difference in the calcium sensitivity of myofilaments, indicating that the increased contractile force in intact hypertrophied muscle does not reside at the level of the myofilaments, but altered intracellular calcium handling pathways could be responsible for the increased contractile performance. The remaining experiments, therefore, focused on intracellular calcium handling in hypertrophied muscle.

135

The force-interval relationship was used to reflect the early recovery of SR Ca^{2+} release channels and Ca^{2+} influx via sarcolemmal Na-Ca exchange at longer diastolic intervals. The characteristics of SR Ca^{2+} release channels were not altered at early recovery, however, the SR Ca^{2+} release was significantly increased at longer diastolic intervals, suggesting that Ca^{2+} influx, probably via sarcolemmal Na-Ca exchange, was enhanced in hypertrophied muscle.

An examination of the force-frequency response showed a biphasic relationship in a broad range of stimulation frequencies (0.1 ~ 2.5Hz) in rat right ventricular trabecula. At frequencies of 0.1 to 0.5 Hz, the force-frequency relationship was negative. Above 0.5 Hz, this response was strongly positive. In hypertrophied muscle, the positive rate staircase was significantly increased. Studies using rapid cooling contracture (RCC) suggest that SR Ca^{2+} content was altered with different frequencies of stimulation and the SR Ca^{2+} release was proportional to SR Ca^{2+} storage. Ryanodine (0.1 uM), which can unload SR Ca^{2+}, decreased steady-state twitch force at low frequencies and transformed the negative response to a positive one. Blockage of the L-type Ca^{2+} channels with nifedipine (0.1 uM) eliminated the positive force-frequency response and had no effect on the negative phase. These results suggest that both the diastolic Ca^{2+} influx, probably via sarcolemmal Na-Ca exchange, and the SR Ca^{2+} loading contribute to the negative rate staircase, whereas the Ca^{2+} influx via L-type channel at high frequencies of stimulation dominates the positive force-frequency response. In hypertrophied muscle, the enhanced positive rate staircase and RCC suggest an increased functioning of L-type Ca^{2+} channel and subsequently a greater SR Ca^{2+} content.

The Ca^{2+} influx via L-type channel at various stimulation rates was further studied

136

by measuring action potential duration at 50% of its amplitude (APD_{50}) using flexible microelectrodes. An increase of stimulation rate leads to a consistent prolongation of APD_{50} in both control and hypertrophied muscles. However, the APD_{50} was significantly increased in hypertrophied muscle compared to control ($p < 0.001$) at all frequencies. These results suggest that (1) there was a frequency-induced enhancement of Ca^{2+} influx in both groups and (2) the transsarcolemmal Ca^{2+} influx is significantly amplified in hypertrophied muscle.

To investigate the removal of cytoplasmic Ca^{2+} during a relaxation in hypertrophied muscle, the paired RCCs and post-rest-potentiation-decay were used to examine the relative contributions of the SR Ca-ATPase pump and sarcolemmal Na-Ca exchange pathways. The paired RCCs showed that there was a significant frequency-dependent increase of the SR Ca^{2+} sequestration in both groups, which can be explained by an increase of intracellular Na^+ concentration at higher stimulation rates due to more action potentials per unit time. An increase in intracellular Na^+ would inhibit calcium efflux via sarcolemmal Na-Ca exchange and in turn, favor SR Ca^{2+} uptake. Also, the relative proportion of SR Ca^{2+} sequestration or Ca^{2+} efflux via Na-Ca exchange was unchanged in either potentiation decay or paired RCCs in hypertrophied muscle. Because the total intracellular Ca^{2+} transient is enhanced during a contraction in hypertrophied muscle, the unchanged relative proportion suggests that there was an increase of absolute amount of either SR Ca^{2+} uptake or Ca^{2+} extrusion via Na-Ca exchange.

In summary, the increased intracellular calcium handling pathways, such as Ca^{2+} influx via L-type Ca^{2+} channels, SR Ca^{2+} content, Na-Ca exchange activity, and SR Ca-ATPase pump, contribute to the enhanced contractile function in this model of cardiac

hypertrophy.

REFERENCES

Aceto, J.F. and K.M. Baker (1990). [Sar]Angiotensin II receptor-mediated stimulation of protein synthesis in chick heart cells. Am. J. Physiol., 258:H806-H813.

Allard, M.F., M.F. Devenny, L.K. Doss, W.E. Grizzle, and S.P. Bishop (1990). Alterations in dietary sodium affect isoproterenol-induced cardiac hypertrophy. J. Mol. Cell Cardiol. 22:1135-1145.

Amrani, F.C.E., E. Mayoux, C. Mouas, R. Clapier-Ventura, D. Henzel, D. Charlemagne, and B. Swynghedauw (1990). Normal responsiveness to external Ca and to Ca-channel modifying agents in hypertrophied rat heart. Am. J. Physiol. 258: H1727-1734.

Argibay, J.A., R. Fischmeister, and H.C. Hartzell (1988). Inactivation, reaction and pacing dependence of calcium current in frog cardiocytes: Correlation with current density. J. Physiol (Lond). 401:201-226.

Arlock, P., B. Liu, B. Wohlfart, and B.W. Johansson (1988). A comparison of some force-interval relation in rat, hedgehog and human cardiac preparations. Cardiovasc. Res. 22:601-613.

Armstrong, C.M., F.M. Benzanilla and P. Horowicz (1972). Twitches in the presence of ethylene glycol (Beta-aminoethylether)-N,N-tetraacetic acid. Biochem. Biophys. Acta. 267:605-608.

Armstrong, S.C, and C.E. Ganote (1991). Effect of 2,3-butanedione monoxime (BDM) on contracture and injury of isolated rat myocytes following metabolic inhibition and ischemia. J. Mol. Cell. Cardiol. 23:1001-1004.

Aronson, R.S. (1980). Characteristics of action potentials of hypertrophied myocardium from rats with renal hypertension. Circ. Res. 47:443-454.

Babu, A., E. Sonnenblick, and G. Jagdish (1988). Molecular basis for the influence of muscle length on myocardial performance. Science. 240:74-76.

Baker, K.M. and H.A. Singer (1988). Identification and characterization of guinea pig angiotension II ventricular and atrial receptors: coupling to inositol phosphate production. Circ. Res. 62:896-904.

Baker, K.M. and J.F. Aceto (1990a). Angiotension II stimulation of protein synthesis and cell growth in chick heart cells. Am. J. Physiol. 359:H610-H618.

Baker, K.M., M.I. Chernin, S.K. Wixson, and J.F. Aceto (1990b). Renin-angiotensin system involvement in pressure overload cardiac hypertrophy in rats. Am. J. Physiol.

259:H324-H332.

Baldwin, K.M., S.B. Ernst, W.I. Mullin, L.F. Schrader, and R.E. Herrick (1982). Exercise capacity and cardiac function of rats with drug-induced cardiac enlargement. J. Appl. Physiol. 52:(3)591-595.

Banijamali, H.S., W.D. Gao, B.R. MaCIntosh, and H.E.D.J. Ter Keurs (1991). Force-interval relations of twitch and cold contractures in rat cardiac trabeculae. Circ. Res. 69:937-948.

Baudet, S. and R. V. Clapier (1990). Differential effects of caffeine on skinned fibers from control and hypertrophied ferret hearts. Am. J. Physiol. 259:H1803-H1808.

Basset, A.L., and H. Gelband (1973). Chronic partial occlusion of the pulmonary artery in cats. Changes in ventricular action potential configuration during early hypertrophy. Circ. Res. 32:15-26.

Bean, B.P. (1985). Two kinds of calcium channels in canine atrial cells. Differences in kinetics, selectivity, and pharmacology. J. Gen. Physiol. 86:1-30.

Benjamin, I.J., J.E. Jalil, L.B. Tan, K.Cho, K.T. Weber and W.A. Clark (1989). Isoproterenol-induced myocardial fibrosis in relation to myocyte necrosis. Circ. Res. 65:657-670.

Bers, D.M. (1983). Early transient depletion of extracellular calcium during individual cardiac muscle contractions. Am. J. Physiol. 244:H462-H468.

Bers, D.M. (1987). Mechanisms contributing to the cardiac inotropic effect of Na-pump inhibition and reduction of extracellular Na. J. Gen. Physiol. 90:479-504.

Bers, D.M. and J.H.B. Bridge (1988). The effects of acetylstrophanthidin on twitches, microscopic tension fluctuations and cooling contractures in rabbit ventricular muscle. J. Physiol. 404:53-69.

Bers, D.M. and J.H.B. Bridge (1989). Relaxation of rabbit ventricular muscle by Na-Ca exchange and sarcoplasmic reticulum Ca-pump: Ryanodine and voltage sensitivity. Circ. Res. 65:334-342.

Bers, D.M. and D.M. Christensen (1990). Functional interconvension of rest decay and ryanodine effects in rabbit and rat ventricle depends on Na-Ca exchange. J. Mol. Cell. Cardiol. 22:715-723.

Bers, D.M. (1991a). Excitation-contraction coupling and cardiac force. Kluwer Academic Publishers. pp. 72-98.

Bers, D.M. (1991b). Excitation-contraction coupling and cardiac force. Kluwer Academic Publishers. pp.148-191.

Beznak, R., B. Konecky, and G. Thomas (19f 9). Regression of cardiac hypertrophy of various origin. Can. J. Physiol. Pharmacol., 47:579-586.

Bishop, S.P. (1982). Animal models. In: Congestive Heart Failure, E. Braunwald et al eds, pp. 125-149. Grune & Stratton, New York.

Bishop, S.P. (1990). The myocardial cell: normal growth, cardiac hypertrophy and response to injury. Toxicol. Pathol. 18:438-453.

Blinks, J.R. (1986). Intracellular calcium measurements. In: The Heart and Cardiovascular System, H.A. Fozzard et al., eds., 671-701. Raven Press, New York.

Borzak, S., M. Stephanie, and J.D. Marsh (1991). Mechanisms of rat staircase in rat ventricular cells. Am. J. Physiol. 260:H884-H892.

Bouchard, R.A. and D. Bose (1989). Analysis of the interval-force relationship in rat and canine ventricular myocardium. Am. J. Physiol. 257:H2036-H2047.

Bouron, A., D. Potreao, and G. Raymond (1992). The L-type Ca current in single hypertrophied cardiac myocytes isolated from right ventricle of ferret heart. Cardiovas. Res. 26:662-670.

Bridge, J.H.B. (1986). Regulations between the SR and transsarcolemmal Ca transport revealed by rapidly cooling rabbit ventricular muscle. J. Gen. Physiol. 88:437-473.

Bridge, J.H.B., J.R.Smolley, and K.W. Spitzer (1990). The relationship between charge movements associated with Ica and I_{Na-Ca} in cardiac myocytes. Science. 248:376-378.

Bugaisky, L., and R. Zak (1986). Biological mechanisms of hypertrophy. In The Heart and Cardiovascular System, H.A. Fozzard et al., eds., pp1491-1493. Raven Press, New york.

Buxton, I.L.O. and L.L. Brunton (1986). Alpha-adrenergic receptor on rat ventricular myocytes: characteristics and linkage to cAMP metabolism. Am. J. Physiol. 251:H307-H313.

Caldwell, J.J.S. and A.H. Caswell (1982). Identification of a constituent of the junctional feet linking the terminal cisternae to transverse tubules in skeletal muscle. J. Cell. Biol. 93:543-550.

Capasso, J.M., A. Malhotra, J.Scheuer, and H.E. Sonnenblick (1986). Myocardial biochemical, contractile and electrical performance after imposition of hypertension in young and old rats. Circ. Res. 58:445-460.

Caroni, P. and E. Carafoli (1980). An ATP-dependent calcium pumping system in dog heart sarcolemma. Nature (London). 283:765-767.

Charnet, P., J. Nerbonne, and S. Richard (1988). The calcium current inactivation in

isolated rat ventricular cells: Dependence on membrane pote ntial and frequency of activation (abstract). J. Physiol (Lond). 406:80.

Chien, K.R., K.U. Knowlton, Hong Zhu, and Shu Chien (1991). Regulation of cardiac gene expression during myocardial growth and hypertrophy: molecular studies of an adaptive physiologic response. FASEB J. 5:3037-3046.

Chizzonite, R.A. and R.Zak (1984). Regulation of myosin isoenzyme composition in fetal and neonatal rat ventricle by endogenous thyroid hormones. J. Biol. Chem. 259:12628-12632.

Chua, B.H.L., L.A.Russo, E.E. Gordon, B.J. Kleinhans and H.E. Morgan (1987). Faster ribosome synthesis induced by elevated aortic pressure in rat. Am. J. Physiol. 252:C323-327.

Clough, D.L., M.B. Pamnani, and F.J. Haddy (1983). Decreased myocardial Na-K-ATPase activity in one-kidney, one-clip hypertensive rats. Am. J. Physiol. 245:H244-H251.

Cohen, J., J.M. Aroesty, and M.G. Rosenfeld (1966). Determinants of thyroid-induced cardiac hypertrophy in mice. Circ. Res. 18:388-397.

Cohn, C.J., H.A. Fozzard, and S.S. Sheu (1982). Increase in intracellular sodium ion activity during stimulation in mammalian cardiac muscle. Circ. Res. 50:651-662.

Collins, P., C.G. Billings, G.R.Barber, J.J. Daly, and A. Jolly (1975). Quantitation of isoproterenol-induced changes in the ventricular myocardium. Cardiovasc. Res. 9:797-806.

Conway, G., R.A. Heazlitt, N.O. Fowler, M. Gabel, and S. Green (1976). The effect of hyperthyroidism on the SR and myosin ATPase of dog hearts. J. Mol. Cell. Cardiol, 8:39-51.

Cooper, G.IV., R.J. Tomanek, J.C. Ehrhardt, and M.L. Marcus (1981). Chronic progressive pressure-overload at the cat right ventricle. Circ. Res., 48:488-497.

Cooper, G.IV. (1987). Cardiocyte adaptation to chronically altered load. Ann Rev. Physiol. 49:501-518.

Crie, J.S., J.R. Wakeland, B.A. Mayhew, and K. Wildenthal (1983). Direct anabolic effects of thyroid hormone on isolated mouse heart. Am. J. Physiol. 245:C328-333.

Crompton, M., M. Capana, and E. Carafoli (1976). The sodium induced efflux of calcium from mitochondria. A possible mechanism for the regulation of mitochondria calcium. Eur. J. Biochem. 69:453-462.

Crompton, M. (1985). The regulation of mitochondria calcium transport in heart. Curr. Top. Memb. Transp. 25:231-276.

Crompton, M. (1990). The role of calcium in the function and dysfunction of the heart mitochondria. In: Calcium and The Heart. Langer G.A., et al, eds. 167-198. Raven, New York.

Crozatier, B., L. Hittinger, and M. Chavance (1987). Modification of force-interval relations during early adaptation to pressure overload in dogs. Am. J. Physiol. 253(22): H1506-1513.

Cutilletta, A.F., R.T. Dowell, M. Rudnik, R.A. Arcilla, and R. Zak (1975). Regression of myocardial hypertrophy. (1). Experimental model, changes in heart weight, nucleic acids and collagen. J. Mol. Cell. Cardiol., 7:767-780.

Dani, A.M., A. Cittadini, and G. Inesi (1979). Calcium transient and contractile activity in dissociated mammalian heart cells. Am. J. Physiol. 237:C274-281.

Dela, Bastie D., D. Levitsky, L. Rappaport, J.J. Mercadier, F. Marotte, C. Wisnewsky, V. Brovkovich, K. Schwartz, and A.M. Lompre (1990). Function of the SR and expression of its Ca-ATPase gene in pressure over-load-induced cardiac hypertrophy in the rat. Circ. Res. 66:554-564.

Denton, R.M. and J.G. McCormack (1980). On the role of the calcium transport cycle in heart and other mammalian mitochondria. FEBS Lett. 119:1-8.

Endo, M. (1977). Calcium release from the SR. Physiol. Rev. 57:71-108.

Fabiato, A. (1980). Sarcomere length dependence of calcium release from the SR of skinned cardiac cells demonstrated by differential microspectrophotometry with Arsenzo III. J. Gen. Physiol. 76:15a.

Fabiato, A. (1981). Myoplasmic free calcium concentration reached during the twitch of an intact isolated cardiac cell and during calcium-induced release of calcium from the SR of a skinned cardiac cell from the adult rat or rabbit ventricle. J. Gen. Physiol. 78:457-497.

Fabiato, A. (1983). Calcium-induced release of calcium from the cardiac SR. Am. J. Physiol. 245:C1-C14.

Fabiato, A. (1985a). Rapid ionic modifications during the aequorin-detected calcium transient in skinned canine cardiac Purkinje cell. J. Gen. Physiol. 254:189-246.

Fabiato, A. (1985b). Time and calcium dependence of activation and inactivation of calcium-induced release of calcium from the SR of a skinned canine Purkinje cell. J. Gen. Physiol. 254:249-289.

Fabiato, A. (1985c). Stimulated calcium current can cause both calcium loading in and trigger calcium release from the SR of a skinned cardiac Purkinje fiber. J. Gen. Physiol. 245:291-320.

143

Fedida, D, D. Noble, and A.J. Spindler (1988). Use-dependent reduction and facilitation of calcium current in guinea-pig myocytes. J. Physiol (Lond). 405:439-460.

Fedida, D, S. Sethi, B.J.M. Mulder and H.E.D.J. Ter Keurs (1990). An ultracompliant glass microelectrode for intracellular recording. Am. J. Physiol. 258: C164-C170.

Fozzard, H.A., E. Haber, R.B. Jennings, A.M. Katz, and H.E. Morgan (1986). The heart and cardiovascular system. Raven Press. pp.1502-1503.

Franch, H.A., R.A.F. Dixon, E.H. Blaine, and P.K.S. Siegl (1988). Ventricular atrial natriuretic factor in the cardiomyopathic hamster model of congestive heart failure. Circ. Res. 62:31-42.

Franzini-Armstrong C. (1970). Studies of the triad. I. Structure of the junction in frog twitch fibers. J. Cell. Biol. 47:488-499.

Fried, R., and L.M. Reid (1985). The effect of isoproterenol on the development and recovery of hypoxic pulmonary hypertension. Am. J. Pathol. 121:102-111.

Fry, C.H., T. Powell, V.W. Twist, and J.P.T. Ward (1984). The effects of sodium hydrogen and magnesium ions on mitochondrial calcium sequestration in adult rat ventricular myocytes. Proc. Roy. Soc. Lond. 223:239-254.

Fuller, S.J., C.J. Gaitanaki, and P.H. Sugden (1990). Effects of catecholamines on protein synthesis in cardiac myocytes and perfused hearts isolated from adult rats. Biochem. J. 266:727-736.

Gulch, R.W., R. Baumann, and R. Jacob (1979). Analysis of myocardial action potential in left ventricular hypertrophy of Goldblatt rats. Basic Res Cardiol. 74:69-82.

Gustafson, T.A., B.E. Markham, J.J. Bahl, and E. Morkin (1987). Thyroid hormone regulates expression of a transfected alpha-myosin heavy-chain fusion gene in fetal heart cells. Proc. Natl. Acad. Sci. USA. 84:3122-3126.

Gwathmey, J.K. and J.P. Morgan (1985). Altered calcium handling in experimental pressure-overload hypertrophy in the ferret. Circ. Res. 57:836-843.

Gwathmey, J.K. and R.J. Hajjar (1992). Calcium-activated force in a Turkey model of spontaneous dilated cardiomyopathy: adaptive changes in thin myofilament calcium regulation with resultant implications on contractile performance. J. Mol. Cell. Cardiol. 24:1459-1470.

Haddad, F., and K.M. Baldwin (1991). Effects of low carbohydrate provision on isomyosin expression in the isoproterenol stressed rat heart. J. Mol. Cell. Cardiol. 23:453-460.

Hagiwara, S., S. Ozawa, and O. Sand (1975). Voltage clamp analysis of two inward current mechanisms in the egg cell membrane of a starfish. J. Gen. Physiol. 65:617-

644.

Hagiwara, N., H. Irisawa, and M. Kameyama (1988). Contribution of two types of calcium currents to the pacemaker potentials of rabbit sino-atrial node cells. J. Physiol. 359:233-253.

Hajjar, R.J. and J.K. Gwathmey (1991). Modulation of calcium activation in control and pressure-overload hypertrophied ferret hearts: effect of DPI 201-106 on myofilament calcium responsiveness. J. Mol. Cell. Cardiol. 23:65-75.

Harrison, S.M. and D.M. Bers (1990). Modification of temperature-dependence of myofilament Ca-sensitivity by troponin-C replacement. Am. J. Physiol. 258:C282-288.

Harsdorf, R.V., R.E. Lang, M.Fullerton, and E.A. Woodcock (1989). Myocardial stretch stimulates phosphatidyl inositol turnover. Circ. Res. 65:494-501.

Henry, P.D., G.G. Ahumada, W.F. Friedman, and B.E. Sobel (1972). Simultaneously measured isometric tension and ATP hydrolysis in glycerinated fibers from normal and hypertrophied rabbit heart. Circ. Res. 31:740-749.

Hess, P., J.B. Lansman, and R.W. Tsien (1984). Modulation of single calcium channels by the calcium agonist Bay K 8644. Nature. 311:538-541.

Hirano, Y., H.A. Fazzard, and C.T. January (1989). Characteristics of L- and T-type calcium currents in canine cardiac Purkinje cells. Am. J. Physiol. 256:H1478-H1492.

Homcy, C.J., S.F. Vatner, and D.E. Vatner (1991). Beta-adrenergic receptor regulation in the heart in pathophysiologic states: abnormal adrenergic responsiveness in cardiac disease. Ann. Rev. Physiol. 53:137-159.

Hryshko, L.V., V. Stiffel, and D.M. Bers (1989). Rapid cooling contractures as an index of SR calcium content in rabbit ventricular myocytes. Am. J. Physiol. 257:H1369-H1377.

Ingber, D.E., D. Prusty, J.V. Frangioni, E.J. Cragoe, C. Lechene, and M.A. Schwartz (1990). Control of intracellular pH and growth by fibronectin in capillary endothelial cells. J. Cell. Biol. 110:1803-1811.

Irisawa, H., and S. Kokubun (1983). Modulation by intracellular ATP and cAMP of the slow inward current in isolated single ventricular cells of the guinea pig. J. Physiol. 338:321-327.

Jalil, J.E., J.S. Janicki, R. Pick, C. Abrahams, and K.T. Weber (1989). Fibrosis induced reduction of the endomyocardium in the rat after isoproterenol treatment. Circ. Res. 65:258-264.

Jasmin, G., L. Proschek, and C. Dechesne (1986). Effect of isoproterenol, D-600 and digitoxin on ventricular heavy chain (HC) myosins in normal and cardiomyopathic

hamsters (abs). J. Mol. Cell. Cardiol. 18:127.

Kaplan, J.H. (1985). Ion movements through the sodium pump. Ann. Rev. Physiol. 47:535-544.

Karin, M. (1992). Signal transduction from cell surface to nucleus in development and disease. FASEB J. 6:2581-2590.

Kaze, A.M., H. Takenaka, and J. Watras (1986). The sarcoplasmic reticulum. In: The Heart and Cardiovascular System, H.A. Fozzard et al., eds., Raven Press, New York, pp.731-746.

Kawaguchi, H., H. Sano, K. Hizuka, H. Okada, T. Kudo, K. Kageyama, S. Muramoto, T. Murakami, H. Okamoto, N. Mochizuki, and A. Kitabatake (1993). Phosphatidylinositol metabolism in hypertrophic rat heart. Circ. Res. 72:966-972.

Kent, R.L., J.K. Hoober, and G. Cooper IV. (1989). Load responsiveness of protein synthesis in adult mammalian myocardium: role of cardiac deformation linked to sodium influx . Circ. Res. 64:74-85.

Kentish, J.C. (1986). The effects of inorganic phosphate and creatine phosphate on force production in skinned muscles from rat ventricle. J. Physiol. 370:585-604.

Keung, E.C.H., and R.S. Aronson (1981). Non-uniform electrophysiological properties and electronic interaction in hypertrophied rat myocardium. Circ. Res. 49:150-158.

Keung, E.C. (1989). Calcium current is increased in isolated adult myocytes from hypertrophied rat myocardium. Circ. Res. 64:753-763.

Kleiman R.B., and S.R. Houser (1988). Calcium currents in normal and hypertrophied isolated feline ventricular myocytes. Am. J. Physiol. 255:H1434-H1442.

Kimara, S., Bassett A.C., K. Saida, M. Shimiza, and R.J. Megerburg (1989). SR function in skinned fibers of hypertrophied rat ventricle. Am. J. Physiol. 256:H1006-H1011.

Kuribayashi, T., K. Furukawa, H. Katsume, H. Ijichi, and Y. Ibata (1986). Regional difference of myocyte hypertrophy and three dimentional deformation of the heart. Am. J. Physiol. 249:H378-H388.

Kuyayama, H. (1988). The membrane potential modulates the ATP-dependent Ca-pump of cardiac sarcolemma. Biochim. Biophys. Acta. 940:295-299.

Lakatta, E.G. (1993). Cardiovascular regulatory mechanisms in advanced age. Physiol. Rev. 73:413-453.

Lai, F.A., K. Anderson, E. Rousseau, Q. Liu, and G. Meissner (1988). Evidence for a calcium channel within the ryanodine receptor complex from cardiac SR. Biochem.

Biophys. Res. Commun. 151:441-449.

Lai, F.A., M. Misra, L. Xu, H.A. Smith and G. Meissner (1989). The ryanodine receptor-calcium release channel complex of skeletal muscle SR. J. Biol. Chem. 264:16766-16785.

Lamers, J.M.J., and J.T. Stinis. (1979). Defective calcium pump in the SR of the hypertrophied rabbit heart. Life Sci. 24:2313-2319.

Langer, G.A. (1992). Calcium and the heart:exchange at the tissue, cell, and organelle levels. FASEB J. 6:893-902.

Larson, D.F., J.G. Copeland and D.H. Russell (1985). Catacholamine-induced cardiac hypertrophy in a denervated, hemodynamically non-stressed heart transplant. Life Sci. 360:2477-2489.

Leblanc, N., and J.R. Hume (1990). Sodium current induced release of calcium from cardiac SR. Science. 248:372-376.

Lecarpentier, Y., A. Waldenstrom, M. Clerque, D. Chemla, P. Oliviero, J.L. Martin, and B. Swynghedauw (1987a). Major alterations in relaxation during cardiac hypertrophy induced by aortic stenosis in guinea pig. Circ. Res. 61:107-116.

Lecarpentier, Y., L.B. Bugaisky, D. Chemla, J.J. Mercadier, K. Schwartz, G. Whalen, and J.L. Martin (1987b). Coordinated changes in contractility, energetics, and isomyosin after aortic stenosis. Am. J. Physiol. 252: H275-H282.

Lee, C.O., D.H. Kang, and J.H. Sokol (1980). Relation between intracellular sodium ion activity and tension in sheep cardiac Purkinje fibers exposed to dihydroouabain. Biophys. J. 29:314-330.

Lee, H., S. Henderson, R. Reynold, P. Dunnmon, D. Yuan, and K.R. Chien (1988). Alpha-1 adrenergic stimulation of cardiac gene transcription in neonatal rat myocardial vells:effects on myosin light chain-2 gene expression. J. Biol. Chem. 263:7352-7358.

Levitsky, D.O., D.S. Benevolensky, T.S. Levchenko, V.N. Smirnov, and E.I. Chazov (1981). Calcium-binding rate and capacity of cardiac SR. J. Mol. Cell. Cardiol. 13:785-796.

Lewartowski, B., R.G. Hansford, G.A. Langer, and E.G. Lakatta (1990). Calcium content in single myocytes of guinea pig heart: effect of ryanodine. Am. J. Physiol. 259:H1222-1229.

Li, T., and N. Sperelakis (1983). Calcium antagonist blockade of slow action potentials in cultured chick heart cells. Can. J. Physiol. Pharmacol. 61:957-966.

Lin, Y.C. (1973). Hemodynamics in the rat with isoproterenol induced cardiac hypertrophy. Res. Commun. Chem. Pathol. Pharmacol. 6:213-220.

Lynch III, C. (1991). Pharmacological evidence for two types of myocardial SR Ca release. Am. J. Physiol. 260:H785-H795.

Mann D.L., R.L. Kent and G.IV Cooper (1989). Load regulation of the properties of adult feline cardiocytes: growth induction by cellular deformation. Circ. Res. 64:1079-1090.

Mansier, P., B. Chevalier, and B. Swynghedauw (1989). Characterization of the beta adrenergic system in adult rat hypertrophied hearts (abs.). J. Mol. Cell. Cardiol. 21, Suppl.:S.17.

Maughan, D., E. Low, R. Litten, J. Brayden, and N. Alpert (1975). Calcium activated muscle from hypertrophied rabbit heart. Circ. Res. 44:274-287.

Mayoux, E., F. Callen, B. Swynghedauw, and D. Charlemagne (1988). Adaptational process of the cardiac Ca channels to pressure overload: biochemical and physiological properties of the dihydropyridine receptors in normal and hypertrophied rat hearts (1988). J. Cardiovasc. Pharmacol. 12:390-396.

McCollum, W.B., H.R. Beshchjr, M.L. Entman, and A. Schwartz (1972). Apparent initial binding rate of calcium by canine cardiac relaxing system. Am. J. Physiol. 223:H608-614.

McDonough, P.M., and C.C. Glembotski (1992). Induction of ANF and MHC-2 gene expression in cultured ventricular myocytes by electrical stimulation of contraction. J. Biol. Chem. 267:11665-11668.

McIvor, M.E., C.H. Orchard, and E.G. Lakatta (1988). Dissociation of changes in apparent myofibrillar Ca sensitivity and twitch relaxation induced by adrenergic and cholinergic stimulation in isolated ferret cardiac muscle. J. Gen. Physiol. 92:509-529.

Meidell, R.S., A. Sen, S.A. Henderson, M.F. Slahetka, and K.R. Chein (1986). Alpha1-adrenergic stimulation of rat myocardial cells increases protein synthesis. Am. J. Physiol. 251:H1076-H1084.

Meissner, G. (1975). Isolation and characterization of two types of SR vesicles. Biochim. Biophys. Acta 389:51-68.

Meissner, G. (1986), Ryanodine activation and inhibition of the calcium release channel of SR. J. Biol. Chem. 261:6300-6306.

Meissner, G., and J.S. Henderson (1987). Rapid calcium release from cardiac SR vesicles is dependent on Ca and is modulated by Mg, adenine nucleotide and calmodulin. J. Biol. Chem. 262:3065-3073.

Mercadier, J.J., A.M. Lompre, C. Wisnewsky, J.L. Samuel, J. Bercovici, B. Swynghedauw, and K. Schwartz (1981). Myosin isoenzyme changes in several models of rat cardiac hypertrophy. Circ. Res. 49:525-532.

148

Mirsky, I., and M.M. Laks (1980). Time course of changes in the mechanical properties of the canine right and left ventricles during hypertrophy caused by pressure overload. Circ. Res. 46:530-542.

Mitchell, M.R., T. Powell, D.A. Terrar, and V.W. Twist (1985). Influence of a change in stimulation rate on action potentials, currents and contractions in rat ventricular cells. J. Physiol. (Lond). 365:527-544.

Mochly-Rosen, D., C.J. Henrich, L. Cheever, H. Khaner, and P.C. Simpson (1990). A protein kinase C isozyme is translocated to cytoskeletal elements on activation. Cell Regul. 693-706.

Moolenaar, W.H. (1986). Effects of growth factors on intracellular pH regulation. Ann. Rev. Physiol. 48:363-376.

Morad, M., and Y. Goldman (1973). Excitation-contraction coupling in heart muscle: membrane control of development of tension. Progr. Biophys. Mol. Biol. 27:257-313.

Morgan, H.E., E.E. Gordon, Y. Kira, B.H.L. Chua, L.A. Russo, C.J. Peterson, P.J. McDermott, and P.A. Watson (1987). Biochemical mechanisms of cardiac hypertrophy. Ann. Rev. Physiol. 49:533-543.

Morgan, J.P. (1991). Abnormal intracellular modulation of calcium as a major cause of cardiac contractile dysfunction. New England J. Med. 325:625-632.

Morano, I., C. Wojciechowski, and J.C. Ruegg (1991). Modulation of cross-bridge kinetics by myosin isoenzymes in skinned human heart fibers. Circ. Res. 68:614-618.

Morris, C.E. (1990). Mechanosensitive ion channels. J. Membrane Biol. 113:93-107.

Moss, R.L. (1992). Calcium regulation of mechanical properties of striated muscle. Circ. Res. 70:865-884.

Mullins, L.J. (1979). The generation of electric currents in cardiac fibers by Na-Ca exchange. Am. J. Physiol. 236:C103-C110.

Nabauer, M. and M. Morad (1990). Ca induced Ca release as examined by photolysis of caged Ca in single ventricular myocytes. Am. J. Physiol. 258:C189-C193.

Nag, A.C. and M. Cheng (1984). Expression of myosin isoenzymes in cardiac muscle cell in culture. Biochem. J. 221:21-26.

Niedergerke, R. (1956). The staircase phenomenon and the action of calcium on the heart. J. Physiol. 134:569-583.

Niggli, V., E.S. Adunyah, J.T. Penniston, and E. Carafoli (1981). Purified (Ca-Mg)-ATPase of the erythrocyte membrane. J. Biol. Chem. 256:395-401.

Nordin, C., F. Siri, and R.S. Aronson (1989). Electrophysiological characteristics of single myocytes isolated from hypertrophied guinea-pig hearts. J. Mol. Cell. Cardiol. 21:729-739.

Nowychy, M.C., A.P. Fox, and R.W. Tsien (1985). Three types of neuronal calcium channel with different calcium agonist sensitivity. Nature. 316:440-443.

Okazaki, O., N. Suda, K. Hongo, M. Konishi, and S. Kurihara (1990). Modulation of calcium transients and contractile properties by beta-adrenergic receptor stimulation in ferret ventricular myocytes. J. Physiol. 423:221-240.

Orchard, C.H., and E.G. Lakatta (1985). Intracellular calcium transients and developed tension in rat heart muscle. a mechanism for the negative interval strength relationship. J. Gen. Physiol. 86:637-651.

Parker, T.G., S.E. Packer, and M.D. Schneider (1990). Peptide growth factors can provoke fetal contractile protein gene expression in rat cardiac myocytes. J. Clin. Invest. 85:507-514.

Perreault, C.L., O.H.L. Bing, W.W. Brooks, B.J. Ransil, and J.P. Morgan (1990). Differential effects of cardiac hypertrophy and failure on right versus left ventricular calcium activation. Circ. Res. 67:707-712.

Peterson, M.B., and M. Lesch (1972). Protein synthesis and amino acid transport in isolated rabbit right ventricular muscle. Circ. Res. 31:317-327.

Philipson, K.D., and A.Y. Nishimoto (1982). Na-Ca exchange in inside-out cardiac sarcolemmal vesicles. J. Biol. Chem. 257:5111-5117.

Poggesi, C., M. Everts, B. Polla, F. Tanzi, and C. Reggiani (1987). Influence of thyroid state on mechanical restitution of rat myocardium. Circ. Res. 60:142-151.

Post, J.A., J.I.Sen, S.L. Kenneth, and G.A. Langer (1991). Effects of charged amphiles on cardiac cell contractility are mediated via effects on calcium current. Am. J. Physiol. 260:H759-H769.

Ragnarsdottir, K., B. Wohltart, and M. Johannsson (1982). Mechanical restitution of the rat papillary muscle. Acta. Physiol. Scand. 115:183-191.

Raine, A.E.G., A.F.C. Roberts, B.S. Manley, J.V. Jones, and J.G.G Ledingham (1983). Calcium sensitivity and cardiac performance in genetic and renal models of hypertension. J. Hypertens. 1:85-87.

Re, R.N., R.J. Michalik, and V.J. Dzau (1983). Cardiac myocytes contain renin. Clin. Res. 32:845A.

Reuter, H., and H. Seitz (1968). The dependence of calcium efflux from cardiac muscle on temperature and external ion composition. J. Physiol. 195:451-470.

Reuter, H., C.F. Stevens, R.W. Tsien, and G. Yellen (1982). Properties of single calcium channels in cardiac cell culture. Nature (Lond). 297:501-504.

Reuter, H. (1983). Calcium channel modulation by neurotransmitters, enzymes and drugs. Nature. 301:569-574.

Rich, T.L., G.A. Langer, and M.G. Klassen (1988). Two components of coupling calcium in single ventricular cell of rabbits and rats. Am. J. Physiol. 254:H937-H946.

Rich, T.L., and G.A. Langer (1991). Na-Ca exchange contribution to the rapid exchangeable Ca compartment of rat heart cells. FASEB J. 5, A1051 (abs.).

Rousseau, E., J.S. Smith, J.S. Henderson, and G. Meissner (1986). Single channel and Ca flux measurements of the cardiac SR Ca channel. Biophys. J. 50:1009-1014.

Rousseau, E., and G. Meissner (1989). Single cardiac SR Ca-release channel: Activation by caffeine. Am. J. Physiol. 256:H328-H333.

Rupp, H., R. Wahl, and R. Jacob (1987). Chronic cardiac reactions IV. Effects of drugs and altered functional loads on cardiac energetics as inferred from myofibrillar ATPase and the myosin isoenzyme population. Basic. Res. Cardiol (supp 2). 82:173-182.

Rupp, H., V. Elimban, and N.S. Dhalla (1988). Sucrose feeding presents changes in myosin isoenzymes and SR Ca-ATPase in pressure loaded rat heart. Biochem. Biophys. Res. Commun. 156:917-923.

Sadoshima, J.I., L. Jahn, T. Takahashi, T.J. Kalik, and S. Izumo (1992). Molecular characterization of the stretch-induced adaptation of cultured cardiac cells: an in vitro model of load induced cardiac hypertrophy. J. Biol. Chem. 267:10551-10560.

Scamps, F., E. Mayoux, D. Charlemagne, and G. Vassort (1990). Calcium current in single cells isolated from normal and hypertrophied rat heart. Circ. Res. 67:199-208.

Schouten, V.J.A. (1985). Excitation-contraction coupling in heart muscle. Graduate thesis. pp.14-23.

Schouten, V.J.A., J.K. Van Deen, P.D. Tombe, and A.A. Verveen (1987). Force interval relationship in heart muscle of mammalians. Biophys. J. 51:13-26.

Schouten, V.J.A. (1990). Interval dependence of force and twitch duration in rat heart explained by calcium pump inactivation in the SR. J.Physiol. 431:427-444.

Schouten, V.J.A., and H.E.D.J. Ter Keurs (1991). Role of Ica and Na-Ca exchange in the force-frequency relationship of rat heart muscle. J. Mol. Cell. Cardiol. 23:1039-1050.

Schwartz, K., D. De La Bastie, P. Bouveret, P. Oliviero, S. Alonso, and M. Buckingham (1986). Alpha-skeletal muscle actin mRNAs accumulate in hypertrophied adult rat

hearts. Circ. Res. 59:551-555.

Schwartz, M.A., G. Both, and C. Luchene (1989). Effect of cell spreading on cytoplasmic pH in normal and transformed fibroblasts. Proc. Natl. Acad. Sci. USA 86:4525-4529.

Schwartz, M.A., E.J. Jr. Cragoe, and C.P. Lechence (1990). pH regulation in spread cells and round cells. J. Biol. Chem. 265:1327-1332.

Sen, S., G. Kundu, N.Mekhail, J. Castel, K. Misono, and B. Healy (1990). Myotrophin: purification of a novel peptide from spontaneously hypertensive rat heart that influences myocardial growth. J. Biol. Chem. 265:16635-16643.

Sham, J.S.K., L. Cleemann, and M. Morad (1992). Gating of the cardiac calcium release channel: the role of sodium current and sodium calcium exchange. Science. 255:850-853.

Shattock, M.J., and D.M. Bers (1989). Rat vs. rabbit ventricle: calcium flux and intracellular sodium by ion selective microelectrodes. Am. J. Physiol. 256:C813-822.

Sheng, M., M.A. Thompson, and M.E. Greenberg (1991). A calcium regulated transcription factor phosphorylated by calmodulin-dependent kinases. Science 252 (5011):1427-1430.

Sheu, S.S., and M.P. Blaustein (1986). The heart and cardiovascular system. Fozzard H.A. et al, eds. Raven Press. 509-537.

Shigekawa, M., J.A.M. Finegan, and A.M. Katz (1976). Calcium transport ATPase of canine cardiac SR. J. Biol. Chem. 251:6894-6900.

Shoki, M., H. Kawaguchi, H. Okamoto, H. Sano, H. Sawa, T. Kudo, N. Hirao, Y. Sakata, and H. Yasuda (1992). Phosphatidylinositol and inositolphosphatide metabolism in hypertrophied rat heart. Japan. Circ. J. 56:142-147.

Shubeita, H.E., P.M. McDonough, A. Harris, K.U. Knowlton, C. Glembotski, J.H. Brown, and K.R. Chien (1990). Endothelin induction of sarcomere assembly and cardiac gene expression in ventricular myocytes: a paracrine mechanism for myocardial cell hypertrophy. J. Biol. Chem. 265:20555-20562.

Simpson, P., A. McGrath, and S. Savion (1982). Myocyte hypertrophy in neonatal rat heart cultures and its regulation by serum and by catecholamines. Circ. Res. 51:787-801.

Simpson, P. (1985). Stimulation of hypertrophy of cultured neonatal rat heart cells through an alpha1-adrenergic receptor and induction of beating through an alpha1- and beta1-adrenergic receptor interaction. Circ. Res. 56:884-894.

Simpson, P.C., C.S. Long, L.E. Waspe, C.J. Henrich, and C.P. Ordahl (1989).

transcription of early developmental isogenes in cardiac myocyte hypertrophy. J. Mol. Cell. Cardiol. 21(sup.5):79-89.

Simon, G. (1989). Is intracellular sodium increased in hypertension? Clin. Sci. 76:455-461.

Singh, J. (1982). Stretch stimulates cyclic nucleotide metabolism in the isolated frog ventricle. Pflugers Arch. 395:162-164.

Siri, F.M., J. Krueger, C. Nordin, Z. Ming and R.S. Aronson (1991). Depressed intracellular calcium transients and contraction in myocytes from hypertrophied and failing guinea pig hearts. Am. J. Physiol. 261:H514-H530.

Sperelakis, N. and J.A. Schneider (1976). A metabolic control mechanism for calcium ion influx that may protect the ventricular myocardial cell. Am J. Cardiol. 37:1079-1085.

Sperelakis, N. (1984). Cyclic AMP and phosphorylation in regulation of calcium influx into myocardial cells, and blockade by calcium antagonistic drugs. Am. Heart J. 107:347-357.

Sperelakis, N. (1988). Regulation of calcium slow channels of cardiac muscle by cyclic nucleotides and phosphorylation. J. Mol. Cell. Cardiol. 20 (suppl. II) 75-105.

Solaro, R.J., and F.N. Briggs (1974). Estimating the functional capacities of the sarcoplasmic reticulum in cardiac muscle. Circ. Res. 34:531-540.

Sreter, R.A., R. Faris, I. Balogh, E. Somogyi, and P. Sotonyi (1982). Changes in isomyosin distribution induced by low doses of isoproterenol. Arch. Int. Pharmacodyn. Ther. 229:872-879.

Stemmer, P., and A. Tai (1986). Concealed positive-force-frequency relationships in rat and mouse cardiac muscle by ryanodine. Am. J. Physiol. 251:H1106-1110.

Stern, M.D., and E.G. Lakatta (1992). Excitation-contraction coupling in the heart: the state of the question. FASEB J. 6:3092-3100.

Strauss, J.D., C. Zeugner, J.E. Van Eyk, B. Christel, T. Monika, and J.C. Ruegg (1992). Troponin replacement in permeabilized cardiac muscle. FEBS 310:229-234.

Stone, J.A. Backx P.H.M., and H.E.D.J. Ter Keurs (1990). The effects of atrial natriuretic factor on force development in rat cardiac trabeculae. Can. J. Physiol. Pharmacol. 68:1247-1254.

Sutko, J.L., and J.L. Kenyon (1983). Ryanodine modification of cardiac muscle response to potassium free solutions: evidence for inhibition of SR calcium release. J. Gen. Physiol. 82:385-404.

Taylor, P.B., R.K. Helbing, S. Rourke, and D. Churchill (1988). Effects of catecholamine-induced cardiac hypertrophy on the force-interval relationship. Can. J. Physiol. Pharmacol. 67:40-46.

Tang, Q., P.B. Taylor, and R.K. Helbing (1987). Catacholamine induced cardiac hypertrophy. Can. J. Cardiol. 3:311-316.

Ten Eick, R.E., D.W. Whalley, and H.H. Rasmussen (1992). Connections: heart disease, cellular electrophysiology, and ion channels. FASEB J. 6:2568-2580.

Thollon, C., P. Kreher, V. Charlon, and A. Rossi (1989). Hypertrophy induced alteration of action potential and effects of an inhibition of angiotensin converting enzyme by perindopril in infarcted rat heart. Cardiovasc. Res. 23:224-230.

Tse, J., J.R. Powell, C.A. Baste, R.E. Friest, and F. Kuo (1979). Isoproterenol-induced cardiac hypertrophy: modulation in characteristics of beta-adrenergic receptor, adenylate cyclase, and ventricular contraction. Endocrinology. 105:246-255.

Tsuda, T., and R.W. Alexander (1990). Angiotensin II stimulates phosphorylation of nuclear lamins via a protein kinase C-dependent mechanism in cultured vascular smooth muscle cells. J. Biol. Chem. 264:1165-1170.

Ventura-Clapier, R., R.H. Mekhfi, P. Oliviero, and B. Swynghedauw (1988). Pressure overload changes cardiac skinned fiber mechanics in rats, not in guinea pigs. Am. J. Physiol. 254:H517-H524.

Vogel, S. and N. Sperelakis (1977). Blockade of myocardial slow inward current at low pH. Am. J. Physiol. 233:99-103.

Walsh, L.G., and J.M. Tormey (1988). Cellular compartment in ischemic myocardium: indirect analysis by electron microprobe. Am. J. Physiol. 255:H929-H936.

Watson, P.A. (1989a). Accumulation of cAMP and calcium in S49 mouse lymphoma cells following hyposmotic swelling. J. Biol. Chem. 264:14735-14740.

Watson, P.A., T. Haneda, and H.E. Morgan (1989b). Effect of higher aortic pressure on ribosome formation and cAMP content in rat heart. Am. J. Physiol. 256:C1257-C1261.

Watson, P.A. (1990). Direct stimulation of adenylate cyclase by mechanical forces in S49 mouse lymphoma cells during hyposmotic swelling. J. Biol. Chem. 265:6569-6575.

Whitmer, K.R., J.L. Lee, A.F. Martin, L.K. Lane, S.W. Lee, A. Schwarz, H.W. Overbeek, and E.T. Wallick (1986). Myocardial Na-K-ATPase in one kidney, one-clip hypertensive rats. J. Mol. Cell. Cardiol. 18:1085-1095.

Wibo, M., G. Bravo, and T. Godfraind (1991). Postnatal maturation of excitation-contraction coupling in rat ventricle in relation to the subcellular localization and surface density of 1,4-dihydropyridine and ryanodine receptors. Circ. Res. 68:662-673.

Wohlfart, B., and M.I.M. Noble (1982). The cardiac excitation-contraction cycle. Pharmol. Ther 16:1-43.

Yang, X., and F. Sachs (1989). Block of stretch-activated ion channels in Xenopus oocytes by gadolinium and calcium ions. Science. 264:1068-1071.

Zierhut, W., and H.G. Zimmer (1989a). Significance of myocardial alpha- and beta-adrenergic receptors in catecholamine-induced cardiac hypertrophy. Circ. Res. 65:1417-1425.

Zierhut, W., and H.G. Zimmer (1989b). Triiodothyronine-induced changes in function, metabolism, and weight of rat heart: effects of alpha- and beta-adrenergic blockade. Basic. Res. Cardiol. 84:359-370.

Zimmer, H.G., and H. Peffer (1986). Metabolic aspects of the development of experimental cardiac hypertrophy. Basic. Res. Cardiol. 81(suppl 1):127-137.

Table 1. Influence of $[Ca^{2+}]_o$ on isometric force in both control and hypertrophied trabeculae.

$[Ca^{2+}]_o$ (mM)	Isometric Force (mN/mm^2)	
	Control (n = 6)	Hypertrophy (n = 9)
0.25	8.38 ± 1.5	11.5 ± 1.5
0.50	20.2 ± 2.4	34.4 ± 3.6
0.75	27.9 ± 3.8	47.2 ± 4.4
1.00	32.6 ± 4.5	52.9 ± 4.9
1.25	34.5 ± 4.8	56.5 ± 5.4
1.50	37.8 ± 5.3	58.9 ± 5.8
1.75	39.6 ± 5.9	60.5 ± 5.8
2.00	40.6 ± 5.8	60.7 ± 5.6

Note that values are expressed as mean ± S.E. Muscle contracted at optimal sarcomere length.

Table 2(a). DT at various sarcomere lengths in control trabeculae. $[Ca^{2+}]_o = 2.0$ mM.

Developed Force (mN/mm^2)

SL(um)	G1	G2	G3	G4	G5	G6
1.67						2.77
1.69			1.33	1.71		
1.70					1.61	
1.71	2.43	3.71				
1.79				3.00		
1.80		8.44				4.33
1.81	7.39					
1.82					8.93	
1.84		13.4	7.99			
1.89						6.07
1.91				7.01	14.9	
1.92			10.3			
1.95				12.7		8.92
1.97	13.4					
1.98			13.8			
2.00		22.5				
2.03	16.9			20.0		
2.04					21.1	14.9
2.05		34.0				
2.10						18.4
2.12			21.5	25.0		
2.15						25.2
2.16					32.2	
2.18	24.6					
2.19			28.7			
2.20						34.6
2.21		45.9				
2.23			35.7			
2.24				41.1	39.6	
2.25		51.9				
2.27	37.5					
2.28					44.7	
2.29			39.4			
2.33	43.7				43.9	
2.35		63.4				
2.39					50.4	
2.40						38.8

Note: this Table continues on next page.

Table 2(b). DT at various sarcomere lengths in control trabeculae. $[Ca^{2+}]_o = 2.0$ mM.

SL(um)	Developed Force (mN/mm^2)		
	G7	G8	G9
1.69	0.00	2.59	
1.72			2.56
1.79	9.68		
1.86			10.7
1.91		7.98	
1.94	18.3		
1.96	24.0	11.8	
2.03		18.7	
2.06		19.5	
2.08		22.6	
2.09			16.2
2.11	34.9		
2.15		27.1	
2.17			21.8
2.19	39.3		
2.27			30.5
2.29			37.0
2.30	43.6		
2.32		37.7	

Note that this Table follows Table 2(a) on the preceding page. DT = developed tension. SL = sarcomere length. G1 ~ G9 represent the number of preparation.

Table 3. DT at various SL in hypertrophied trabeculae. $[Ca^{2+}]_0 = 2.0$ mM.

SL(um)	Developed Force (mN/mm^2)					
	G1	G2	G3	G4	G5	G6
1.60				2.30		
1.64	1.40					
1.65		9.10				
1.66					4.00	
1.69						5.51
1.70			6.30			
1.72			8.40			
1.73	8.00					
1.81			12.4			
1.82						7.73
1.84		19.3			7.50	
1.85			20.3	13.6		
1.86	13.3	25.3				
1.88				15.8		
1.89					13.3	
1.90						10.9
1.91			27.6			
1.94	16.3					
1.95		32.0		28.5		
1.96					20.3	
2.00				30.1		19.2
2.01	22.0					
2.04						29.4
2.06			34.5			
2.07					33.8	
2.09				40.5		
2.10		40.0				
2.13		48.5	43.0		43.3	
2.14						40.0
2.15	28.3					
2.16						56.5
2.18	37.3			60.0		
2.20		55.9	51.6			
2.23					55.3	
2.25				76.3		
2.26	44.5				61.9	71.1
2.28						81.3
2.29				81.1		
2.30	49.5					
2.31					67.8	
2.35		68.0	57.4			

APPENDIX 2

METHODS FOR MUSCLE SKINNING

1. ELECTRODE CALIBRATION OF THE PH METER

The substantial liquid junction potential can produce misleading pH measurements (Kentish et al. 1986). The liquid junction potential varies with the ionic strength of the solution under test, and thus it will be present if the electrode has been calibrated in standard buffers that typically have different ionic strentch from test solutions. To calibrate my pH electrode (Fisher Accument, Model 620) two standard solutions were prepared and used:

(A). 50 mM potassium acid phthalate solution ($KHC_8O_4H_4$) with pH 4.010 at 25 °C;

(B). 25 mM sodium phosphate (Na_2HPO_4) + 25 mM potassium phosphate (KH_2PO_4) with pH of 6.865 at 25 °C.

After calibration of the electrode with these two solutions above, the pH of equimolar solution (B) (25mM) is 6.86 ± 0.01, and that of the 10 X diluted solution (2.5 mM) is 7.06 ± 0.01. The pH measured by my pH meter in the undiluted and diluted solution is 6.88 and 7.05, respectively. Since this is within an acceptable range, I believe that the electrode does not suffer from liquid junction potential and

160

ionic strength effects, and hence provided accurate measurement of pH.

2. ESSENTIAL SOLUTIONS

Solution 1: Chelexed-KOH

To make virtually Ca^{2+} free solution it is essential to remove the contaminant Ca^{2+} from the stock solution as much as possible. Since I used plastic ware for preparing these solutions, the contaminant Ca^{2+} was probably from water, ATP, creatine phosphate and BES buffer. The maximal removal of Ca^{2+} was accomplished by using an ion exchange resin Chelex-100 (Na^+ form, 100~200 mesh). Chelex-100 has a very high affinity for Ca^{2+}, Mg^{2+}, Fe^{2+} and Cu^{2+}. Because $[K^+]_i$ is higher than $[Na^+]_i$ in excitable cells such as cardiomyocytes, I used K^+ (in K-Chelex) to replace Ca^{2+} in these solutions. The K-Chelex was prepared from Na-Chelex-100. Conversion of Na-Chelex into K-Chelex involves two steps. The following describes the converting processes from Na-Chelex into K-Chelex:

Step 1. Na-Chelex + HCL <----> H-Chelex + NaCL

Step 2. H-Chelex + KOH <----> K-Chelex + H_2O

Procedures for Chelexed-KOH (1000 ml, 1M):

1). In a plastic beaker, 100 ml of HCL (1M) was mixed with 130~150 ml Na-Chelex. This was stirred with a teflon stirrer for 10 minutes following which the beads were allowed to settle and the HCL was decanted off.

161

2). This procedure was repeated once with fresh 100 ml of 1 M HCL. With this procedure, the resin shrank to about 50% of its original volume.

3). This resin was washed once with 100 ml deionized water for 5 minutes. The Chelex is now in the H-Chelex form.

4). The resin was washed again in a beaker with 100 ml water and allowed to settle. Sebsequently 50% of the water was decanted off. The rest of the solution was mixed and poured very slowly into a plastic column (Inside Diameter = 35mm, Length = 450mm).

5). The peristaltic pump was started and the water was suctioned out at a rate of 1 drop/second.

6). Before the level of water reaches the surface of the Chelex, 20 ml KOH (1 M) was slowly run down the column without disturbing the bed, while samples were continued to be removed at a rate of 1 drop/second room temperature.

7). Then 1500 ml KOH (1 M) was slowly run down and the pH of the eluting solution was checked until the pH was the same as that of the entering KOH (pH = 14). The H-Chelex resin is now converted to the K-Chelex and the eluted KOH was the Chelexed-KOH solution. The Chelexed-KOH solution was kept in a plastic container at room temperature.

Solution 2: Chelexed K-BES

The buffer N,N-bis[2-Hydroxyethyl]-2 Aminoethane Sulfonic Acid (H-BES, Sigma) was used to control the pH of all solutions. The reason for using this buffer is that its pKa is 7.1 at 25 °C which is close to physiological pH. For H^+ buffering it is generally considered that ± 1 pH unit from pKa value is the maximal useful buffer range, and

the maximum buffering capacity of any buffer is actually at the point where pH = pKa (i.e., point where [OH⁻] = [H⁺]), BES buffer was the best choice.

To make the Chelexed K-BES, two steps were involved. First, transformation of H-BES into K-BES; second, formation of the Chelexed K-BES. The transformation of H-BES into K-BES is given by:

$$H\text{-}BES + KOH \longleftrightarrow K\text{-}BES + H_2O$$
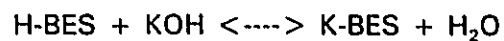
Procedures for Chelexed K-BES (300 ml, 500 mM):

1). 500 ml of 500 mM BES stock buffer was prepared by dissolving 53.33 g of H-BES in deionized water.

2). The pH of this solution was adjusted to 7.1 at room temperature with 100-150 ml Chelexed-KOH solution which transformed H-BES into K-BES.

3). About 100 ml of H-chelex resin was prepared by following step 1 ~ 3 of **The Procedure for Chelexed-KOH**. This was washed once by adding 100 ml water to the beaker containing the H-Chelex, stirring for 5 minutes and then decanting the water.

4). Adjust pH to 7.1 by adding Chelexed-KOH to the H-Chelex solution while stirring. At pH of 7.1, the H-Chelexed was converted to the K-Chelexed form.

5). This solution was washed once with 100 ml deionized water and poured slowly into the column.

6). The K-BES solution was Chelexed in this column. The first 150 ml was discarded until the pH of entering and exiting solutions were the same (pH = 7.1) after which the Chelexed K-BES (~300 ml) was collected in a plastic container and stored at -20 °C.

Solution 3: KPr

The preparation of KPr (CH_3CH_2COOK, BDH Inc.) was based on the following chemical equation:

$$CH_3CH_2COOH + KOH ----> CH_3CH_2COOK + H_2O$$
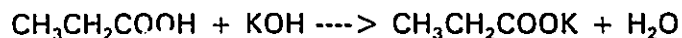
Precedures For KP; (100 ml, 1 M) Preparation:

1). I titrated 200 ml of 1 M Chelexed-KOH with pure concentrated propionic acid (~ 13.5 M) to pH 7.0 at room temperature. Since this reaction is exothermic, the acid was added slowly and the pH was continually monitored and fixed to 7.0 at room temperature.

2). KPr was subsequently chelexed by using the similar procedures $3 \sim 6$ of **the Chelexed K-BES.**

3). The Chelexed-KPr was stored at -20 °C for < 1 year.

Solution 4: Parent Solution

This solution was the most fundamental one. The "parent solution" contains the following components: Chelexed-BES buffer, ATP (Sigma), CP (Sigma), Chelexed-KPr, $MgCl_2$ (BDH Inc.) and Dithiothreitol (DTT, Sigma). The concentrations of these chemicals were determined by using a computer programme while considering the total concentration of this solution, free concentrations of ligands, metals, ligand-metal complex, ionic strength and net charge. The essential free ion concentrations that were

Table 4. Composition of the parent solution at pH = 7.1 and 25 °C as determined by computer program. Total concentration before dilution in each case is 1.25X concentrated.

NAME	1.25X* (mM)	1X (mM)	1.25X* (g/100 ml)	1.25X (ml/100 ml)
BES	125	100	---	25.0
Na_2ATP	8.5	6.8	0.5170	---
Na_2CP	12.5	10	0.4402	---
KPr	68.75	55	---	6.875
$MgCl_2$	7.31	5.85	---	0.731
DTT**	1.25	1.0	0.0195	---

* "1.25X" refers to the concentrated solution of 1.25 times in mM.
** DTT is a reagent that prevents breakage of the S-H groups with permeabilization which will otherwise act to reduce the stability of the muscle by generation of oxygen free radicals.

monitored were [$MgATP^{2-}$], [Mg^{2+}], [Ca^{2+}], [Na^+] and [K^+]. Since ATP and CP are acidic compounds, the addition of these chemicals to the BES buffer might reduce the pH. The pH of the "parent solution" was fixed to 7.1 (by using Chelexed-KOH) at 25 °C. The pH was checked after thawing. The amount for each chemical in the "parent solution" is given in Table 4.

Solution 5 and 6: K_2H_2EGTA and CaK_2EGTA

In order to accurately regulate Ca^{2+} levels at nM concentrations a buffer (H_4EGTA) with a high buffering capacity for Ca^{2+} was used. Theoretically, the easiest method to obtain various Ca^{2+} is to add Ca^{2+} to an H_4EGTA solution. However, this will not produce otherwise identical solutions with various Ca^{2+}. Every time Ca^{2+} is added to such a solution H^+ is released and the pH drops. Therefore, the solutions with more Ca^{2+} will also have a lower pH. To overcome this problem various Ca^{2+} concentrations were obtained by combining appropriate amounts of two extreme solutions with a constant final 10 mM total EGTA and hence a constant pH in all solutions. The two extreme solutions were: 1) one solution (K_2H_2EGTA) with zero free Ca^{2+} and 10 mM total EGTA and 2) one solution (CaK_2EGTA) with a free Ca^{2+} that will maximally activate the myofilaments and 10 mM total EGTA.

Procedures for K_2H_2EGTA (1000 ml, 50 mM)

1). In a plastic beaker, H_4EGTA for 50 mM concentration was mixed with 500 ml deionized water and stirred.

2). Amounts of stock $MgCl_2$ was added which was enough to make a 5X final concentration (i.e. 5 X 0.45 mM).

3). While measuring the pH, 1 M Chelexed-KOH was added to help dissolve H_4EGTA.

4). The volume was increased with deionized water to near 1000 ml and pH was fixed to 7.0 at room temperature with 1 M Chelexed-KOH.

5). The final volume was made with water to 1000 ml. This solution was kept at -

20 °C. The pH was always checked after thawing.

The reaction is described by the following:

$$H_4EGTA + 2\ KOH \longrightarrow K_2H_2EGTA + 2\ H_2O$$
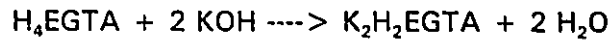
Procedures for CaK$_2$EGTA (1000 ml, 50 mM)

1). In a plastic beaker, enough H$_4$EGTA (50 mM) and CaCO$_3$ (50 mM) were dissolved in 500 ml deionized water.

2). Chelexed-KOH solution was added to help dissolving H$_4$EGTA while stirring.

3). pH was fixed to 7.0 at room temperature with Chelexed-KOH.

4). The final volume was adjusted to 1000 ml with water and stored at -20 °C. The pH was always checked after thawing.

The following describes the reactions:

$$H_4EGTA + CaCO_3 \longrightarrow CaEGTA^{2-} + H_2O + CO_2 + 2H^+$$

$$CaEGTA^{2-} + 2H^+ + 2KOH \longrightarrow CaK_2EGTA + 2H_2O$$
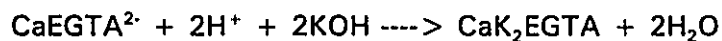
3. ACTIVATING SOLUTION (AS)

The AS was made by mixing 4 parts of the 1.25X concentrated "parent solution" with 1 part of stock CaK$_2$EGTA (50 mM). The AS was used to maximally activate the muscle contraction (pCa = 4.5). Table 5 shows the composition and concentration of the AS.

Table 5. Concentrations of ingredients in the final AS after mixing 1.25X concentrated parent solution with 50 mM CaK_2EGTA stock solution in 4:1 ratio. pH = 7.1. Temperature = 25 °C. Ionic strength = 0.2 M. Net charge = -0.000003.

NAME	TOTAL (mM)	FREE (mM)
Ligands		
BES	100.0	H-BES/K-BES = 48/52
EGTA	10.0	0.000009
ATP	6.8	0.7469
CP	10	9.7910
DTT	1.0	1.0
Metals		
K^+	140.0	139.17
Na^+	33.6	3.20
Ca^{++}	10.0	27.67 uM (pCa 4.5)
Mg^{++}	5.85	1.05
Cl^-	11.7	11.7
Pr^-	55.0	54.77

Table 6. Concentrations of ingredients in the final RS after mixing 1.25X concentrated parent solution with stock K_2H_2EGTA (50 mM) solution in 4:1 ratio. pH = 7.1. Temperature = 25 °C. Ionic strength = 0.2 M. Net charge = -0.000906.

NAME	TOTAL (mM)	FREE (mM)
Ligands		
BES	100	H-BES/K-BES = 48/52
EGTA	10	0.00106
ATP	6.80	0.75484
CP	10.0	9.79517
DTT	1.0	1.0
Metals		
K^+	140	139.164
Na^+	33.6	33.201
Ca^{++}!	0.0	0.0
Mg^{++}	6.30	1.048
Cl^-	12.6	12.6
Pr^-	55.0	54.77

! Eventhough we added no Ca^{2+} and we used the chelexing procedure, it is estimated that total contaminant Ca^{2+} may actually be about 10 ~ 20 nM.

4. RELAXING SOLUTION (RS)

The relaxing solution was made by mixing 4 parts of the 1.25X concentrated "parent solution" with 1 part stock K_2H_2EGTA (50 mM). The RS was used to relax the muscle. Table 6 shows the composition and concentration of the RS.

Table 7. Volumes of AS and RS required to prepare 1 ml final working solutions of various [Ca^{2+}].

Total [Ca^{2+}](mM)	RS(uL)	AS(uL)
10.0	0.0	1000
9.95	5	995
9.90	10	990
9.85	15	985
9.80	20	980
9.75	25	975
9.70	30	970
9.65	35	965
9.60	40	960
----	--	---
0.00	1000	0.0

5. FINAL WORKING SOLUTION

The final working solutions with varoius concentration of total Ca^{2+} were prepared by mixing appropriate volumes of RS with AS (Table 7). The computer programme was used to determine the free Ca^{2+} from the total Ca^{2+} in all cases (Table 8).

Table 8. Composition of solutions with various pCa, at 25°C and pH = 7.1. Ionic stretch = 0.2 M, Net charge range = -0.0009.

TOTAL [Ca^{2+}](mM)	FREE [Ca^{2+}](uM)	pCa
10.0	27.6706	4.55
9.90	16.5032	4.78
9.80	10.7874	4.97
9.70	7.75069	5.11
9.60	5.95970	5.22
9.50	4.80223	5.32
9.00	2.33273	5.63
8.50	1.47585	5.83
8.00	1.04354	5.89
7.00	0.60950	6.22
6.00	0.39201	6.41
5.00	0.26138	6.58
4.00	0.17425	6.76
3.00	0.11203	6.95
2.00	65.3552 nM	7.18
1.00	29.0469 nM	7.54

6. PREACTIVATING SOLUTION

To speed up the response of the muscle when it was exposed to a particular $[Ca^{2+}]$ (pCa) buffer, a solution known as the pre-activating solution was used. This contained zero Ca^{2+} and a reduced [EGTA] (part of EGTA was replaced with a buffer with a much lower affinity for Ca^{2+}, ie, 1,6-diaminohexane-N,N,N,N tetraacetic acid- HDTA). This did not induce any activation, but rather it equilibrated the muscle with a very low [EGTA] such that when it was exposed to a Ca^{2+}-containing solution, the Ca^{2+} would not bind to Ca^{2+}-free EGTA in RS. The content of the preactivating stock solution is given in Table 9. The ingredients of the preactivating solution are shown in Table 10.

Table 9. Concentrations of the preactivating stock solution.

NAME	5X (mM)*	1X (mM)
K_2H_2EGTA	2.5	0.50
HDTA	47.5	9.5
$MgCl_2$	1.65	0.33

* This refers to dilution of the preactivating stock solution with 1.25 X concentrated parent solution in 1:4.

7. SKINNING SOLUTION

Using Triton X-100, the total cell membrane structures including sarcolemmal, sarcoplasmic reticulum, and most other intracellular membranes are permeabilized. This is typically used to study twitch force-pCa relation of a preparation since the limiting

172

Table 10. Concentrations of ingredients in the "preactivating solution" after mixing 1.25X concentrated parent solution with the preactivating stock solution in 4:1 ratio. Temperature 25 °C, pH = 7.1. Ionic stretch = 0.2 M, Net charge = 0.000298.

NAME	TOTAL(mM)	FREE(mM)
Ligands		
BES	100	BES-H/BES-K = 48/52
EGTA	0.50	0.000053
HDTA	9.50	0.0000023
ATP	6.80	0.753911
CP	10.0	9.79481
DTT	1.0	1.0
Metals		
K^+	140.0	139.167
Na^+	33.6	33.2032
Ca^{2+}	0.0	0.0
Mg^{2+}	5.970	1.050
Cl^-	11.94	11.94
Pr^-	55.0	54.77

factor of the sarcoplasmic reticulum will be absent and the major determinant of force

will then be myofilaments binding to Ca^{2+}. A 1% (v/v) Triton X-100 dissolved in RS

was used to skin the muscle for about 30 minutes at room temperature. After skinning, the solution was replace by RS.

Table 11. Data for force-pCa relationship in both control and hypertrophied trabeculae.

pCa	Developed Force (mN/mm^2)	
	Control	Hypertrophy
7.18	0.00 ± 0.00	0.00 ± 0.00
6.67	3.90 ± 0.95	3.30 ± 1.00
6.11	30.0 ± 7.90	19.8 ± 4.00
5.74	58.0 ± 11.0	53.2 ± 2.60
5.32	77.7 ± 11.2	67.5 ± 6.20
5.04	78.7 ± 11.3	74.1 ± 6.40
4.55	83.5 ± 10.9	84.7 ± 10.8

Note that values are expressed as mean ± S.D. for 6 control and 6 hypertrophied trabecular muscles. The average muscle size for control and hypertrophy, respectively, was 0.03 ± 0.003 mm^2 and 0.029 ± 0.002 mm^2.

Table 12. Data for force-interval relationships in both control and hypertrophied muscles.

	Ft/Fc	
Time (s)	Control	Hypertrophy
0.40	0.5049 ± 0.008	0.5049 ± 0.05
0.54	0.5797 ± 0.009	0.5499 ± 0.04
0.73	0.6356 ± 0.013	0.6199 ± 0.05
0.99	0.6966 ± 0.015	0.6724 ± 0.04
2.00	0.8236 ± 0.019	0.7398 ± 0.02
2.50	0.8760 ± 0.014	0.7999 ± 0.02
3.50	0.9382 ± 0.065	0.8961 ± 0.01
4.50	0.9725 ± 0.002	0.9613 ± 0.01
6.00	1.0345 ± 0.010	1.0698 ± 0.01
10.5	1.1538 ± 0.019	1.2998 ± 0.03
15.0	1.2991 ± 0.040	1.6042 ± 0.06
20.0	1.4306 ± 0.054	1.9273 ± 0.10
27.0	1.6047 ± 0.070	2.3294 ± 0.15
36.5	1.7400 ± 0.105	2.7412 ± 0.10
49.0	1.9737 ± 0.123	3.3707 ± 0.12
66.5	2.0787 ± 0.137	3.6190 ± 0.10
89.5	2.1786 ± 0.147	4.0577 ± 0.14
121.0	2.2574 ± 0.139	4.5952 ± 0.20
163.0	2.2695 ± 0.147	4.7727 ± 0.41

Note that values are expressed as mean $\pm$ S.E. Ft, potentiated force following test interval. Fc, contractile force at priming frequency. Sarcomere length for control and hypertrophied muscles, respectively, was 1.90 ± 0.02 um (n = 7) and 1.86 ± 0.02 um (n = 5). $[Ca^{2+}]_o = 1.0$ mM.

Table 13. Relative developed force of both control and hypertrophied muscles at various frequencies of stimulation. $[Ca^{2+}]_o = 0.5$ mM.

Frequency (Hz)	% of DT at 0.2 Hz	
	Control (n = 7)	Hypertrophy (n = 6)
0.1	1.359 ± 0.049	1.197 ± 0.066
0.2	1.000 ± 0.000	1.000 ± 0.000
0.3	0.858 ± 0.016	0.920 ± 0.025
0.5	0.773 ± 0.044	0.952 ± 0.039
1.0	0.874 ± 0.108	1.195 ± 0.106
1.5	1.175 ± 0.136	1.711 ± 0.137
2.0	1.438 ± 0.162	2.089 ± 0.197
2.5	2.032 ± 0.164	2.598 ± 0.213

Note that values are expressed as mean ± S.E. DT at 0.2 Hz, developed tension normalized by contractile force at 0.2 Hz.

Table 14. Relative developed force at various frequencies of stimulation. $[Ca^{2+}]_o = 1.0$ mM.

Frequency (Hz)	% of DT at 0.2 Hz	
	Control (n = 7)	Hypertrophy (n = 7)
0.1	1.179 ± 0.021	1.226 ± 0.066
0.2	1.000 ± 0.000	1.000 ± 0.000
0.3	0.939 ± 0.011	0.936 ± 0.024
0.5	0.849 ± 0.012	0.917 ± 0.055
1.0	0.913 ± 0.020	1.082 ± 0.119
1.5	1.267 ± 0.025	1.421 ± 0.158
2.0	1.455 ± 0.045	1.623 ± 0.152
2.5	1.927 ± 0.061	1.831 ± 0.142

Note that values are expressed mean ± S.E. DT at 0.2 Hz, developed force normalized by contractile force at 0.2 Hz.

Table 15. Relative developed force of both control and hypertrophied muscles at various frequencies of stimulation. $[Ca^{2+}]_o = 2.0$ mM.

% of DT at 0.2 Hz

Frequency (Hz)	Control (n = 5)	Hypertrophy (n = 6)
0.1	1.347 ± 0.056	1.127 ± 0.059
0.2	1.000 ± 0.000	1.000 ± 0.000
0.3	0.812 ± 0.037	0.903 ± 0.032
0.5	0.700 ± 0.051	0.855 ± 0.054
1.0	0.715 ± 0.077	0.877 ± 0.085
1.5	0.877 ± 0.119	0.983 ± 0.112
2.0	0.987 ± 0.153	1.047 ± 0.122
2.5	1.256 ± 0.195	1.125 ± 0.155

Note that values are expressed as mean ± S.E. DT at 0.2 Hz, developed force normalized by contrctile force at 0.2 Hz.

Table 16. Frequency dependence of contractile force in nifedipine-treated and untreated muscles. $[Ca^{2+}]_o = 0.5$ mM.

Frequency (Hz)	Developed Force (mN/mm²)			
	CON (n = 10)	CON + NIF (n = 7)	HYP (n = 5)	HYP + NIF (n = 6)
0.1	2.72 ± 0.30	2.73 ± 0.43	4.56 ± 0.5	6.05 ± 1.16
0.2	1.99 ± 0.21	1.72 ± 0.20	4.18 ± 0.53	3.63 ± 0.62
0.3	1.51 ± 0.15	1.20 ± 0.12	3.80 ± 0.42	2.69 ± 0.41
0.5	1.37 ± 0.17	1.00 ± 0.09	3.84 ± 0.43	2.20 ± 0.31
1.0	1.37 ± 0.16	0.88 ± 0.10	4.67 ± 0.72	1.70 ± 0.19
1.5	2.00 ± 0.31	0.83 ± 0.12	6.66 ± 1.00	1.37 ± 0.17
2.0	2.45 ± 0.43	0.74 ± 0.10	7.90 ± 1.20	1.26 ± 0.17
2.5	3.54 ± 0.77	0.75 ± 0.13	9.73 ± 1.50	1.08 ± 0.18

Note that values are expressed as mean ± S.E. CON = control. HYP = hypertrophy. NIF = nifedipine.

Table 17. Frequency dependence of contractile force in ryanodine-treated and untreated muscles. $[Ca^{2+}]_o = 0.5$ mM.

Developed Force (mN/mm^2)

Freq (HZ)	CON (N = 10)	CON + RYAN (n = 6)	HYP (n = 5)	HYP + RYAN (n = 7)
0.1	2.72 ± 0.30	0.33 ± 0.07	4.56 ± 0.51	1.37 ± 0.27
0.2	1.99 ± 0.21	0.43 ± 0.09	4.18 ± 0.53	1.70 ± 0.32
0.3	1.51 ± 0.15	0.63 ± 0.12	3.80 ± 0.42	2.37 ± 0.35
0.5	1.37 ± 0.17	0.96 ± 0.15	3.84 ± 0.43	3.23 ± 0.47
1.0	1.37 ± 0.16	1.52 ± 0.30	4.67 ± 0.72	5.09 ± 0.67
1.5	2.00 ± 0.31	2.23 ± 0.32	6.66 ± 1.00	7.19 ± 0.79
2.0	2.45 ± 0.43	2.58 ± 0.36	7.90 ± 1.20	7.97 ± 0.79
2.5	3.54 ± 0.77	3.20 ± 0.40	9.73 ± 1.50	8.85 ± 0.97

Note that values are expressed as mean ± S.E. CON = control. HYP = hypertrophy. RYAN = ryanodine. Freq = frequency.

Table 18. Data for RCC and DT in both control and hypertrophied muscles at various stimulation frequencies. $[Ca^{2+}]_o = 0.5$ mM.

Frequency (Hz)	Control		Hypertrophy	
	$DT/DT_{0.2Hz}$ (n = 5)	$RCC/RCC_{0.2Hz}$ (n = 6)	$DT/DT_{0.2Hz}$ (n = 4)	$RCC/RCC_{0.2Hz}$ (n = 10)
0.1	1.25 ± 0.10	1.10 ± 0.03	1.36 ± 0.16	1.14 ± 0.05
0.2	1.00 ± 0.00	1.00 ± 0.00	1.00 ± 0.00	1.00 ± 0.00
0.5	0.84 ± 0.07	0.95 ± 0.04	0.98 ± 0.04	1.07 ± 0.06
1.0	1.01 ± 0.12	1.17 ± 0.05	1.32 ± 0.07	1.43 ± 0.09
1.5	1.45 ± 0.23	1.39 ± 0.05	1.88 ± 0.16	1.86 ± 0.19
2.0	1.59 ± 0.21	1.49 ± 0.05	2.22 ± 0.19	2.18 ± 0.21
2.5	1.73 ± 0.30	1.74 ± 0.11	2.49 ± 0.12	2.57 ± 0.30

Note that values are expressed as mean ± S.E. DT, developed tension at any frequency of stimulation. $DT_{0.2Hz}$, developed tension at 0.2 Hz. RCC, rapid cooling contracture at any frequency. $RCC_{0.2Hz}$, rapid cooling contracture at 0.2 Hz.

Table 19. Data for APD_{50} in control and hypertrophied muscles at various frequencies of stimulation. $[Ca^{2+}]_o = 0.5$ mM.

APD_{50} (ms)

Frequency (Hz)	Control (n = 6)	Hypertrophy (n = 6)
0.2	17.53 ± 1.76	34.73 ± 1.96
0.5	18.19 ± 1.89	36.07 ± 2.08
1.0	20.36 ± 2.26	39.35 ± 2.73
1.5	23.87 ± 2.96	41.78 ± 2.85
2.0	26.04 ± 3.37	44.91 ± 2.70
2.5	28.38 ± 2.88	49.60 ± 2.62
3.0	30.88 ± 3.58	52.10 ± 3.65

Note that values are expressed as mean ± S.E. APD_{50}, 50% duration of action potential. ms = millisecond.

Table 20. Data for double RCCs in both control and hypertrophied muscles. $[Ca^{2+}]_o$ = 0.5 mM.

RCC$_2$/RCC$_1$ (%)

Frequency (Hz)	Control (n = 7)	Hypertrophy (n = 6)
0.2	58.6 ± 1.9	58.6 ± 3.8
0.5	68.0 ± 2.1	62.6 ± 3.9
1.0	74.5 ± 2.9	70.1 ± 2.2
1.5	75.1 ± 3.1	73.6 ± 2.5
2.0	81.7 ± 1.5	78.7 ± 3.0
2.5	83.4 ± 2.1	84.2 ± 2.6

Note that values are expressed as mean ± S.E. RCC$_2$/RCC$_1$, second rapid cooling contracture was normalized by first rapid cooling contracture at the same frequency of stimulation.

VITA AUCTORIS

NAME   Lihui Tang

PLACE OF BIRTH   Heilongjiang, China

YEAR OF BIRTH   1962

EDUCATION   Harbin Medical University, Harbin, China
                                1979 - 1984. M.D.

                                Harbin Medical University, Harbin, China
                                1984 - 1987, M.Sc.

                                University of Windsor, Windsor, Ontario
                                1990 - 1993, Ph.D.